University of Alberta

Kinetics of the Catalytic Dehydration of 2-Propanol in an Aqueous Medium

By

Jean-Marc Rivard

A thesis submitted to the Faculty of Graduate Studies and Research in partial fulfillment of the requirements for the degree of **Master of Science**

in

Chemical Engineering

Department of Chemical and Materials Engineering

Edmonton, Alberta

Fall 2000

National Library of Canada
Acquisitions and Bibliographic Services
395 Wellington Street
Ottawa ON K1A 0N4
Canada

Bibliothèque nationale du Canada
Acquisitions et services bibliographiques
395, rue Wellington
Ottawa ON K1A 0N4
Canada

Your file Votre référence

Our file Notre référence

The author has granted a non-exclusive licence allowing the National Library of Canada to reproduce, loan, distribute or sell copies of this thesis in microform, paper or electronic formats.

L'auteur a accordé une licence non exclusive permettant à la Bibliothèque nationale du Canada de reproduire, prêter, distribuer ou vendre des copies de cette thèse sous la forme de microfiche/film, de reproduction sur papier ou sur format électronique.

The author retains ownership of the copyright in this thesis. Neither the thesis nor substantial extracts from it may be printed or otherwise reproduced without the author's permission.

L'auteur conserve la propriété du droit d'auteur qui protège cette thèse. Ni la thèse ni des extraits substantiels de celle-ci ne doivent être imprimés ou autrement reproduits sans son autorisation.

0-612-59871-3

Canada

University of Alberta

Library Release Form

Name of Author: Jean-Marc Rivard

Title of Thesis: Kinetics of the Catalytic Dehydration of 2-Propanol in an Aqueous Medium

Degree: Master of Science

Year this Degree Granted: 2000

Permission is hereby granted to the University of Alberta Library to reproduce single copies of this thesis and to lend or sell such copies for private, scholarly or scientific research purposes only.

The author reserves all other publication and other rights in association with the copyright in the thesis, and except as herein before provided, neither the thesis nor any substantial portion thereof may be printed or otherwise reproduced in any material form whatever without the author's prior written permission.

Jean-Marc Rivard

Department of Chemical and
Materials Engineering
University of Alberta
Edmonton, Canada T6G 2G6

Date: Sept 21, 2000

Abstract

The liquid-phase catalytic dehydration of 2-propanol was investigated in a batch slurry reactor. Alumina, zeolite 13X, SAPO-5 and silicalite are all active in the liquid phase dehydration of 2-propanol at 463 K with silicalite being the most active catalyst. Propylene was found to be the major reaction product, with diisopropyl ether and acetone formed in trace amounts. The reaction kinetics over silicalite was determined at a temperature range of 434 – 463 K and at a concentration range of 4 – 10 mol % 2-propanol in water. A single site Langmuir-Hinshelwood-Hougen-Watson type mechanism was found to describe the kinetic data well. The rate equation was determined to be

$$r = k K_A C_A / (1 + K_A C_A + K_W C_W)$$

The activation energy over silicalite was determined to be 226.8 kJ/mol while the heat of adsorption model parameters for 2-propanol and water were -45.5 and -9.6 kJ/mol, respectively.

A simplified first order rate model was also found to describe the kinetic data well at low 2-propanol concentrations. An activation energy of 195.8 kJ/mol was determined over silicalite. For the purpose of designing an appropriate separation process for wastewater purification it is recommended that the simple first order model be used, due to its simplicity and accuracy at low 2-propanol concentrations.

University of Alberta

Faculty of Graduate Studies and Research

The undersigned certify that they have read, and recommend to the Faculty of Graduate Studies and Research for acceptance, a thesis entitled **Kinetics of the Catalytic Dehydration of 2-Propanol in an Aqueous Medium** submitted by **Jean-Marc Rivard** in partial fulfillment of the requirements for the degree of **Master of Science** in **Chemical Engineering**.

K.T Chuang

Dr. K. T. Chuang (Supervisor)

Dr. R. E. Hayes

Dr. M. Cowie

Date: Sept. 18, 2000

Acknowledgements

The completion of this thesis would not have been possible without the gracious assistance of several fine individuals in this department. I would like to thank my supervisor Dr. Karl Chuang for his patience and encouragement throughout this work and for suggesting this very interesting project.

I would also like to thank Dr. Qinglin Zhang for his many invaluable suggestions, for his assistance in helping me write this thesis and for sharing his knowledge with me through many enlightening discussions.

I would like to thank Andrée Koenig for her assistance in the analytical aspects of this project. The outstanding work done by Walter Boddez and Richard Cooper of the instrument shop and Bob Scott and James McKinnon of the machine shop on the experimental apparatus is greatly appreciated.

I am extremely grateful for the generous financial assistance provided by the University of Alberta and the Natural Science and Engineering Research Council.

I would like to thank my fellow graduate students for providing a stimulating and enjoyable atmosphere during my stay here in Edmonton.

I will always be in debt to my parents, Roch and Lise Rivard for their love and support in whatever I chose to embark upon. They are without a doubt, the finest individuals I have ever met.

Table of Contents

1 Introduction **1**

1.1 2-Propanol Dehydration 2

1.2 Mechanism of 2-Propanol Dehydration over Solid Acid Catalysts 5

1.2.1 Alumina 5

1.2.2 Silica-Alumina 6

1.2.3 Zeolites – HZSM-5 Substitutional Series 8

1.2.4 Silicoaluminophosphates 8

1.2.5 Ion Exchange Resins 10

1.3 Problem Definition 11

1.4 Nomenclature 12

1.5 Literature Cited 13

2 Experimental **22**

2.1 Experimental Apparatus 22

2.2 Analysis Techniques and Experimental Procedure 22

3 Kinetic Modeling **26**

3.1 Determination of the Rate of Formation of Propylene 26

3.2 Determination of the Rate Equation 35

3.2.1 Single-Site Mode Adsorption with the Water Term Excluded (SSM-1) 36

3.2.2 Single-Site Mode Adsorption with the Water Term Included (SSM-2) 37

3.2.3 Dual-Site Mode Adsorption with the Water Term Excluded (DSM-1) 38

3.2.4 Dual-site Mode Adsorption with the Water Term Included (DSM-2) 40

3.3 Nomenclature 42

3.4 Literature Cited 47

4 Experimental Results and Discussion 49

4.1 Determination of the Vapor-Liquid Equilibria for 2-Propanol/Water System 49

4.2 Catalyst Screening 57

4.2.1 Preliminary Screening 57

4.2.2 Validation of Irreversible Reaction 60

4.3 Mass Transfer Limitations 66

4.4 Kinetic Study 71

4.5 Catalyst Loading 80

4.6 First Order Model 83

4.7 Nomenclature 87

4.8 Literature Cited 91

5 Conclusions and Recommendations 92

5.1 Conclusions 92

5.2 Recommendations for Future Work 94

5.2.1 Simulation of Wastewater Purification Process 94

5.2.2 Hydration of Propylene over Solid Acid Catalysts 94

5.2.3 Effect of Silica/Alumina Ratio on the Rate of Propylene Formation 95

5.2.4 Effect of Metal Ion Concentration in Wastewater on the Rate of Propylene Formation 95

5.3 Literature Cited 98

Appendices **99**

A1 Maple V Worksheet for the Determination of the Amount of Propylene Produced 99

A2 Raw Data for the Kinetic Runs 103

List of Tables

3.1	Critical Constants of Reactants, Products and Inerts	46
3.2	COSTALD Correlation Parameters	46
4.1	BET Surface Area for the Screened Catalysts	90
4.2	Enthalpy and Gibbs Free Energy of Formation and the Temperature Dependency of the Heat Capacity for Reactant and Products	90
4.3	Parameters and Predictions of the Developed LHHW Kinetic Models	90
A2.1	Catalyst Screening Raw Data: Alumina	103
A2.2	Catalyst Screening Raw Data: Zeolite 13X	104
A2.3	Catalyst Screening Raw Data: Silicalite S-115 SiO_2 ExT.	105
A2.4	Catalyst Screening Raw Data: SAPO-5	106
A2.5	External Mass Transfer Raw Data: Stirrer Speed = 883 rpm	107
A2.6	External Mass Transfer Raw Data: Stirrer Speed = 1004 rpm	108
A2.7	External Mass Transfer Raw Data: Stirrer Speed = 1182 rpm	109
A2.8	Internal Mass Transfer Raw Data: 100-170 Mesh Particle Size	110
A2.9	Internal Mass Transfer Raw Data: 20-30 Mesh Particle Size	111
A2.10	Temperature Dependence Raw Data: 463 K	112
A2.11	Temperature Dependence Raw Data: 453 K	113
A2.12	Temperature Dependence Raw Data: 444 K	114
A2.13	Temperature Dependence Raw Data: 434 K	115
A2.14	Concentration Dependence Raw Data: 8 mol % Initial 2-Propanol/Water Concentration in the Feed at 463 K	116
A2.15	Concentration Dependence Raw Data: 6 mol % Initial 2-Propanol/Water Concentration in the Feed at 463 K	117

A2.16 Concentration Dependence Raw Data: 4 mol % Initial 2-Propanol/Water Concentration in the Feed at 463 K 118

A2.17 Catalyst Reusability Raw Data: Used Catalyst at 463 K 119

A2.18 Catalyst Loading Raw Data: 0.762 wt % 120

A2.19 Catalyst Loading Raw Data: 1.106 wt % 121

List of Figures

1.1 E_2 Mechanism for 2-Propanol Dehydration (S_1 = Lewis Basic Site, S_2 = Lewis Acid Site): Fikis, D. V.,W. J. Murphy and R. A. Ross, *Can. J. Chem.* **56**, 2530-2537 (1978) 7

1.2 E_1 Mechanism for 2-Propanol Dehydration (S = Brønsted Acid Site, H^+): de Miguel, S. R., A.C. Martinez, A. A. Castro, and O. A. Scelza, *J. Chem. Tech. Biotechnol.* **65**, 131-136 (1996) 9

2.1 Experimental Setup 23

4.1 Minimization of Function f_1 for the Determination of the van Laar Binary Parameters: ( ) 433 K, (■) 443 K, (▲) 453 K, (◆) 463 K, (—) van Laar model fit 52

4.2 Minimization of Function f_2 for the Determination of the van Laar Binary Parameters: ( ) 433 K, (■) 443 K, (▲) 453 K, (◆) 463 K, (—) van Laar model fit 53

4.3 Minimization of Function f_3 for the Determination of the van Laar Binary Parameters: ( ) 433 K, (■) 443 K, (▲) 453 K, (◆) 463 K, (—) van Laar model fit 54

4.4 The Equilibrium Pressure versus Liquid Composition : PRSV Equation of State with the van Laar Excess Gibbs Free Energy Model: (◆) 433 K, (●) 443 K, (▲) 453 K, (■) 463 K, (—) van Laar model fit 55

4.5 Temperature Dependence of the Binary Parameters for the van Laar excess Gibbs Free Energy Model (1 = 2-Propanol, 2 = Water): (▲) C_{12}, (■) C_{21} 56

4.6 X-Ray Diffraction Pattern for the Screened Catalysts: 1 = S-115 Al_2O_3 ExT., 2 = S-115 SiO_2 ExT., 3 = SAPO-5, 4 = Zeolite 13X, 5 = Alumina 58

4.7 Catalyst screening – Reaction Temperature = 463 K, Stirrer Speed = 1004 rpm, 30-40 Mesh Particle Size (Except Powder SAPO-5), 1.5 wt % Catalyst Loading, 10 mol % 2-Propanol /Water Feed 59

4.8 Chemical Equilibrium Constant for the Liquid-Phase Dehydration of 2-Propanol to Propylene at Various Reaction Temperatures 63

4.9 Influence of Reactor Temperature and Initial 2-Propanol Concentration on the Equilibrium Conversion of 2-Propanol to Propylene in a Batch Slurry Reactor 65

4.10 Effect of Stirrer Speed on the Observed Rate of Propylene Formation over Silicalite S-115 Al_2O_3 : 10 mol % 2-Propanol / water feed, 100-170 mesh particle size, 463 K Reaction Temperature 68

4.11 Effect of Particle Size on the Observed Rate of Propylene Formation over Silicalite S-115 Al_2O_3 : 10 mol % 2-Propanol / water feed, 1080 rpm Stirrer Speed, 463 K Reaction Temperature 70

4.12 Comparison of Experimental Rate Data with the Fitted SSM-2 Model at a Temperature Range of 434 – 463 K: (◆) 434 K, (▲) 444 K, (●) 453 K, (■) 463 K, (—) SSM-2 Model Fit 73

4.13 Temperature Dependence of the Kinetic Parameters k, Determined from the Fitted SSM-2 LHHW Model 74

4.14 Temperature Dependence of the Adsorption/Desorption Equilibrium Constants Determined from the Fitted SSM-2 LHHW Model: (◆) 2-Propanol, (■) Water 75

4.15 Comparison of SSM-2 Model Prediction with the Rate of Propylene Produced under Different Initial 2-Propanol Mole Fraction: (▲) 4 mol % 2-Propanol Feed, (□ 6 mol % 2-Propanol Feed, (■) 8 mol % 2-Propanol Feed, ( ) 10 mol % 2-Propanol Feed, (—) SSM-2 Model 76

4.16 Comparison of X-Ray Diffraction Pattern of Fresh Silicalite (S-115 Al_2O_3 ExT.) with Reacted Silicalite: 1 = Fresh, 2 = Reacted 78

4.17 Silicalite S-115 Al_2O_3 ExT. Catalyst Reusability: Initial 2-Propanol Concentration of 10 mol %, 30-40 Mesh Particle Size, 1080 rpm Stirrer Speed, Reaction Temperature of 463 K: Used Catalyst Reacted for 2.5 Hours 79

4.18 Effect of Silicalite S-115 Al_2O_3 ExT. Loading on the Rate of Propylene Formation: 10 mol % 2-Propanol Feed at a Reaction Temperature of 463 K: ( ) 1.556 wt %, (▲) 1.106 wt %, (■) 0.762 wt %, (—) SSM-2 Model Fit 81

4.19 Effect of Silicalite S-115 Al_2O_3 ExT. Loading on the Kinetic Parameters: 10 mol % 2-Propanol Feed at a Reaction Temperature of 463 K 82

4.20 Concentration Dependence of 2-Propanol on the Rate of Propylene Formation at 463 K:(▲) 4 mol % 2-Propanol Feed, (□ 6 mol % 2-Propanol Feed, (■) 8 mol % 2-Propanol Feed, ( ) 10 mol % 2-Propanol Feed, (—) 1st Order Model Fit 84

4.21 Comparison of Experimental Rate Data with the Fitted 1st Order Model at a Temperature Range of 434 – 463 K: (◆) 434 K, (▲) 444 K, (●) 453 K, (■) 463 K, (—) 1st Order Model Fit 85

4.22 Temperature Dependence of the Kinetic Parameters k, Determined from the Fitted 1st Order Model 86

5.1 Effect of Metal Ions Present in Tap Water on the Rate of Propylene Formation and Catalyst Deactivation: 10 mol % 2-Propanol Feed, Reaction Temperature of 463 K (Used Catalyst from Tap Water Reaction used in Kinetic Run with Deionized Water in the Feed) 97

Chapter 1

Introduction

The increased industrial usage of water in recent years has led to an increase in the volume of wastewater effluent [Terzis, 1994]. Wastewater from various industries, such as pharmaceutical, cosmetic, textile, and rubber contain aliphatic organic solvents which are often flammable, malodorous and potentially toxic to aquatic organisms [Henry et al., 1996]. 2-Propanol is a common organic solvent and its removal from wastewater is an important environmental issue.

Wastewater containing 2-propanol can be purified in many manners. Distillation, aerobic biological treatment [McKinney and Jeris, 1955; Hatfield, 1957; Ludzack and Ettinger, 1960] and anaerobic biological treatment [Hovious et al., 1973; Chou et al., 1978; Terzis, 1994; Henry et al., 1996] are known methods in purifying wastewater containing 2-propanol. These methods are not without their flaws. Distillation is very energy intensive and the 2-propanol/water separation may be complicated if the 2-propanol concentration of the wastewater approaches the azeotropic value. Biological treatment of wastewater may require further disinfection via chlorination to kill harmful bacteria. Although 2-propanol has not been found in the literature to be toxic to the microorganisms in biological treatment processes [Ludzack and Ettinger, 1960; Chou et al., 1978], it can be expected that a high concentration of 2-propanol in wastewater would be potentially harmful to the organisms.

It is known that 2-propanol can dehydrate in the presence of an acid catalyst to form propylene and water. In the literature, vapor-phase catalytic dehydration reactions are often carried out in plug-flow reactor systems with little or no water in the feed. The

use of a vapor-phase reactor to convert 2-propanol to propylene is expensive because of the large amount of energy required to vaporize the aqueous 2-propanol/water feed. For this reason, the reaction must be conducted in the liquid-phase. The liquid-phase dehydration of 2-propanol has potential application for wastewater purification where 2-propanol is present as an impurity.

Catalytic distillation is a potential separation process for wastewaters containing 2-propanol as an impurity. Making use of a solid acid catalyst, 2-propanol would dehydrate in the liquid-phase to form propylene and water. This process is potentially attractive because the propylene/water separation is much easier than the 2-propanol/water separation. To design such a process, the liquid-phase 2-propanol dehydration kinetics must first be determined. The development of the kinetic model is the focus of this thesis.

1.1 – 2-Propanol Dehydration

It is well known that alcohols can dehydrate in the presence of solid acid catalysts to form olefinic products [Pines and Manassen, 1966]. In the case of 2-propanol, the olefin produced is propylene

$$C_3H_8O(l) \leftrightarrow C_3H_6(g) + H_2O(l) \qquad K_{L,298} = 0.094 \qquad (1.1.1)$$

$$\Delta H^{o}_{f,298} = 52.6 \text{ kJ mole}^{-1}$$

Depending on the relative strength of the solid acid, the dehydration product can also include ether, in the case of 2-propanol dehydration the product is diisopropyl ether

$$C_3H_8O(l) \leftrightarrow \frac{1}{2}C_6H_{14}O(l) + \frac{1}{2}H_2O(l) \qquad K_{L,298} = 2.912 \qquad (1.1.2)$$

$$\Delta H^{o}_{f,298} = -0.5 \text{ kJ mole}^{-1}$$

If the basic sites are sufficiently strong, alcohol dehydrogenation can also occur. For the case of 2-propanol, the dehydrogenation product is acetone

$$C_3H_8O(l) \leftrightarrow H_2(g) + C_3H_6O(l) \qquad K_{L,298} = 4.15 \times 10^{-5} \qquad (1.1.3)$$

$$\Delta H^{\circ}_{f,298} = 69.9 \text{ kJ mole}^{-1}$$

The vapor-phase dehydration of 2-propanol is widely used as a reaction to qualitatively characterize the acidity of solid catalysts and to study the mechanism of the catalytic dehydration of alcohols over solid acids [Jain and Pillai, 1968; Jacobs et al., 1977; Gervasini and Auroux, 1991; Gervasini et al., 1997]. Gervasini and Auroux (1991) concluded that the "number, the nature and the strength of the acid sites affect the catalytic activity".

The vapor-phase dehydration of 2-propanol over a γ-alumina catalyst has been proposed for propylene production [Fukuhara et al., 1991], although it is not a common practice to do so.

Several solid acid catalysts have been reported to be active in the vapor phase dehydration of 2-propanol. It is known that some metal oxide catalysts, such as alumina, possess acidic properties, which are useful in dehydration reactions. Gamma alumina (γ-Al_2O_3) is a solid acid known to be active in the vapor-phase dehydration of 2-propanol. The acid-base properties of alumina and ion-exchanged alumina have been well studied in the literature [Pines and Haag, 1960; Jain and Pillai, 1967; de Mougues et al., 1967; Knözinger and Ratnasamy, 1978; Knözinger and Stübner, 1978; Luy and Parera, 1986; Berteau et al., 1987; Auroux and Gervasini, 1990; Gervasini and Auroux, 1991; Mostafa et al., 1991; de Canio et al., 1992; Saad et al., 1993; Gervasini et al., 1995; Shi and Davis, 1995; de Miguel et al., 1996; Gervasini et al., 1997; El-Hakam and El-Sharkawy, 1998].

There has been recent interest in the activity of alumina in reactions requiring strong acids. Solid acid catalysts, such as alumina, are known to be active in the chemical abatement of some chemical pollutants. A process has been proposed to use γ-alumina in ceramic filters for flue gas cleaning [Saracco and Montanaro, 1995; Saracco and Specchia, 1995a,b]. The use of ceramic as a porous filter allows for a high temperature to be used, as conventional polymer-based filter bags cannot withstand temperatures exceeding 200 °C. Once the filters are activated with a suitable catalyst (γ-Al_2O_3), the flue gas can be cleaned with a combined action of mechanical particulate removal and catalytic abatement of some chemical pollutants, such as nitrogen oxides and volatile organic compounds [Saracco and Montanaro, 1995].

Mixed oxides are often prepared to produce a material with properties superior to a linear combination of the constituents [Youssef et al., 1992]. Various mixed oxides have been found in the literature to be active in the vapor-phase 2-propanol dehydration. Some of these include mixed oxides of SnO_2 with P_2O_5 and V_2O_5 [Ai, 1975a,b], silica (SiO_2) with MgO and SnO_2 [Youssef et al., 1992; Salas et al., 1997], and MoO_3 with SnO_2, Fe_2O_3, P_2O_5, and TiO_2 [Ai and Suzuki, 1973; Tanabe et al., 1986; Bond et al., 1994]. A special series of mixed oxides containing alumina and silica (silica-aluminates) are known to be very active in the dehydration of 2-propanol [Youssef et al., 1990; López et al., 1992]. Their acidity and catalytic activity are related to the Al/Si ratio.

Recently, zeolites have been given attention because of their high activity in reactions involving strong acids. The vapor-phase dehydration of 2-propanol over various zeolite molecular sieves is discussed in the literature [Jacobs et al., 1977; Yue and Olaofe, 1984ab; Bezoukhanova and Kalvachev, 1994]. Other solid acids such as

aluminophosphates [Mishra et al., 1998; El-Sharkawy et al., 1999] and ion exchange resins [Gottifredi et al., 1968] are also known to be active in the vapor-phase dehydration of 2-propanol.

1.2 – Mechanism of 2-Propanol Dehydration over Solid Acid Catalysts

1.2.1 – Alumina

The mechanism of alcohol dehydration over a solid acid catalyst was first studied using active alumina [Pines and Manassen, 1966; Jain and Pillai, 1967]. Alumina is known to be active in reactions requiring strong acids, such as hydrocarbon cracking and alcohol dehydration. Amphoteric oxides, such as alumina, have a balanced strength of acid and basic sites [Gervasini et al., 1997]. There has been considerable debate upon the nature of these acid and basic sites. The general consensus is that the active sites on alumina consists of electron pair donors (Lewis bases) and electron pair acceptors (Lewis acids). Using FT-IR spectroscopy of adsorbed pyridine, Berteau and co-workers (1991) found no Brønsted-acid sites on alumina and modified aluminas. Knözinger and Kaerlein (1971) previously concluded that alumina surfaces do not develop Brønsted acidity at temperatures up to 300 °C which are strong enough to protonate pyridine.

The formation of Lewis acidity on the dehydrated surface of alumina was postulated by a model suggested by Hindin and Weller (1956).

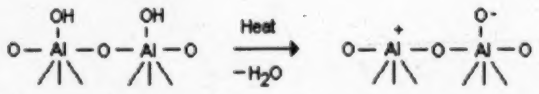

(1.1.4)

The resulting structure contains coordinately unsaturated aluminum atoms.

An E_2 type mechanism has been proposed for 2-propanol dehydration over alumina to form propylene [Krylov, 1965 ab; Fikis et al., 1978; de Miguel et al., 1996; Gervasini et al., 1996]. The acid site induces the abstraction of the hydroxyl group and the basic site induces the abstraction of the β-hydrogen. Figure 1.1 illustrates the E_2 dehydration mechanism for olefin formation, where S_1 and S_2 represent the basic and acidic sites respectively.

1.2.2 – Silica-Alumina

Silica-alumina is a mixed metal oxide catalyst commonly used in alcohol dehydration reactions. On pure alumina, the Lewis-acid site consists of an aluminum atom which is incompletely coordinated (electron pair acceptor). Unlike pure aluminas, both Brønsted and Lewis acids occur on silica-aluminas because of the isomorphous substitution of tetravalent silicon by trivalent aluminium in the silica lattice [Berteau et al., 1991]. The aluminum atom, which is normally hexacoordinated, is forced to adopt a tetracoordinated structure. The aluminum atom in the silica-alumina lattice behaves as a Lewis acid in the absence of water and as a Brønsted acid in the presence of water. It is generally accepted that silica-aluminas contain both Brønsted and Lewis acid sites [Basila et al., 1964; Fripiat et al., 1965; Luy and Parera, 1986]. Brønsted acidity is believed to be responsible for the catalytic activity of silica-alumina [Thomas, 1949], hence it has been proposed that 2-propanol dehydrates via an E_1 type mechanism [Luy and Parera, 1986]. Unlike the E_2 mechanism, which requires both acid and basic sites, the E_1 mechanism only requires acids and involves a carbenium intermediate. This carbenium cation is later transformed to an olefin by proton abstraction. This mechanism

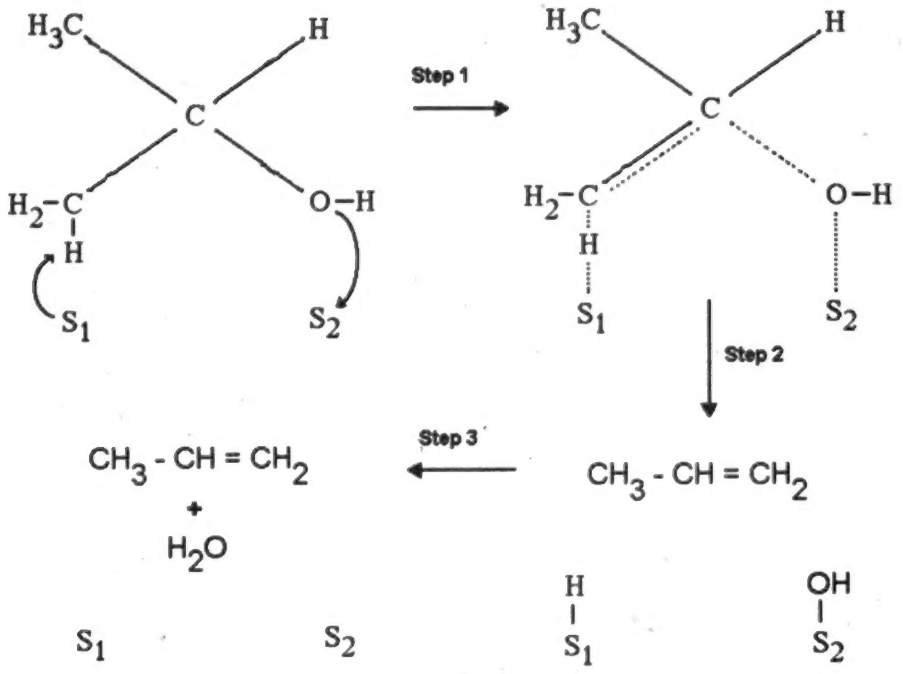

Figure 1.1 – E_2 Mechanism for 2-Propanol Dehydration (S_1 = Lewis Basic Site, S_2 = Lewis Acid Site): Fikis, D. V., W. J. Murphy and R. A. Ross, *Can. J. Chem.* **56**, 2530-2537 (1978)

is illustrated in Figure 1.2. A more detailed explanation of E_1 and E_2 mechanisms can be found in the literature [Lowry and Richardson, 1981].

1.2.3 – Zeolites – HZSM-5 Substitutional Series

Zeolites are a class of hydrated aluminum silicates consisting of a 3D network of –Al-O-Si- atoms in the form of linked tetrahedra [Tanabe, 1970]. They differ from silica-aluminas in terms of their crystal structure and acidity. There is evidence to suggest that zeolites, notably H-ZSM-5, act as Brønsted acids [Anderson et al., 1980; Bolis et al., 1980]. Gorte and co-workers confirmed the Brønsted acidity of ZSM-5 zeolites by the characterization of 2-propanol adsorption by temperature programmed desorption (TPD), thermogravimetric analysis (TGA) and transmission infrared spectroscopy [Grady and Gorte, 1985; Aronson et al., 1986;1987].

The structural aluminum atoms responsible for the Brønsted acidity of H-ZSM-5 zeolites are very dilute, due to the zeolite's highly siliceous nature. This dilution causes the active sites to be similar in nature [Grady and Gorte, 1985] as illustrated in the linear increase in hexane cracking with aluminum content [Olson et al., 1980]. Despite the dilute concentration of acid sites on H-ZSM-5 zeolites, the sites themselves are strong and are active in reactions requiring strong acids, such as catalytic cracking. It has been proposed that alcohols dehydrate to propylene over zeolites via an E_1 mechanism [Jacobs et al., 1977]. 2-Propanol can also dehydrate over zeolites to form diisopropyl ether, although both acid and basic sites are involved in the mechanism.

1.2.4 – Silicoaluminophosphates

Silicon and aluminum in the zeolite framework can be isomorphously substituted by elements such as gallium, cerium, beryllium, boron, iron, phosphorus, and magnesium

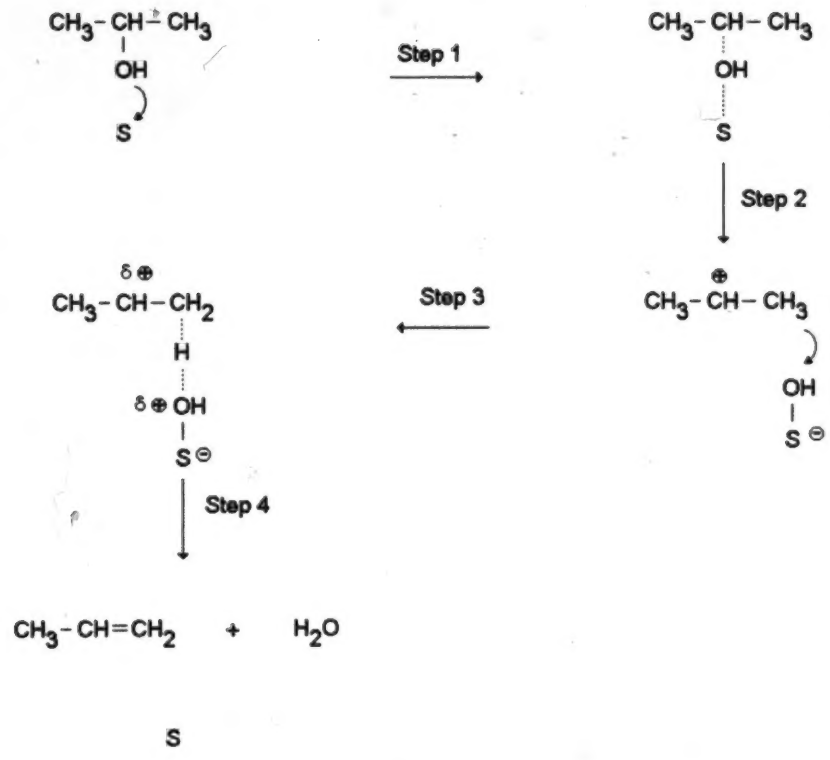

Figure 1.2 – E_1 Mechanism for 2-Propanol Dehydration (S = Brønsted Acid Site, H^+): de Miguel, S. R., A. C. Martinez, A. A. Castro, and O. A. Scelza, *J. Chem. Tech. Biotechnol.* **65**, 131-136 (1996)

[Chu and Chang, 1985]. Much attention has been drawn to the introduction of pentavalent phosphorus in the zeolite lattice [Bezoukhanóva and Kalvachev, 1994]. Aluminophosphates (AlPO) and silicoaluminophosphates (SAPO) have been synthesized in this manner [Wilson et al., 1982; Lok et al., 1984]. These molecular sieves have been classified by x-ray and neutron diffraction [Flanigen et al., 1988].

Silicoaluminophosphates are produced by a replacement of the pentavalent phosphorus by tetravalent silicon [Bezoukhanova and Kalvachev, 1994]. Based on the IR spectra of cyclohexanol on SAPO-5, SAPO-11 and SAPO-31, it has been concluded that Brønsted acid sites and hydrogen-accepting sites (probably basic in character) exist in SAPO molecular sieves which is similar to what was found for H-ZSM-5 zeolites [Bezoukhanova et al., 1991]. The acidity and activity of SAPO molecular sieves are related to the (Al + P)/Si ratio. Unlike H-ZSM-5 molecular sieves, a simple relation between activity and the (Al + P)/Si ratio is not known.

1.2.5 – Ion Exchange Resins

Macroporous cation exchange resins, such as Amberlyst 15 have recently found use in the synthesis of MTBE [Subramaniam and Bhatia, 1987; Izqulerdo et al., 1992; Nicolaides et al., 1993]. These resins are a polymeric three-dimensional cross-linked structure obtained by the sulphonation of a copolymer made of polystyrene and divinyl benzene. The reaction mechanism for alcohol dehydration is strongly dependent on the concentration of water as was determined from the vapor-phase dehydration of methanol, tertiary butyl alcohol and 2-propanol [Gates and Rodriguez, 1973; Thornton and Gates, 1974]. There is a transition from catalysis by bound $-SO_3H$ groups to hydrated protons

in the polymer matrix upon addition of water. The catalytic activity is proportional to the proton concentration.

The main problem with the use of polymer ion exchange resins is that they are very sensitive to temperature and lose their activity at temperatures exceeding 393 K. Current work is being performed to develop catalysts that are more thermally stable [Beasly and Jokovac, 1984; Helfferich and Hwang, 1988].

1.3 – Problem Definition

To design a process for a 2-propanol/water separation, kinetic data for 2-propanol dehydration in an aqueous media are essential. Although the vapor-phase dehydration of 2-propanol has been well studied, there exists no information in the literature on the liquid-phase dehydration of 2-propanol. Furthermore, the influence of a high concentration of water on the rate of 2-propanol dehydration is not well understood.

In this study, the performance of several well-known acid catalysts including alumina, zeolite 13X, SAPO-5 and silicalite (similar to H-ZSM-5 in structure) were evaluated with an initial 2-propanol concentration of 10 mol % at 463 K in a batch slurry reactor. The kinetic study was carried out at temperatures ranging from 434 to 463 K and initial 2-propanol concentrations of 4 – 10 mol %. The kinetic equation was derived based on a Langmuir-Hinshelwood-Hougen-Watson (LHHW) type reaction mechanism. The LHHW method of generating rate models is based on Langmuir adsorption and is often used in developing rate models for heterogeneous catalytic reactions. LHHW models have been used in developing rate equations for the catalytic vapor-phase 2-propanol dehydration [Jacobs et al., 1977; Yue and Olaofe, 1984a; Hamzaoui and Batis, 1992].

1.4 – Nomenclature

ΔH^{o}_{f} = heat of formation, kJ $mole^{-1}$

K = chemical equilibrium constant

Subscripts

298 = at 298 K

L = liquid

1.5 – Literature Cited

Ai, M. and S. Suzuki, "Oxidation Activity and Acidity of MoO_3-P_2O_5 Catalysts", *J. Catal.* **30**, 362-371 (1973)

Ai, M., "The Oxidation Activity and Acid-Base Properties of SnO_2-Based Binary Catalysts I. The SnO_2-V_2O_5 System", *J. Catal.* **40**, 318-326 (1975a)

Ai, M., "The Oxidation Activity and Acid-Base Properties of SnO_2-Based Binary Catalysts II. The SnO_2-MoO_3 and SnO_2-P_2O_5 Systems", *J. Catal.* **40**, 327-333 (1975b)

Anderson, J. R., T. Mole and V. Christov, "Mechanism of Some Conversions over ZSM-5 Catalyst", *J. Catal.* **61**, 477-484 (1980)

Aronson, M. T., R. J. Gorte and W. E. Farneth, "The Influence of Oxonium Ion and Carbenium Ion Stabilities on the Alcohol/H-ZSM-5 Interaction", *J. Catal.* **98**, 434-443 (1986)

Aronson, M. T., R. J. Gorte and W. E. Farneth, "An Infrared Spectroscopy Study of Simple Alcohols Adsorbed on H-ZSM-5", *J. Catal.* **105**, 455-468 (1987)

Auroux, A. and A. Gervasini, "Microcalorimetric Study of the Acidity and Basicity of Metal Oxide Surfaces", *J. Phys. Chem.* **94**, 6371-6379 (1990)

Basila, M. R., T. R. Kantner and K. H. Rhee, "The Nature of the Acidic Sites on a Silica-Alumina. Characterization by Infrared Spectroscopic Studies on Trimethylamine and Pyridine Chemisorption", *J. Phys. Chem.* **68**, 3107-3207 (1964)

Beasley, G. H. and I. J. Jakovac, "Ion Exchange Resin Catalysts Having Improved Catalytic Activity and Enhanced Thermal Stability", in *Ion Exchange Technology* (B. Naden and M. Streat eds.), Chichester, West Sussex, p. 441 (1984)

Berteau, P., B. Delmon, J-L. Dallons, and A. Van Gysel, "Acid-Base Properties of Silica-Aluminas: Use of 1-Butanol Dehydration as a Test Reaction", *Appl. Catal.* **70**, 307-323 (1991)

Berteau, P., M. Ruwet and B. Delmon, "1-Butanol Dehydration on Aluminas and Modified Aluminas. Evolution of Activity and Selectivity", *Acta Chem. Hung.* **124 (1)**, 25-33 (1987)

Bezoukhanova, C. P. and Y. A. Kalvachev, "Alcohol Reactivity on Zeolites and Molecular Sieves", *Catal. Rev. –Sci. Eng.* **36(1)**, 125-143 (1994)

Bezoukhanova, C. P., Y. A. Kalvachev and H. Lechert, "Infrared Study of Cyclohexanol Chemisorption in SAPO Molecular Sieves", *J. Chem. Soc. Faraday Trans.* **87**(19), 3315-3317 (1991)

Bolis, V., J. C. Vedrine, J. P. Van de Berg, J. P. Wolthuizen, and E. G. Debrouane, "Adsorption and Activation of Ethene by Zeolite-H-ZSM-5", *J. Chem. Soc., Faraday Trans. 1* **76**, 1606-1616 (1980)

Bond, G. C., S. A. Halawy, K. M. A. El-Salaam, E. A. Hassan, and H. M. Ragih, "MoO_3-Fe_2O_3 Catalysts : Characterization and Activity for Isopropyl Alcohol Decomposition", *J. Chem. Tech. Biotechnol.* **59**, 181-191 (1994)

Chou, W. L., R. E. Speece, R. H. Siddiqi, and K. McKeon, "The Effect of Petrochemical Structure on Methane Fermentation Toxicity", *Prog. Wat. Tech.* **10**, 545-558 (1978)

Chu, C. T-W. and C. D. Chang, "Isomorphous Substitution in Zeolite Frameworks. 1. Acidity of Surface Hydroxyls in [B]-, [Fe]-, [Ga]-, and [Al]-ZSM-5", *J. Phys. Chem.* **89**, 1569-1571 (1985)

de Canio, E. C., V. P. Nero and J. W. Bruno, "Identification of Alcohol Adsorption Sites on γ-Alumina", *J. Catal.* **135**, 444-457 (1992)

de Miguel, S. R., A. C. Martinez, A. A. Castro, and O. A. Scelza, "Effect of Lithium Addition upon γ-Al_2O_3 for Isopropanol Dehydration", *J. Chem. Tech. Biotechnol.* **65**, 131-136 (1996)

de Mourgues, I., F. Peyron, Y. Trambouze, and M. Prettre, "Kinetics of the Catalytic Dehydration of 2-Propanol", *J. Catal.* **7**, 117-125 (1967)

El-Hakam, S. A. and E. A. El-Sharkawy, "Structural Characterization and Catalytic Properties of Aluminum Borates-Alumina Catalysts", *Mat. Letters* **36**, 167-173 (1998)

El-Sharkawy, E. A., M. R. Mostafa and A. M. Youssef, "Changes in Surface and Catalytic Dehydration Activities of 2-Propanol on AlPO-5 Induced by Silver Impregnation", *Colloids Surf. A.* **157**, 211-218 (1999)

Fikis, D. V., W. J. Murphy and R. A. Ross, "The Formation of Propane, Propylene, and Acetone from 2-Propanol over Vanadium Pentoxide and Modified Vanadium Pentoxide Catalysts", *Can. J. Chem.* **56**, 2530-2537 (1978)

Flanigen, E. M., R. L. Patton and S. T. Wilson, "Structural, Synthetic and Physicochemical Concepts in Aluminophosphate-Based Molecular Sieves", in *Innovations in Zeolite Materials Science* (P. J. Grobet et al., eds.), Stud. Surf. Sci. Catal., Vol. 37, Elsevier, Amsterdam, p. 13. (1988)

Fripiat, J. J., A. Léonard and J. B. Uytterhoeven, "Structure and Properties of Amorphous Silicoaluminas. II. Lewis and Brønsted Acid Sites", *J. Phys. Chem.* **69**, 3274-3279 (1965)

Fukuhara, H., W. Matsanaga, M. Yasuhara, S. Araki, and T. Isaka, "Preparation of Propylene by Dehydration of Isopropanol in the Presence of a Pseudo-Bohemite Derived Gamma Alumina Catalyst", U.S. Pat. 5,227,563 (1991)

Gates, B. C. and W. Rodriguez, "General and Specific Acid Catalysts in Sulfonic Acid Resin", *J. Catal.* **31**, 27-31 (1973)

Gervasini, A. and A. Auroux, "Acidity and Basicity of Metal Oxide Surfaces. II. Determination by Catalytic Decomposition of Isopropanol", *J. Catal.* **131**, 190-198 (1991)

Gervasini, A., G. Bellussi, J. Fenyvesi, and A. Auroux, "Microcalorimetric and Catalytic Studies of the Acidic Character of Modified Metal Oxide Surfaces. 1. Doping Ions on Alumina, Magnesia, and Silica", *J. Phys. Chem.* **99**, 5117-5125 (1995)

Gervasini, A., J. Fenyvesi and A. Auroux, "Study of the Acidic Character of Modified Metal Oxide Surfaces Using the Test of Isopropanol Decomposition", *Cat. Letters* **43**, 219-228 (1997)

Gottifredi, J. C., A. A. Yeramian and R. E. Cunningham, "Vapor-Phase Reactions Catalyzed by Ion Exchange Resins I. Isopropanol Dehydration", *J. Catal.* **12**, 245-256 (1968)

Grady, M. C. and R. J. Gorte, "Adsorption of 2-Propanol and Propene on H-ZSM-5: Evidence for Stable Carbenium Ion Formation", *J. Phys. Chem.* **89**, 1305-1308 (1985)

Hamzaoui, H. and H. Batis, "Propriétés Physico-Chimiques des Phosphates de Zirconium. II. Cinétique de Déshydratation de L'Isopropanol en Propène", *J. Chim. Phys.* **89**, 111-122 (1992)

Hatfield, R., "Biological Oxidation of Some Organic Compounds", *Ind. Eng. Chem.* **49**, 192-196 (1957)

Helfferich, F. G. and Y-L. Hwang, "Ion Exchangers as Catalysts", in *Ion Exchange for Industry* (M. Streat ed.), Chichester, New York, p. 585 (1988)

Henry, M. P., B. A. Donlon, P. N. Lens, and E. M. Colleran, "Use of Anaerobic Hybrid Reactors for Treatment of Synthetic Pharmaceutical Wastewaters Containing Organic Solvents", *J. Chem .Tech. Biotechnol.* **66**, 251-264 (1996)

Hindin, S. G. and S. W. Weller, *J. Phys. Chem* **60**, 1501 (1956)

Hovious, J. C., R. A. Conway and C. W. Ganze, "Anaerobic Lagoon Pretreatment of Petrochemical Wastes", *J. Wat. Pollut. Control Fed.* **45**, 71-84 (1973)

Izqulerdo, J. F., F. Cunill, M. Vila, J. Tejero, and M. Iborra, "Equilibrium Constants for Methyl *tert*-Butyl Ether Liquid-Phase Synthesis", *J. Chem. Eng. Data* **37**, 339-343 (1992)

Jacobs, P. A., M. Tielen and J. B. Uytterhoeven, "Active Sites in Zeolites. Part 6. Alcohol Dehydration over Alkali Cation-Exchanged X and Y Zeolites", *J. Catal.* **50**, 98-108 (1977)

Jain, J. R. and C. N. Pillai, "Catalytic Dehydration of Alcohols over Alumina. Mechanism of Ether Formation", *J. Catal.* **9**, 322-330 (1967)

Knözinger, H. and B. Stübner, "Adsorption of Alcohols on Alumina 1. Gravimetric and Infrared Spectroscopic Investigation", *J. Phys. Chem.* **82**, 1526-1532 (1978)

Knözinger, H. and C-P. Kaerlein, "A Test for the Development of Protonic Acidity in Alumina at Elevated Temperatures", *J. Catal.* **24**, 436-438 (1971)

Knözinger, H. and P. Ratnasamy, "Catalytic Aluminas : Surface Models and Characterization of Surface Sites", *Catal. Rev. –Sci. Eng.* **17(1)**, 31-70 (1978)

Krylov, O. V., "Mechanism of the Dehydration of Alcohols", *Russ. J. Phys. Chem.* **39**, 1422 (1965a)

Krylov, O. V., "Mechanism of the Dehydrogenation of Alcohols", *Russ. J. Phys. Chem.* **39**, 1554 (1965b)

Lok, B. M., C. A. Messina, R. L. Patton, R. T. Gajek, T. R. Cannan, and E. M. Flanigen, "Silicoaluminophosphate Molecular Sieves: Another New Class of Microporous Crystalline Inorganic Solids", *J. Am. Chem. Soc.* **106**, 6092-6093 (1984)

López, T., M. Asomoza and R. Gómez, "Catalytic Properties of Silico-Aluminates Prepared by the Sol-Gel Method : Isopropanol Dehydration", *J. Non-Cryst. Solids* **147-148**, 769-772 (1992)

Lowry, T. H. and K. S. Richardson, "Mechanism and Theory in Organic Chemistry", 2nd. Ed.. p. 531-542. Harper & Row, New York (1981)

Ludzack, F. J. and M. B. Ettinger, "Chemical Structures Resistant to Aerobic Biochemical Stabilization", *J. Wat. Pollut. Control Fed.* **32**, 1173-1200 (1960)

Luy, J. C. and J. M. Parera, "Acidity Control in Alcohol Dehydration", *Appl. Catal.* **26**, 295-304 (1986)

McKinney, R. E. and J. S. Jeris, "Metabolism of Low Molecular Weight Alcohols by Activated Sludge", *Sewage and Ind. Wastes*, **27**, 728-735 (1955)

Mishra, T., K. M. Parida and S. B. Rao, "Transition Metal Promoted $AlPO_4$ Catalyst 2. The Catalytic Activity of $M_{0.05}Al_{0.95}PO_4$ for Alcohol Conversion and Cumene Cracking/Dehydrogenation Reactions", *Appl. Catal. A.* **166**, 115-122 (1998)

Mostafa, M. R., A. M. Youssef and S. M. Hassan, "Conversion of Ethanol and Isopropanol on Alumina, Titania and Alumina-Titania Catalysts", *Mat. Letters* **12**, 207-213 (1991)

Nicolaides, C. P., C. J. Stotijn, E. R. A. van der Veen, and M. S. Visser, "Conversion of Methanol and Isobutanol to MTBE", *Appl. Catal.* **103**, 223-232 (1993)

Olson, D. H., W. O Haag and R. M. Lago, "Chemical and Physical Properties of the ZSM-5 Substitutional Series", *J. Catal.* **61**, 390-396 (1980)

Pines, H. and J. Manassen, "The Mechanism of Dehydration of Alcohols over Alumina Catalysts", *Advan. Catal.* **16**, 49-93 (1966)

Pines, H. and W. O. Haag, "Alumina : Catalyst and Support. IX. The Alumina Catalyzed Dehydration of Alcohols", *J. Am. Chem. Soc.* **83**, 2847-2852 (1961)

Saad, A. B. M., V. A. Ivanov, J. C. Lavalley, P. Nortier, and F. Luck, "Comparative Study of the Effects of Sodium Impurity and Amorphisation on the Lewis Acidity of γ-Alumina", *Appl. Catal. A.* **94**, 71-83 (1993)

Salas, P., J. G. Hernández, J. A. Montoya, J. Navarrete, J. Salmones, I. Schifter, and J. Morales, "Effect of Tin Content on Silica Mixed Oxides : Sulfated and Unsulfated Catalysts", *J. Mol. Catal. A.* **123**, 149-154 (1997)

Saracco, G. and L. Montanaro, "Catalytic Ceramic Filters for Flue Gas Cleaning. 1. Preparation and Characterization", *Ind. Eng. Chem. Res.* **34**, 1471-1479 (1995)

Saracco, G. and V. Specchia, "Catalytic Ceramic Filters for Flue Gas Cleaning. 2. Performance and Modeling Thereof", *Ind. Eng. Chem. Res.* **34**, 1480-1487 (1995a)

Saracco, G. and V. Specchia, "Studies on Sol-Gel Derived Catalytic Filters", *Chem. Eng. Sci.* **50**, 3385-3394 (1995b)

Shi, B. and B. H. Davis, "Alcohol Dehydration : Mechanism of Ether Formation using an Alumina Catalyst", *J. Catal.* **157**, 359-367 (1995)

Subramainam, C. and S. Bhatia, "Liquid Phase Synthesis of Methyl *tert*-Butyl Ether Catalyzed by Ion Exchange Resin", *Can. J. Chem. Eng.* **65**, 613-620 (1987)

Tanabe, K., "Solid Acids and Bases", Chap. 4. Kodansha, Tokyo and Academic Press, New York (1970)

Tanabe, K., H. Hattori, T. Yamaguchi, T. Iizuka, H. Matsuhashi, A. Kimura, and Y. Nagase, "Function of Metal Oxide and Complex Oxide Catalysts for Hydrocracking of Coal", *Fluid Proc. Technol.* **14**, 247-260 (1986)

Terzis, E., "Anaerobic Treatment of Industrial Wastewater Containing Organic Solvents", *Wat. Sci. Tech.* **29**, 321-329 (1994)

Thomas, C. L., "Chemistry of Cracking Catalysts", *Ind. Eng. Chem.* **41**, 2564-2572 (1949)

Thornton, R. and B. C. Gates, "Catalysis by Matrix-Bound Sulfonic Acid Groups: Olefin and Paraffin Formation from Butyl Alcohols", *J. Catal.* **34**, 275-287 (1974)

Wilson, S. T., B. M. Lok, C. A. Messina, T. R. Cannan, and E. M. Flanigen, "Aluminophosphate Molecular Sieves: A New Class of Microporous Crystalline Inorganic Solids", *J. Am. Chem. Soc.* **104**, 1146-1147 (1982)

Youssef, A. M., A. I. Ahmed and S. E. Samra, "Surface and Acidic Properties of Some Mixed Oxide Catalysts in Relation to Their Catalytic Activities", *Mat. Letters* **10**, 175-180 (1990)

Youssef, A. M., I. B. Khalil and B. S. Girgis, "Decomposition of Isopropanol on Magnesium Oxide/Silica in Relation to Texture, Acidity and Chemical Composition", *Appl. Catal. A*, **81**, 1-13 (1992)

Yue, P. L. and O. Olaofe, "Kinetic Analysis of the Catalytic Dehydration of Alcohols over Zeolites", *Chem. Eng. Res. Des.* **62**, 81-91 (1984a)

Yue, P. L. and O. Olaofe, "Molecular Sieving Effects of Zeolites in the Dehydration of Alcohols", *Chem. Eng. Res. Des.* **62**, 167-172 (1984b)

Chapter 2

Experimental

2.1 – Experimental Apparatus

All experimental runs were conducted in a batch slurry reactor system (Figure 2.1). The reactor was a high pressure Parr reactor (Model 4841, Parr Instruments Inc. USA) made of SS-316 stainless steel. The vessel had a volume of 320 mL and was equipped with an impeller. A thermocouple (J-type) was used to measure the reactor temperature and provide feedback to the heater/controller. The heating device/controller was used to maintain a constant reactor temperature within ± 1 K. The liquid sampling line consisted of a 1/8-inch o.d. stainless steel tube connected to a stainless steel sampling valve. A pressure transducer (Foxboro electronic transmitter, Model 841 GM-D) measured the reactor pressure at an accuracy of ± 6.89 kPa.

2.2 – Analysis Techniques and Experimental Procedure

The liquid samples were analyzed using a Hewlett Packard 5890 Series II Gas Chromatograph with a TCD detector. A 0.914 m long column with Poropak R packing (mesh 50-80) was used to separate 2-propanol, water, diisopropyl ether, and acetone. Despite the formation of propylene as a dehydration product, propylene was not analyzed in the liquid-phase by gas chromatography due to its low solubility in 2-propanol. The column temperature was kept constant at 423 K.

During the kinetic runs, a known amount of 2-propanol (analytical grade, BDH), deionized water and dried catalyst were fed to the reactor. The 2-propanol/water mixture corresponds to a 2-propanol concentration between 4 – 10 mol %. This concentration range was chosen to represent the concentrations one might expect to find in a typical

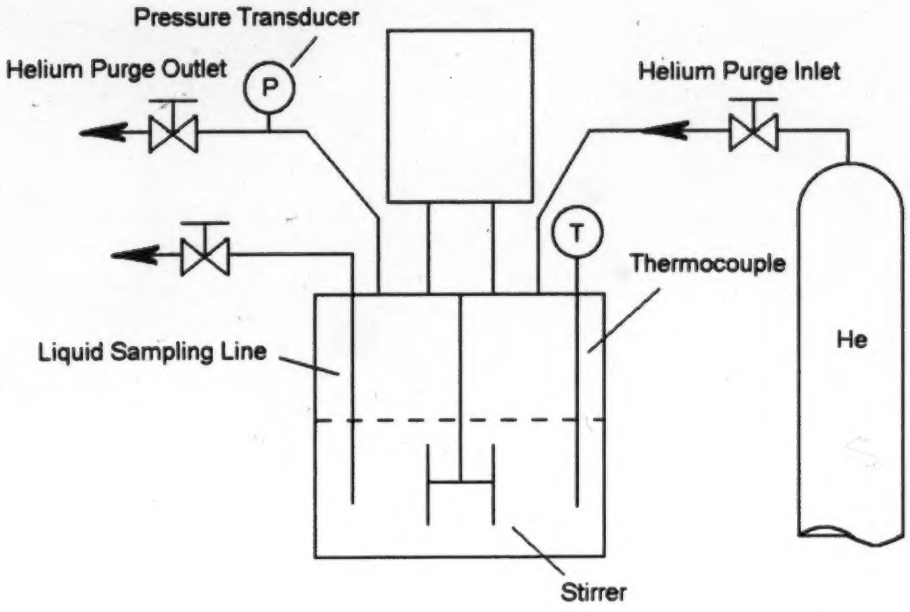

Figure 2.1 – Experimental Setup

wastewater stream, where 2-propanol will be present in low concentrations. Typically, 150 mL of the 2-propanol/water mixture was added to the reactor so that approximately one half of the vessel was initially filled with the liquid. The liquid expands at high temperatures, hence room must be allocated in the vessel for this expansion.

The reactor was then purged with helium to remove air that might be present initially in the reactor. Despite the fact that the catalytic reaction only occurs in the liquid phase, we wish to minimize any possible reactions of the olefin product with air at high-temperatures. For this reason, helium was used to provide an inert atmosphere.

The inlet and outlet of the reactor were then closed. The amount of helium initially present in the reactor prior to heating can be determined based on the initial reactor temperature, pressure and vapor volume. The amount (moles) of helium initially present in the reactor is necessary in performing the material balance on the reactor in determining the reaction rate (see Chapter 3).

The reactor contents were then heated to the desired reaction temperature, between 434 and 463 K. It will be later shown (Chapter 4, section 4.2) that there is a negligible amount of reaction product produced during the heating time. This temperature range was chosen for three reasons. First, 434 K appears to be the minimum temperature at which there is a noticeable amount of propylene produced in a reasonable time period (1.5 hours). Second, because accurate pressure measurements are essential in the determination of the reaction rate (Chapter 3), we are limited to reactor pressures less than 4238 kPa, the range of accuracy of the pressure transducer. For this reason, a maximum temperature of 463 K was chosen so that this maximum pressure was not exceeded. Finally, the liquid-phase catalytic reaction may not be industrially feasible at

temperatures exceeding 463 K due to the high pressure required to liquefy most of the reactants.

The reactor contents were stirred at 1080 rpm for 1.5 to 2.5 hours. The stirrer speed was chosen to minimize the influence of external mass transfer, which will be later discussed (Chapter 4, section 4.3). During the catalyst screening tests, a small sample of liquid (~ 1 mL) was taken every half-hour and analyzed by gas chromatography.

Chapter 3

Kinetic Modeling

3.1 – Determination of the Rate of Formation of Propylene

The rate of propylene formation per gram of catalyst in a batch slurry reactor can be written in the following manner:

$$r = \frac{1}{m_C}\frac{d\alpha}{dt} = f(C_A, C_W, T) \qquad (3.1.1)$$

where α is the cumulative amount of propylene produced, m_C is the mass of catalyst, C_A is the liquid-phase 2-propanol concentration and C_W is the liquid-phase water concentration.

The batch slurry reactor consists of a liquid phase, where 2-propanol reacts over the suspended solid catalyst to form dehydration products and a vapor phase, where the reactants, products and inerts will be present. Since the dehydration occurs only in the liquid phase, 2-propanol, water and product propylene can be assumed to be at their vapor-liquid equilibrium at any given reaction time, t.

If the vapor and liquid phases are in equilibrium, the liquid and vapor phase fugacity of component, i, are equal:

$$\hat{f}_i^V = \hat{f}_i^L \qquad (3.1.2)$$

Theoretically, the above equation can be solved by the use of an equation of state. However, the use of a single equation of state to calculate the vapor-liquid equilibria is reserved for highly ideal systems containing nonpolar compounds. For non-ideal systems such as alcohol/water systems, a "dual method" is often used to compute the phase equilibria. An equation of state is used to model the vapor phase where non-idealities are

not severe and an excess Gibbs free energy model along with vapor-pressure data is used to compute the liquid phase fugacity. The liquid and vapor phase fugacities in equation 3.1.2 can be rewritten in terms of total pressure, P, and the fugacity coefficient, ϕ as

$$\hat{f}_i^V = f_i^{0V} y_i \tag{3.1.3}$$

and

$$\hat{f}_i^L = f_i^{0L} \gamma_i x_i \tag{3.1.4}$$

where

$$\phi_i^0 = \frac{f_i^0}{P} \tag{3.1.5}$$

Equation 3.1.3 – 3.1.5 can be substituted into equation 3.1.2 to yield the following relationship for the vapor-liquid equilibrium for a component i:

$$P\phi_i^V y_i = P\phi_i^{0L} \gamma_i x_i \tag{3.1.6}$$

As the total pressure approaches zero, the vapor-phase fugacity coefficient ϕ_i^V approaches 1 and the value of $P\phi_i^{0L}$ approaches the saturation vapor pressure P_i^{SAT}. At low pressures, equation 3.1.6 simplifies to:

$$P y_i = P_i^{SAT} \gamma_i x_i \tag{3.1.7}$$

A modified Peng-Robinson equation of state (PRSV), developed by Stryjek and Vera (1986) is able to reproduce vapor pressures of nonpolar, polar or associating compounds by calculating the product $P\phi_i^{0L}$. The authors report a reproducibility of vapor pressures down to 1.5 kPa, which is comparable to what can be calculated from Antoine equations. For this reason, the PRSV equation of state was used in calculating the liquid-phase fugacity coefficient for a pure component ϕ_i^{0L}. In general, most cubic

equations of state are considered to be able to reasonably describe the vapor-phase. For this reason the PRSV equation of state was used to calculate the vapor-phase fugacity coefficient for a component in a gas mixture ϕ_i^v.

The Peng-Robinson equation of state [Peng and Robinson, 1976] is of the form:

$$P = \frac{RT}{v - b} - \frac{a}{v^2 + 2bv - b^2} \tag{3.1.8}$$

with

$$a = \left(0.457235R^2T_C^2 / P_C\right)\alpha \tag{3.1.9}$$

and

$$b = 0.077796R\,T_C / P_C \tag{3.1.10}$$

The form proposed by Soave (1972) was used in determining α.

$$\alpha = \left[1 + \kappa\left(1 - T_R^{0.5}\right)\right]^2 \tag{3.1.11}$$

In the PRSV equation of state, the model parameter κ is considered to be a function of the accentric factor ω and temperature:

$$\kappa = \kappa_0 + \kappa_1\left(1 + T_R^{0.5}\right)\left(0.7 - T_R\right) \tag{3.1.12}$$

with

$$\kappa_0 = 0.378893 + 1.4897153\omega - 0.17131848\omega^2 + 0.0196554\omega^3 \tag{3.1.13}$$

Table 3.1 gives the values of T_C, P_C, ω and κ_1 for water, 2-propanol, propylene and helium.

For computational convenience, equation 3.1.8 can be rewritten in terms of the compressibility factor Z [Kyle, 1992]:

$$Z^3 + (B-1)Z^2 + (A - 3B^2 - 2B)Z + (B^3 + B^2 - AB) = 0 \qquad (3.1.14)$$

with

$$A = Pa/(RT)^2 \qquad (3.1.15)$$

and

$$B = Pb/RT \qquad (3.1.16)$$

For a gas-mixture, the following conventional mixing rules were used [Stryjek and Vera, 1986]:

$$b = \sum y_i b_i \qquad (3.1.17)$$

and

$$a = \sum y_i y_j a_{ij} \qquad (3.1.18)$$

with

$$a_{ij} = (a_i a_j)^{0.5}(1 - k_{ij}) \qquad (3.1.19)$$

The binary interaction parameter k_{ij} is set to zero because the non-idealities associated with polar compounds and their mixtures are not as pronounced in the vapor-phase as in the liquid-phase. When the temperature and pressure are fixed, equation 3.1.8 can be solved for the molar volume υ. Below the critical temperature, equation 3.1.8 has three real roots. The smallest and largest roots correspond to the liquid and vapor saturated molar volumes, respectively. When using a cubic equation of state to represent the P-υ isotherm for $T < T_C$, the region between υ_L and υ_G is unstable. A cubic equation of state is too simple to be able to accurately represent the P-υ isotherm for the liquid-vapor region and for this reason the calculated value of υ between υ_L and υ_G has no physical significance. When using equation 3.1.14 to solve for the compressibility factor, Z, the

smallest and largest roots correspond to the liquid and vapor phase respectively. These roots are used in calculating the fugacity coefficient ϕ.

For a pressure-explicit equation of state, the fugacity coefficient for a component in a gas mixture is written mathematically as [Kyle, 1992]:

$$\ln\phi_i^V = \frac{1}{RT}\int_v^\infty \left[\left(\frac{\delta P}{\delta n_i}\right)_{T,V,n_j} - \frac{RT}{v}\right] dv - \ln Z^G \qquad (3.1.20)$$

When evaluated with the PRSV equation of state, this equation yields:

$$\ln\phi_i^V = \frac{A}{2\sqrt{2}\,B}\left[\frac{B_i}{B} - \frac{2\sum_{j=1}^{C} y_i A_{ij}}{A}\right]\ln\left[\frac{Z^G + (1+\sqrt{2})B}{Z^G + (1-\sqrt{2})B}\right] + \frac{B_i}{B}(Z^G - 1) - \ln(Z^G - B) \qquad (3.1.21)$$

The liquid-phase fugacity coefficient for a pure component is written mathematically for a pressure-explicit equation of state as [Kyle, 1992]

$$\ln\phi_i^{0L} = Z_i^L - 1 - \ln Z_i^L + \frac{1}{RT}\int_{v_i}^\infty \left[P - \frac{RT}{v_i}\right] dv_i\,, \qquad (3.1.22)$$

which, when combined with the PRSV equation of state, yields

$$\ln\phi_i^{0L} = Z_i^L - 1 - \ln(Z_i^L - B_i) - \frac{A_i}{2\sqrt{2}B_i}\ln\left[\frac{Z_i^L + (1+\sqrt{2})B_i}{Z_i^L + (1-\sqrt{2})B_i}\right] \qquad (3.1.23)$$

As mentioned previously, an equation of state is not sufficient to describe the vapor-liquid equilibria for systems containing a mixture of polar compounds. The activity coefficient, γ_i, which is dependent on the liquid-phase composition and temperature must be determined experimentally. The compositional dependency of the activity coefficient is often modeled by making use of an excess Gibbs free energy model.

There are several excess Gibbs free energy models with varying degrees of sophistication. Of the more notable models, the van Laar, Margules [Wohl, 1946], Wilson [Wilson, 1963], NRTL [Renon and Prausnitz, 1968] and the UNIQUAC [Abrams and Prausnitz, 1975] models are often used in modeling the activity coefficients of binary and/or multicomponent mixtures. These models are semi-empirical and require experimental data to fit the model parameters. Unfortunately, vapor-liquid-equilibria data for 2-propanol/water mixtures at elevated temperatures are not readily available, hence experiments were performed to determine these empirical constants.

The van Laar model was used due to its simplicity and accuracy in modeling 2-propanol/water vapor-liquid equilibria [Bergmann and Eckert, 1991]. The van Laar excess Gibbs free energy model is written as:

$$\ln \gamma_i = \frac{C_{ij}}{\left[1 + \frac{C_{ij} x_i}{C_{ji} x_j}\right]^2} \tag{3.1.24}$$

The binary interaction parameters C_{12} and C_{21} (1 = 2-propanol, 2 = water) were determined at different temperatures by fitting pressure-liquid composition diagrams. The following function was minimized over the range of 2-propanol concentration at a constant temperature using non-linear least squares regression:

$$\varepsilon = P_{EXP}(1 - y_H) - P_{EXP}\frac{\phi_A^{0L}\gamma_A}{\phi_A^V}x_A - P_{EXP}\frac{\phi_W^{0L}\gamma_W}{\phi_W^V}(1 - x_A) \tag{3.1.25}$$

The temperature dependency of the van Laar binary parameters can be thermodynamically derived by taking the limits of equation 3.1.24 as component x_i approaches zero:

$$(\ln \gamma_i)_{x_i=0} = C_{ij} \tag{3.1.26}$$

The activity coefficient of component, i, approaches a definite limit as x_i becomes smaller and smaller. This limit is often called the limiting activity coefficient at infinite dilution. The governing thermodynamic relationship for the limiting activity coefficient at infinite dilution is:

$$\left[\frac{\delta \ln \gamma_i^{\infty}}{\delta (1/T)}\right]_{P,x} = \frac{h_i^{E\infty}}{R} \qquad (3.1.27)$$

Over a small temperature range, the excess enthalpy at infinite dilution is considered to be relatively constant. A plot of C_{ij} versus 1/T should yield a straight line. Despite the validity of equation 3.1.27, it is not a common practice to determine the excess enthalpy or the limiting activity coefficient at infinite dilution with the above method, i.e. fitting pressure-composition data with an excess Gibbs free energy model. An accurate determination of these limiting parameters is outside the scope of this thesis and is detailed elsewhere [Bergmann and Eckert, 1991; Slocum and Dodge, 1964; Trampe and Eckert, 1990; 1991]. With the binary parameters of the van Laar equation known, the vapor-liquid equilibrium can be completely described.

The amount of diisopropyl ether and acetone formed during the dehydration reaction was assumed to be negligible compared to the amount of propylene produced and will be present in the wastewater in small amounts. The solubility of propylene at elevated temperatures is small enough to be negligible. From the previous statements, the following equation can be written to describe the liquid-phase composition:

$$x_W = 1 - x_A \qquad (3.1.28)$$

The cumulative moles of propylene (α) formed at reaction time t can thus be obtained from the reaction stoichiometry and the overall material balance:

$$V = M_{T0} + \alpha - L \tag{3.1.29}$$

From the component balance of helium and propylene and from equation 3.1.29, the vapor phase mole fractions of helium and propylene are:

$$y_P = \frac{\alpha}{M_{T0} + \alpha - L} \tag{3.1.30}$$

$$y_H = \frac{M_H}{M_{T0} + \alpha - L} \tag{3.1.31}$$

The relationship between the liquid-composition (2-propanol and water) with their vapor counterparts is illustrated in equations 3.1.6, 3.1.21, 3.1.23 and 3.1.24. The reaction temperature T and the reactor pressure P are easily measured and are known to high accuracy at any time t. To be able to completely describe the reactor contents, we need to know, in addition, x_A, y_A, y_W, L, α, and Z^G. The following outlines the set of non-linear equations, which must be solved for each data point.

Compressibility Factor Z

Equation 3.1.10 must be solved for the largest root, which yields Z^G. PRSV parameters A and B are functions of the vapor-composition as well, making the equation highly non-linear.

Water Component Balance

Either the component balance for 2-propanol or the component balance for water needs to be included to describe the system. From the overall material balance and the reaction stoichiometry, the component balance for water is:

$$L(1 - x_A) + (M_{T0} + \alpha - L)y_W = M_{W0} + \alpha \tag{3.1.32}$$

Vapor-Liquid Equilibrium for 2-Propanol and Water

Making use of the PRSV equation of state and the experimentally determined van Laar parameters, the relationship between the liquid-phase components and their vapor-phase counterparts are written as:

$$y_A \phi_A^V = x_A \gamma_A \phi_A^{0L} \tag{3.1.33}$$

$$y_W \phi_W^V = (1 - x_A) \gamma_A \phi_W^{0L} \tag{3.1.34}$$

Vapor-Phase Component Balance

From equations 3.1.30, 3.1.31 and the overall vapor-phase balance, the following equation can be obtained:

$$y_A + y_W + \frac{\alpha + M_H}{M_{T0} + \alpha - L} = 1 \tag{3.1.35}$$

Equation of State for a Closed System

The final equation is derived from the physical limits imposed by the batch reactor itself. A relationship between the reactor pressure, the vapor volume (hence the liquid volume) and the moles of vapor in the vessel can be evaluated using the following equation of state:

$$P \cdot 10^3 \left[319 \cdot 10^{-6} - L \left(\frac{x_A Mw_A}{\rho_A \cdot 10^6} + \frac{(1 - x_A) Mw_W}{\rho_W \cdot 10^6} \right) \right] = ZRT(M_{T0} + \alpha - L) \tag{3.1.36}$$

The saturated liquid densities ρ_A and ρ_W can be calculated using the COSTALD correlation [Hankinson and Thomson, 1979]. The COSTALD correlation is summarized below

$$\frac{V_S}{V^0} = V_R^{(0)} \left[1 - \omega_{SRK} V_R^{(\delta)} \right] \tag{3.1.37}$$

with

$$V_R^{(0)} = 1 + a(1 - T_R)^{1/3} + b(1 - T_R)^{2/3} + c(1 - T_R) + d(1 - T_R)^{4/3} \quad (3.1.38)$$

and

$$V_R^{(\delta)} = \frac{e + f \cdot T_R + g \cdot T_R^{\,2} + h \cdot T_R^{\,3}}{T_R - 1.00001} \quad (3.1.39)$$

Characteristic volumes V^0 and accentric factors from the Soave equation of state ω_{SRK} are given in Table 3.1. The empirical parameters for equations 3.1.38 and 3.1.39 (a - h) are given in Table 3.2. The above set of non-linear equations can be solved numerically using a commercial package (Maple V). The Maple V worksheet used to solve these equations is found in Appendix A1.

From the above analysis, the rate of reaction can thus be described using only pressure and temperature data. As many data points can be taken as required without influencing the reactor condition. The only requirement of using such a method is to have adequate vapor-liquid equilibrium (VLE) data at our disposal. Since VLE data for 2-propanol/water at elevated temperatures greater than 413 K are not readily available, experiments were performed to acquire the required information.

3.2 – Determination of the Rate Equation

The Langmuir-Hinshelwood-Hougen-Watson (LHHW) method of generating rate models based on Langmuir adsorption is often used in developing rate models for heterogeneous catalytic reactions. This model assumes that the adsorbed species are attached to the catalyst surface at definite sites and each active site can only accommodate one adsorbed species. The energy of all the adsorbed species is the same and is independent of the presence or absence of adsorbed species on adjacent sites.

Several LHHW models were developed for catalytic dehydration of 2-propanol in the liquid phase. The adsorption/desorption of 2-propanol and/or water was assumed to either occur via a single-site mode, where acid sites are involved or a dual-site mode, where both acid and basic sites are involved. As well, the rate of propylene formation was considered to be either inhibited or unaffected by the presence of water. For all models derived, the reaction was considered to be irreversible. The validity of this assumption will be further discussed in Chapter 4. In all models, A, W, P, and S represent 2-propanol, water, propylene and the active surface site respectively. The LHHW rate models are derived below.

3.2.1 – Single-Site Mode Adsorption with the Water Term Excluded (SSM-1)

The SSM-1 model involves the chemisorption of 2-propanol on an active site and a surface reaction to form 2-propanol and adsorbed water. In this model, fast desorption of water was assumed, hence water will occupy no active sites during the reaction. Only the forward reaction to form propylene and water will be considered. This model is represented by the following mechanism:

$$A + S \leftrightarrow A \cdot S \qquad \text{(Step 1, chemisorption of 2-propanol)}$$

$$A \cdot S \leftrightarrow W \cdot S + P(g) \qquad \text{(Step 2, surface reaction)}$$

$$W \cdot S \leftrightarrow W + S \qquad \text{(Step 3, desorption of water)}$$

It can be seen that propylene is not an adsorbed entity, which is consistent with other mechanisms previously developed for 2-propanol dehydration in the vapor phase over solid acid catalysts [Youssef et al., 1992]. Let the surface reaction, Step 2, be the rate-determining step, the overall rate of propylene formation can be expressed in terms of the fraction of sites occupied by adsorbed 2-propanol θ_A:

$$(-r_A) = r_S = k_S \theta_A \tag{3.2.1}$$

The rate of adsorption of 2-propanol is given by the Langmuir model as:

$$r_{ads(A)} = k_{a(A)} C_A \theta_V - k_{d(A)} \theta_A \tag{3.2.2}$$

where the fraction of active sites which are vacant, θ_V, can be expressed as:

$$\theta_V = 1 - \theta_A \tag{3.2.3}$$

In the LHHW method of developing kinetic equations, one step is considered to be rate-determining, all other steps are considered to be at equilibrium. In this model, the rate of 2-propanol adsorption is considered to be at equilibrium. Setting equation 3.2.2 equal to zero yields:

$$\theta_A = K_A C_A \theta_V, \tag{3.2.4}$$

where the equilibrium adsorption constant for 2-propanol K_A is defined as:

$$K_A = \frac{k_{a(A)}}{k_{d(A)}} \tag{3.2.5}$$

From equation 3.2.3, the fraction of active sites occupied by 2-propanol can be written as:

$$\theta_A = \frac{K_A C_A}{1 + K_A C_A} \tag{3.2.6}$$

Substituting equation 3.2.6 into equation 3.2.1 yields the SSM-1 kinetic model:

$$r_S = \frac{k_S K_A C_A}{1 + K_A C_A} \tag{3.2.7}$$

3.2.2 – Single-Site Mode Adsorption with the Water Term Included (SSM-2)

The catalytic dehydration mechanism is similar to what was proposed for the SSM-1 model previously derived. The only exception is that the desorption of water is

not instantaneous, hence adsorbed water occupies active sites which are necessary for 2-propanol dehydration which inhibits the reaction. The adsorption/desorption of both 2-propanol and water are considered to be at equilibrium. The fraction of active sites occupied by water can be written as:

$$\theta_W = K_W C_W \theta_V \tag{3.2.8}$$

The fraction of active sites occupied by 2-propanol is the same as in equation 3.2.4. The fraction of vacant active sites is written as:

$$\theta_V = 1 - \theta_A - \theta_W \tag{3.2.9}$$

Making use of equations 3.2.4, 3.2.8 and 3.2.9, the fraction of vacant active sites can be written as:

$$\theta_V = \frac{1}{1 + K_A C_A + K_W C_W} \tag{3.2.10}$$

Substituting equation 3.2.10 into 3.2.4 and 3.2.1 yields the SSM-2 model:

$$r_S = \frac{k_S K_A C_A}{1 + K_A C_A + K_W C_W} \tag{3.2.11}$$

3.2.3 – Dual-Site Mode Adsorption with the Water Term Excluded (DSM-1)

It has been proposed in the literature that the catalytic dehydration over a solid acid catalyst, notably metal oxides, require both acidic and basic sites [Youssef et al., 1992]. 2-Propanol dissociatively adsorbs on an acidic site and a neighboring basic site. Figure 1.1 illustrates this proposed mechanism for olefin formation.

The previous two models assumed that 2-propanol adsorbs only on one type of surface site, i.e. acid site. The following dual-site models attempts to incorporate the above mechanism where both acid and basic sites are involved.

The so-called "dual-site" model, developed by Hougen and Watson (1947), is summarized by the following steps:

$A + S \leftrightarrow A \cdot S$ (Step 1,chemisorption of 2-propanol)

$A \cdot S + S \leftrightarrow W \cdot S + P \cdot S$ (Step 2, surface reaction)

$P \cdot S \leftrightarrow P + S$ (Step 3, desorption of propylene)

$W \cdot S \leftrightarrow W + S$ (Step 4, desorption of water)

In the DSM-1 model, adsorbed 2-propanol reacts with an adjacent vacant site to produced adsorbed water and propylene. Although the above steps do not strictly adhere to the E_2 mechanism proposed in the literature, it has found use in the literature to model 2-propanol dehydration in the vapor phase [Yue and Oloafe, 1984]. In the proposed "dual site" mechanism, two adsorption sites are required for propylene formation although the sites themselves do not differ from one another. This assumption is quite different from the E_2 mechanism where acid and basic sites differ substantially from one another.

Since propylene is assumed to be a vapor-phase product, fast desorption of propylene will be assumed for the derived dual site models. In the DSM-1 model, fast desorption is assumed for water, hence water will not occupy any active sites during the reaction. The rate of propylene formation is written in the following manner:

$$(-r_A) = r_S = k_S \theta_A \theta_V \qquad (3.2.12)$$

The rate of adsorption of 2-propanol on the acid catalyst surface is written in the same manner as in equation 3.2.2. The fraction of sites that contain adsorbed 2-propanol and the fraction of vacant sites are derived in the same manner as in the SSM-1 model and are written as:

$$\theta_V = \frac{1}{1 + K_A C_A} \tag{3.2.13}$$

$$\theta_A = \frac{K_A C_A}{1 + K_A C_A} \tag{3.2.14}$$

Making use of equations 3.2.12 – 3.2.14, the DSM-1 rate model was derived as:

$$r_S = \frac{k_S K_A C_A}{(1 + K_A C_A)^2} \tag{3.2.15}$$

3.2.4 – Dual-Site Mode Adsorption with the Water Term Included (DSM-2)

In this model, 2-propanol dissociatively adsorbs on to an acid and basic site and reacts to form propylene and water. The adsorption/desorption of water on the active sites inhibits the rate of propylene formation by occupying active sites necessary for propylene formation. The model is derived in a similar manner as in the DSM-1 model, except the fraction of sites occupied by water θ_W is included in the mechanism. Making use of equations 3.2.4, 3.2.10 and 3.2.12, the DSM-2 model was derived as:

$$r_S = \frac{k_S K_A C_A}{(1 + K_A C_A + K_W C_W)^2} \tag{3.2.16}$$

Models SSM-1, SSM-2, DSM-1 and DSM-2, expressed mathematically in equations 3.2.7, 3.2.11, 3.2.15 and 3.2.16 respectively, will be used in the model screening procedure. Mathematically, the single-site and dual-site models differ by the exponent in the denominator. For models SSM-2 and DSM-2, the rate of propylene formation is inhibited by the adsorption/desorption of water on the active sites. The rate constant for the surface reaction should follow an Arrhenius type temperature dependency. The temperature dependence of the adsorption/desorption equilibrium

constant K_i can be expressed in terms of the van't Hoff equation. The temperature dependence of the kinetic and adsorption parameters can be expressed mathematically as:

$$k_S = k_S^0 \exp\left(\frac{-E_A}{RT}\right) \tag{3.2.17}$$

$$K_i = K_i^0 \exp\left(\frac{-\Delta H_{A,i}}{RT}\right) \tag{3.2.18}$$

The above parameters were determined by fitting the LHHW models with experimental rate data. The rate equation is integrated numerically with the trapezoidal rule and the model parameters were determined from least-squares non-linear regression. The error to be minimized is written as:

$$\varepsilon = \frac{\alpha_t - \alpha_0}{m_C} - \int_0^t f(t)\,dt, \tag{3.2.19}$$

where f(t) are the models expressed in equations 3.2.7, 3.2.11, 3.2.15, and 3.2.16. For each data point, the absolute value of the error function, ε, is determined. The summation of these absolute errors over the set of data points was minimized using the Solver option in Microsoft Excel 2000. The solver method chosen for the minimization procedure was the "Standard GRG Non-linear" method. The search direction method was chosen through an estimation method, because using the pure form of Newton's method is far too expensive. A quasi-Newton (or BFGS) method, which maintains an approximation to the Hessian matrix, was used instead. The derivatives were determined using a forward difference approximation. Estimations for the forward difference approximation method were determined using the "tangent" method, which uses linear extrapolation from the line tangent to the reduced objective function. For these models, the liquid phase concentration C_i is expressed as:

$$C_i = \frac{x_i}{\sum \frac{x_i Mw_i}{\rho_i \cdot 10^3}} \qquad (3.2.20)$$

3.3 – Nomenclature

a, b = equation of state parameters for the PRSV equation of state

A, B = dimensionless terms, $A = Pa/(RT)^2$; $B = Pb/RT$

a – h = parameters for the COSTALD correlation

C = binary constant for the van Laar equation

= liquid phase concentration of component, mole L^{-1}

E_A = activation energy, kJ $mole^{-1}$

f = fugacity of component, kPa

ΔH_A = heat of adsorption, kJ $mole^{-1}$

h_i^{∞} = partial molar excess enthalpy of component i at infinite dilution, kJ $mole^{-1}$

k = binary interaction parameter for the PRSV equation of state

= rate constant for 2-propanol dehydration, moles g^{-1} min^{-1}

K = adsorption/desorption equilibrium constant, L $mole^{-1}$

k^0 = pre-exponential factor for the rate constant, mole g^{-1} min^{-1}

K^0 = adsorption/desorption pre-exponential factor, L $mole^{-1}$

L = moles of liquid, mole

m = mass, g

M = moles of component prior to reaction, mole

Mw = molecular weight of component, g / mole

n = number of moles, mole

P = pressure, kPa

r = rate of formation, mole g^{-1} min^{-1}

R = gas constant, 8.31451 J $mole^{-1}$ K^{-1}

t = time, min

T = temperature, K

V = moles of vapor, mole

$V_R^{(0)}$ = corresponding states function for normal fluids (COSTALD)

$V_R^{(\delta)}$ = deviation function for COSTALD correlation

V_S = saturated liquid volume, L $mole^{-1}$

V^0 = characteristic volume, L $mole^{-1}$

x = liquid mole fraction

y = vapor mole fraction

Z = compressibility factor

Greek Letters

α = cumulative amount of propylene produced at time t, mole

= function of reduced temperature and accentric factor (Soave)

ε = error in regression fit, mole; kPa

ϕ = fugacity coefficient

γ = activity coefficient

κ = function of reduced temperature and accentric factor (PRSV)

κ_0 = function of accentric factor

κ_1 = pure compound parameter

θ_i = fraction of active sites occupied by component i

θ_V = fraction of vacant sites

ρ = saturated liquid density, g mL^{-1}

Σ = summation

ν = molar volume, m^3 $mole^{-1}$

ω = accentric factor

ω_{SRK} = accentric factor from the Soave equation of state

Subscripts

0 = initial, t = 0

a = adsorption

A = 2-propanol

C = at critical conditions

= catalyst

d = desorption

EXP = experimental

H = helium

i, j = component

P = propylene

R = reduced

S = at catalyst surface

SAT = at saturated conditions

T = total

W = water

Superscripts

0 = pure phase

∞ = infinite dilution

G = gas phase

L = liquid phase

V = vapor phase

Table 3.1 – Critical Constants of Reactants, Products and Inerts

Component	Tc (K)	Pc (kPa)	κ1	ω	ω_{SRK}	V^0 ($L\ mole^{-1}$)
2-Propanol	508.4	4764.25	0.23264	0.66372	0.6637	0.2313
Water	647.286	22089.75	-0.06635	0.3438	-0.65445	0.043567
Propylene	365.57	4664.55	0.044	0.1408	0.1455	0.1829
Helium	5.3	228.99	-	-0.365	-0.4766	0.05457

Table 3.2 – COSTALD Correlation Parameters

a	-1.52816
b	1.43907
c	-0.81446
d	0.190454
e	-0.29612
f	0.386914
g	-0.04273
h	-0.04806

3.4 – Literature Cited

Abrams, D. S. and J. M. Prausnitz, "Statistical Thermodynamics of Liquid Mixtures : A New Expression for the Excess Gibbs Energy of Partly or Completely Miscible Systems", *AIChE J.* **21**, 116-128 (1975)

Bergmann, D. L. and C. A. Eckert, "Measurement of Limiting Activity Coefficients for Aqueous Systems by Differential Ebulliometry", *Fluid Phase Equilibria* **63**, 141-150 (1991)

Hankinson, R. W. and G. H. Thomson, "A New Correlation for Saturated Densities of Liquids and Their Mixtures", *AIChE J.* **25**, 653-663 (1979)

Hougen, O. A. and K. M. Watson, "Chemical Process Principles", Part 3, John Wiley and Sons, New York (1947)

Kyle, B. G., "Chemical and Process Thermodynamics", 2nd Ed., Prentice Hall, Englewood Cliffs (1992)

Peng, D. Y. and D. B. Robinson, "A New Two-constant Equation of State", *Ind. Eng. Chem. Fund.* **15**, 59-64 (1976)

Renon, H. and J. M. Prausnitz, "Local Composition in Thermodynamic Excess Functions for Liquid Mixtures", *AIChE J.* **14**, 135-144 (1968)

Slocum, E. W. and B. F. Dodge, "Activity Coefficients at Infinite Dilution : 2-Propanol – Water System", *AIChE J.* **10**, 364-368 (1964)

Soave, G., "Equilibrium Constants from a Modified Redlich-Kwong Equation of State", *Chem. Eng. Sci.* **27**, 1197-1203 (1972)

Stryjek, R. and J. H. Vera, "PRSV: An Improved Peng-Robinson Equation of State for Pure Compounds and Mixtures", *Can. J. Chem. Eng.* **64**, 323-333 (1986)

Trampe, D. M. and C. A. Eckert, "Calorimetric Measurement of Partial Molar Excess Enthalpies at Infinite Dilution", *J. Chem. Eng. Data* **36**, 112-118 (1991)

Trampe, D. M. and C. A. Eckert, "Limiting Activity Coefficients from an Improved Differential Boiling Point Technique", *J. Chem. Eng. Data* **35**, 156-162 (1990)

Wilson, G. M., "Vapor-Liquid Equilibrium. XI. A New Expression for the Excess Free Energy of Mixing", *J. Am. Chem. Soc.* **86**, 127-130 (1964)

Wohl, K., "Thermodynamic Evaluation of Binary and Ternary Liquid Systems", *Trans. AI ChE* **42**, 215-249 (1946)

Youssef, A. M., I. B. Khalil and B. S. Girgis, "Decomposition of Isopropanol on Magnesium Oxide/Silica in Relation to Texture, Acidity and Chemical Composition", *Appl. Catal. A* **81**, 1-13 (1992)

Yue, P. L. and O. Oloafe, "Kinetic Analysis of the Catalytic Dehydration of Alcohols over Zeolites", *Chem. Eng. Res. Des.* **62**, 81-91 (1984)

Chapter 4

Experimental Results and Discussion

4.1 – Determination of the Vapor-Liquid Equilibria for 2-Propanol/Water System

Total pressure-liquid composition data were collected over a temperature range of 433 to 463 K with a 2-propanol concentration range of 2 – 10 mol % using a procedure similar to that described in Chapter 2, but without added catalyst. Making use of appropriate material balances, the binary parameters for the van Laar equation can be determined from the total pressure at a particular temperature and the initial amounts of 2-propanol, water and helium added to the reactor. The following details the methods used to accomplish this. The liquid phase will contain only water and 2-propanol, since no reaction will occur when the catalyst is absent.

$$x_W = 1 - x_A \tag{4.1.1}$$

The liquid-phase 2-propanol mole fraction can be written in terms of the vapor-phase mole fraction y_A and the total moles of liquid, L, at equilibrium by making use of the total material balance for the system and the component balance for 2-propanol:

$$x_A = \frac{M_{A0} - (M_{T0} - L)y_A}{L} \tag{4.1.2}$$

The vapor-phase water mole fraction can also be written in terms of the vapor-phase 2-propanol mole fraction y_A and the total moles of liquid, L, at equilibrium by making use of the helium component balance, the overall material balance and the vapor-phase material balance:

$$y_W = 1 - y_A - \frac{M_H}{M_{T0} - L} \tag{4.1.3}$$

If the binary parameters of the van Laar equation C_{12} and C_{21} are known (see equation 3.1.24), the equilibrium value of y_A and L can be determined by making use of the vapor liquid equilibrium of 2-propanol/water and an appropriate equation of state for a closed system. These two minimization equations will be referred to as f_1 and f_2

Vapor-Liquid Equilibria for 2-Propanol

$$f_1 = y_A - \left(\frac{\phi_A^{0L}}{\phi_A^{V}}\right) \exp\left[\frac{C_{12}}{\left(1+\frac{C_{12}x_A}{C_{21}(1-x_A)}\right)^2}\right] x_A \qquad (4.1.4)$$

Equation of State for a Closed System

$$f_2 = P\cdot 10^3\left[319\cdot 10^{-6} - L\left(\frac{x_A Mw_A}{\rho_A\cdot 10^6} + \frac{(1-x_A)Mw_W}{\rho_W\cdot 10^6}\right)\right] - Z^G R T(M_T - L) \qquad (4.1.5)$$

The determination of the fugacity coefficients, saturated liquid densities and the compressibility factor are outlined in Chapter 3, section 3.1.

The binary constants for the van Laar equation have to be determined experimentally. An additional function must be developed and minimized for each data point in addition to the functions derived above. Making use of the vapor-liquid equilibria for water, the following minimization function, f_3, was developed:

$$f_3 = 1 - y_A - \frac{M_H}{M_{T0} - L} - \left(\frac{\phi_W^{0L}}{\phi_W^{V}}\right) \exp\left[\frac{C_{21}}{\left(1+\frac{C_{21}(1-x_A)}{C_{12}x_A}\right)^2}\right](1-x_A) \qquad (4.1.6)$$

Function f_3 was minimized by non-linear least-squares regression by varying the binary parameters of the van Laar equation. The minimization procedure is outlined in Chapter 3, section 3.2. The vapor-phase mole fraction of 2-propanol and the equilibrium amount

of liquid in the vessel were calculated by minimizing functions f_1 and f_2. The results of these minimization procedures are shown in Figures 4.1 – 4.3. Figure 4.1 compares the calculated value of y_A with what is expected from the van Laar equation (f_1). Figure 4.2 compares the experimental pressure value P with the pressure calculated using an equation of state for a closed system (f_2). The calculated value of the vapor-phase mole fraction of water, y_W determined from material balances is compared to the mole-fraction determined from the van Laar equation in Figure 4.3 (f_3).

The ability of the van Laar model to fit the experimental pressure-liquid composition data is illustrated in Figure 4.4. A very good fit is found for 2-propanol concentrations greater than 6 mol % over the range of temperatures tested. The temperature dependence of the binary parameters, as expressed mathematically in Chapter 3, equation 3.1.23, is shown in Figure 4.5. It should be noted that these parameters were determined under a relatively small range of 2-propanol concentrations. Caution should be exercised in extrapolating these parameters to other concentration ranges. An accurate description of the vapor-liquid equilibria for the entire range of concentration $0 < x_A < 1$ is outside the scope of this thesis. The temperature dependence of the van Laar binary constants are determined to be:

$$C_{12} = \frac{2299.1}{T} - 3.624, \qquad r^2 = 0.995 \tag{4.1.7}$$

$$C_{21} = -\frac{2228.6}{T} + 5.953, \qquad r^2 = 0.893 \tag{4.1.8}$$

The contents of the reactor vessel can now be completely described using only pressure-temperature data.

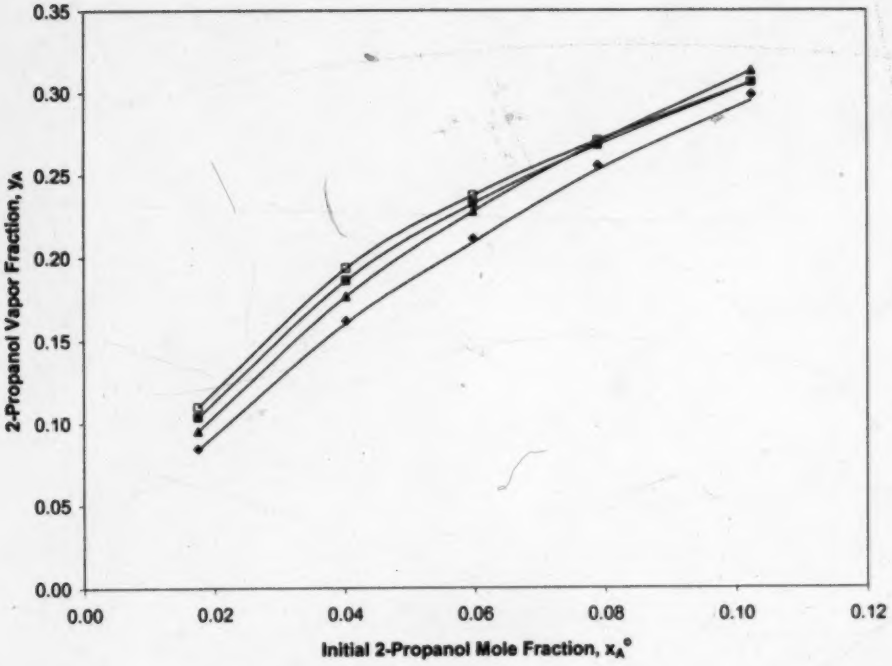

Figure 4.1 – Minimization of Function f_1 for the Determination of the van Laar Binary Parameters: (□) 433 K, (■) 443 K, (▲) 453 K, (◆) 463 K, (—) van Laar model fit

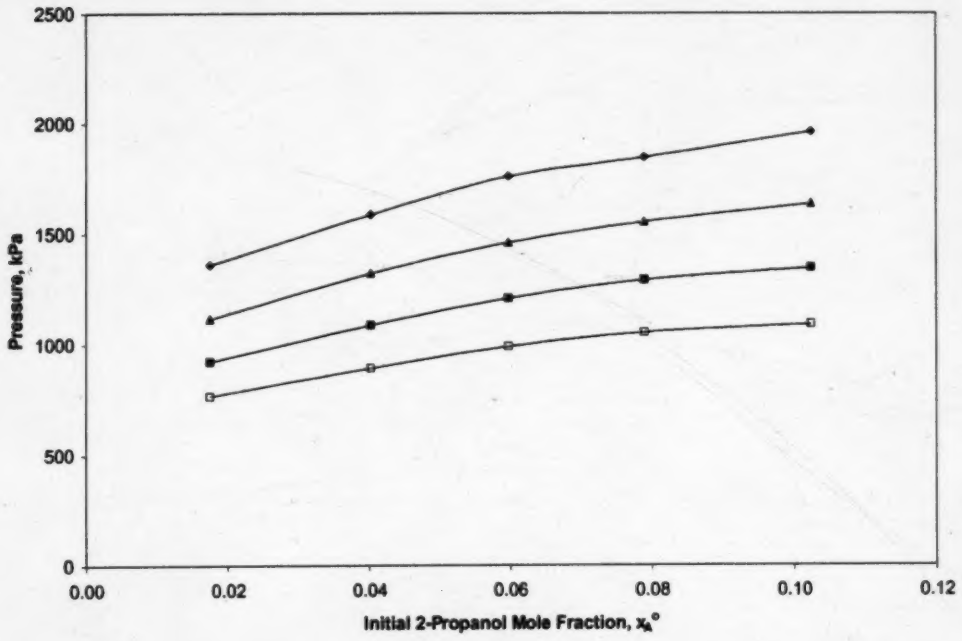

Figure 4.2 - Minimization of Function f_2 for the Determination of the van Laar Binary Parameters: (□) 433 K, (■) 443 K, (▲) 453 K, (◆) 463 K, (—) van Laar model fit

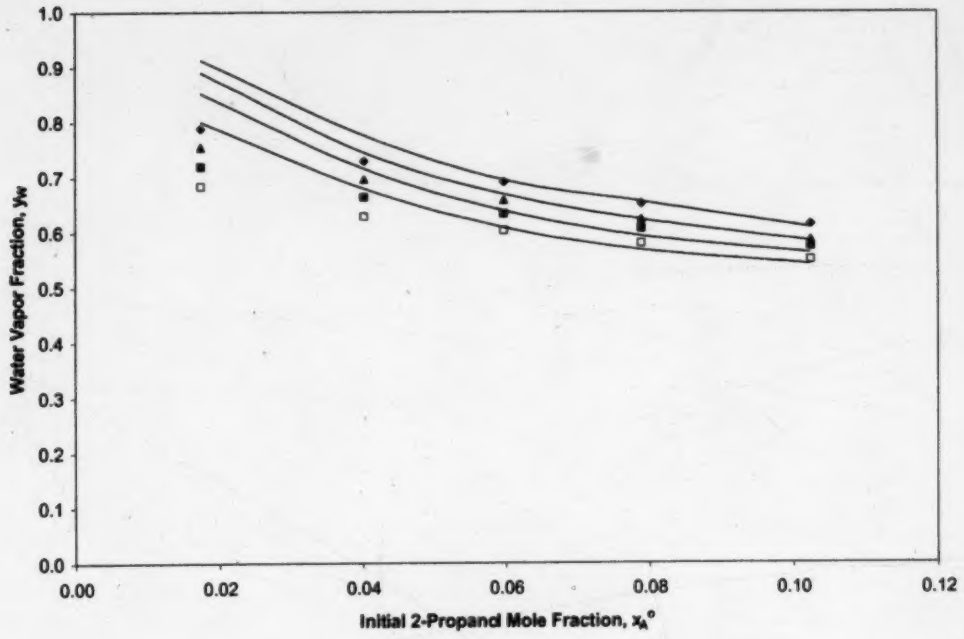

Figure 4.3 - Minimization of Function f_3 for the Determination of the van Laar Binary Parameters: (□) 433 K, (■) 443 K, (▲) 453 K, (◆) 463 K, (—) van Laar model fit

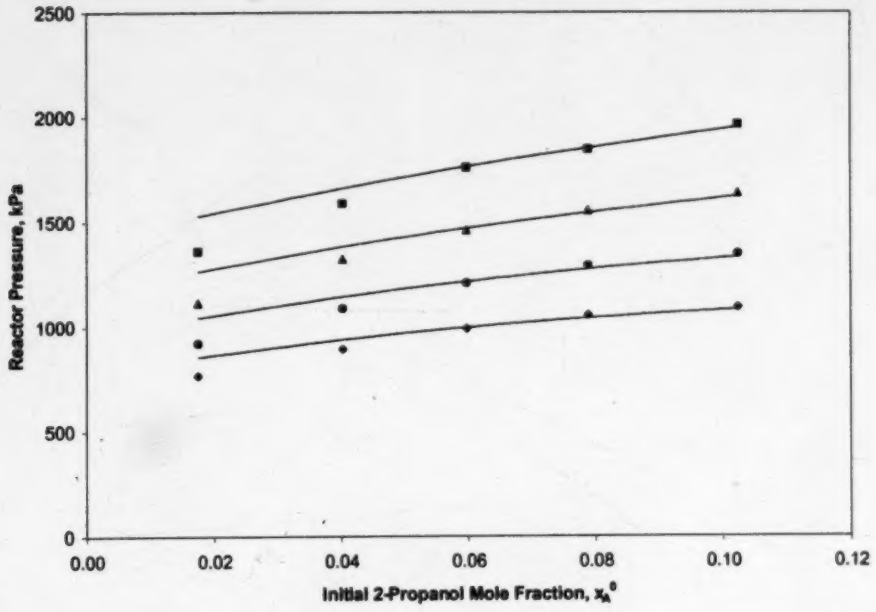

Figure 4.4 - The Equilibrium Pressure versus Liquid Composition : PRSV Equation of State with the van Laar Excess Gibbs Free Energy Model: (◆) 433 K, (●) 443 K, (▲) 453 K, (■) 463 K, (—) van Laar model fit

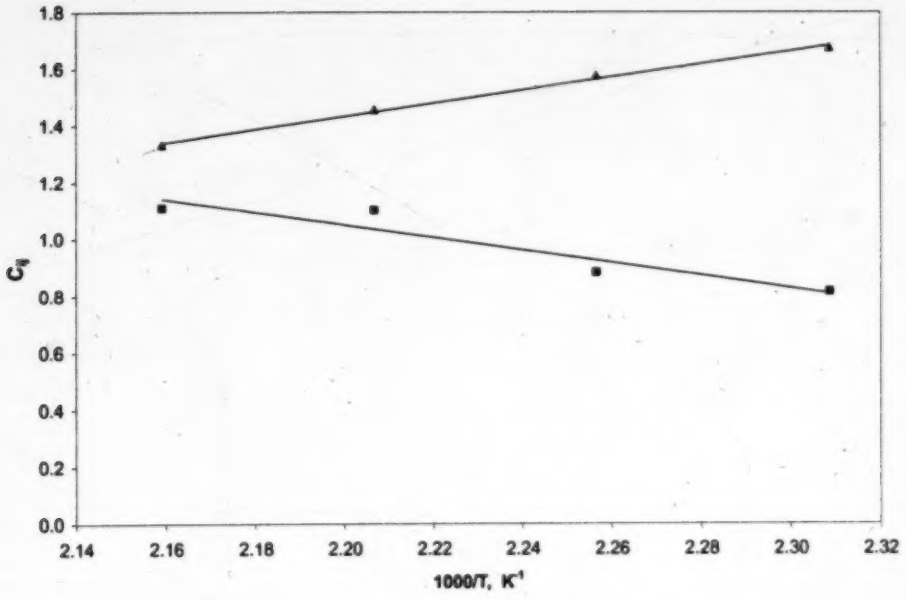

Figure 4.5 - Temperature Dependence of the Binary Parameters for the van Laar Excess Gibbs Free Energy Model (1 = 2-propanol, 2 = water): (▲) C_{12}, (■) C_{21}

4.2 – Catalyst Screening

4.2.1 – Preliminary Screening

Various metal oxide and molecular sieve solid acid catalysts with varying acidities and hydrophobicities were screened for 2-propanol dehydration activity. These include samples of active alumina, zeolite 13X (Aldrich; 20,3864-7), SAPO-5 (MHZN2-34, Laval University, PQ, Canada), silicalite with a silica binder (S-115 SiO_2 ExT., UOP, LOT 15228-32), and silicalite with an alumina binder (S-115 Al_2O_3 ExT., UOP, LOT 09296-29C). The BET surface areas for the screened catalysts and their x-ray diffraction patterns are found in Table 4.1 and Figure 4.6 respectively. Alumina and zeolite 13X were selected for screening due to the fact that they are known to be active in the vapor-phase dehydration of 2-propanol.

HZSM-5 catalysts are known to be active in the vapor-phase catalytic dehydration of ethanol in the presence of water [Phillips and Datta, 1997; Schulz and Bandermann, 1994; Le van Moa et al., 1990; Oudejans et al., 1982]. The dehydration mechanism of ethanol and 2-propanol are considered to be very similar. For this reason, HZSM-5 type zeolites were considered for screening. The silicalite catalysts were chosen because they are very hydrophobic [Flanigen et al., 1978], which is an attractive property for wastewater applications and they are considered to be structurally similar to HZSM-5 catalysts [Olson et al., 1980; Rees, 1982].

Silicoaluminophosphates, such as SAPO-5, are known to be active in reactions requiring strong acids [Hedge at al., 1988]. The results of the catalyst screening are shown in Figure 4.7. The 2-propanol conversion is defined as the mole percent of 2-propanol that is converted to propylene.

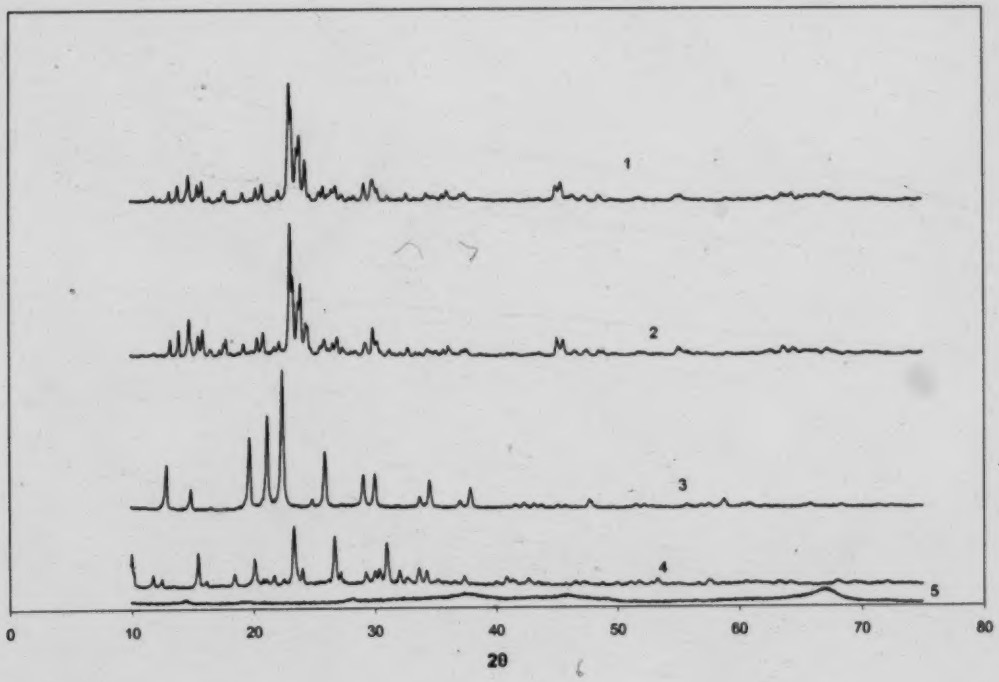

Figure 4.6 – X-Ray Diffraction Pattern for the Screened Catalysts: 1 = S-115 Al_2O_3 ExT., 2 = S-115 SiO_2 ExT., 3 = SAPO-5, 4 = Zeolite 13X, 5 = Alumina

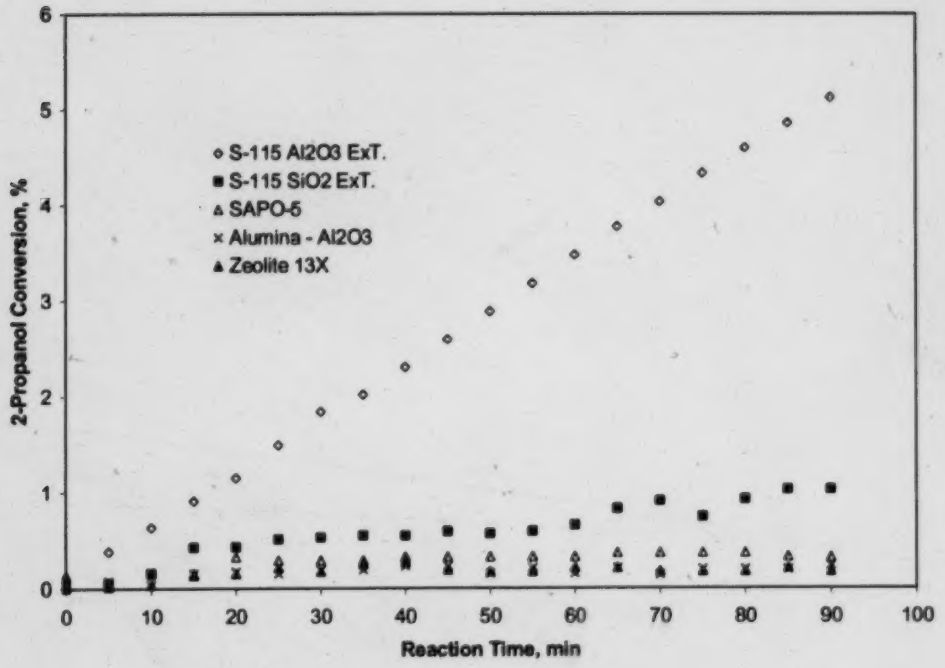

Figure 4.7 - Catalyst screening – Reaction Temperature = 463 K, Stirrer Speed = 1004 rpm, 400 - 595 μm Particle Size (Except Powder SAPO-5), 1.6 wt % Catalyst Loading, 10 mol % 2-Propanol/Water Feed

For all catalysts tested, propylene is the major reaction product. Only trace amounts of di isopropyl ether and acetone were found. These results justify the assumption of a negligible amount of other components in the liquid phase except water and 2-propanol. Further analysis of the liquid samples indeed confirmed that negligible amounts of propylene are present in the liquid phase.

S-115 Al_2O_3 ExT was found to be the most active catalyst among the screened samples, followed by S-115 SiO_2 ExT. In an aqueous media, the rate of propylene formation may depend on the number and strength of acid sites and also on the hydrophobicity of the catalyst. It has been found previously that silicalite is both more hydrophobic and more acidic than SAPO-5 [Hedge et al., 1988]. This may explain the higher activity of the silicalite catalysts compared to the SAPO-5 catalyst. It should be noted that the acidity and hydrophobicity of zeolites, such as silicalite, are dependent on the silica/alumina ratio [Olson et al., 1980]. However, more tests are needed with respect to catalyst acidity and hydrophobicity in order to make definite conclusions with regards to the influence of these parameters on the catalytic activity in the aqueous phase. For all kinetic runs, silicalite S-115 Al_2O_3 ExT is the catalyst used to determine the kinetic parameters.

4.2.2 – Validation of Irreversible Reaction

From the preliminary catalyst screening, the assumption that 2-propanol dehydrates to propylene irreversibly can be validated by calculating the equilibrium conversion in the batch slurry reactor and comparing this conversion with what was found experimentally. A theoretical equilibrium conversion which far exceeds the

conversion attained in the transient mode would indicate that the reaction is not approaching its equilibrium conversion, hence a reverse reaction would not be significant.

The equilibrium conversion calculations were performed by making use of the reactor equations developed in Chapter 3, section 3.1. For the equilibrium conversion calculations the final reactor pressure is not known, hence an additional equation is required to describe the equilibrium product composition. The previous assumptions made with regards to the liquid phase composition and the reaction products are assumed to apply for these calculations as well. In terms of the component activities, the equilibrium constant is given as

$$K = \prod a_i^{\nu_i} = \frac{a_P \cdot a_W}{a_A} \tag{4.2.1}$$

where

$$a_P = \frac{f_P^V}{f_P^{0,V}} = \frac{P\phi_P^V y_P}{101.3} \tag{4.2.2}$$

and

$$a_W = \frac{f_W^L}{f_W^{0,L}} = \frac{P\phi_W^{0L}\gamma_W x_W}{P_W^{SAT}} \tag{4.2.3}$$

and

$$a_A = \frac{f_A^L}{f_A^{0,L}} = \frac{P\phi_A^{0L}\gamma_A x_A}{P_A^{SAT}} \tag{4.2.4}$$

Substituting equations 4.2.2 – 4.2.4 into 4.2.1 yields

$$K = \frac{P}{101.3}\frac{\phi_P^V}{\phi_A^{0L}}\frac{\phi_W^{0L}}{P_W^{SAT}}\frac{P_A^{SAT}}{\gamma_A}\frac{\gamma_W}{(1-x_A)}\frac{y_P}{x_A} \tag{4.2.5}$$

To calculate the equilibrium composition from the above equation, the equilibrium constant must be determined at the required temperature. The temperature dependence of K is known thermodynamically to be [Kyle, 1992]:

$$\frac{d\ln K}{dT} = \frac{\Delta H^0}{RT^2} \tag{4.2.6}$$

where the standard enthalpy change for the reaction ΔH^0 is written as:

$$\Delta H^0 = \Delta H_f^0 + \int_{298}^{T} \left(\sum \nu_i C_{Pi}^0\right) dT \tag{4.2.7}$$

where the heat capacity for the reactants and products have the following temperature dependence:

$$C_{Pi}^0 = a_i + b_i T + c_i T^2 + d_i T^3 \tag{4.2.8}$$

Empirical constants a, b, c, and d for gaseous propylene and liquid water and 2-propanol are given in Table 4.2.

Making use of the temperature dependence of the standard enthalpy change of the reaction and equation 4.2.6, the equilibrium constant can be expressed as

$$\ln K = -\frac{\Delta H_0}{RT} + \left(\frac{\sum \nu_i a_i}{R}\right)\ln T + \left(\frac{\sum \nu_i b_i}{2R}\right)T + \left(\frac{\sum \nu_i c_i}{6R}\right)T^2 + \left(\frac{\sum \nu_i d_i}{12R}\right)T^3 + I \tag{4.2.9}$$

The standard enthalpy change ΔH^0 and the integration factor I were determined to be 67.3 kJ mole^{-1} and 165.3 respectively. The equilibrium constants at a temperature range of 433 to 463 K are shown in Figure 4.8. The liquid-phase dehydration of 2-propanol to form propylene is an endothermic reaction, therefore the equilibrium constant and the equilibrium 2-propanol conversion increases with increasing temperature.

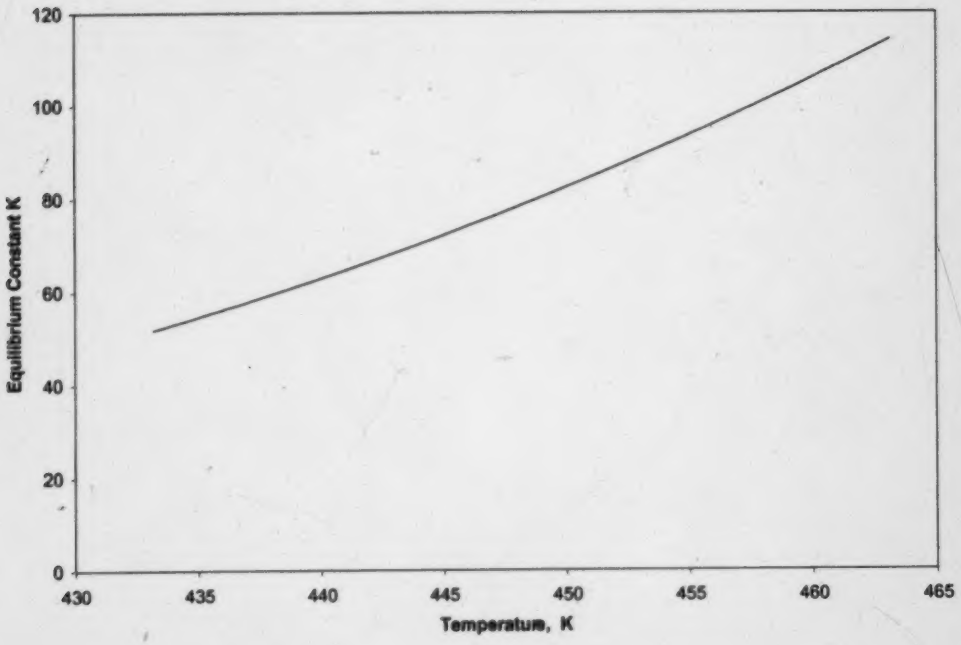

Figure 4.8 – Chemical Equilibrium Constant for the Liquid-Phase Dehydration of 2-Propanol to Propylene at Various Reaction Temperatures

Chemical equilibrium is attained when equation 4.2.5 and the exponential of equation 4.2.9 are equal. Making use of the equations developed in Chapter 3, section 3.1 and this additional equation, the equilibrium conversion of liquid 2-propanol to propylene was calculated at a temperature range of 433 to 463 K at 2-propanol concentrations of 4 – 10 mol %. The results of these calculations are given in Figure 4.9. As is expected from Figure 4.4, the equilibrium conversion increases with increasing temperature. As well, the presence of water in the reactor feed is expected to inhibit the equilibrium conversion to propylene, as can be seen in equation 4.2.5.

It should be noted that these equilibrium conversions were calculated for the experimental batch slurry reactor used to determine the rate data. They do not necessarily reflect the highest conversion one would expect in an industrial setting. As the reactor is operating in a batch mode, the reactor pressure is allowed to increase as volatile propylene is being produced. As can be seen in equation 4.2.5, a high pressure lowers the equilibrium conversion to propylene. If propylene were to be continuously removed (for example, in a catalytic distillation column) very high conversions would be expected.

When comparing Figure 4.7 to 4.9, it is very evident that, even with the relatively active silicalite S-115 Al_2O_3 catalyst, the reaction is far from its equilibrium conversion, even after 1.5 hours. At 463 K with an initial 2-propanol concentration of 10 mol %, the conversion of 2-propanol over silicalite S-115 Al_2O_3 was 5.1 % after 90 minutes. The equilibrium conversion at these conditions was calculated to be 35.3 %, almost seven times higher than the conversions attained during the kinetic runs. These results indicate

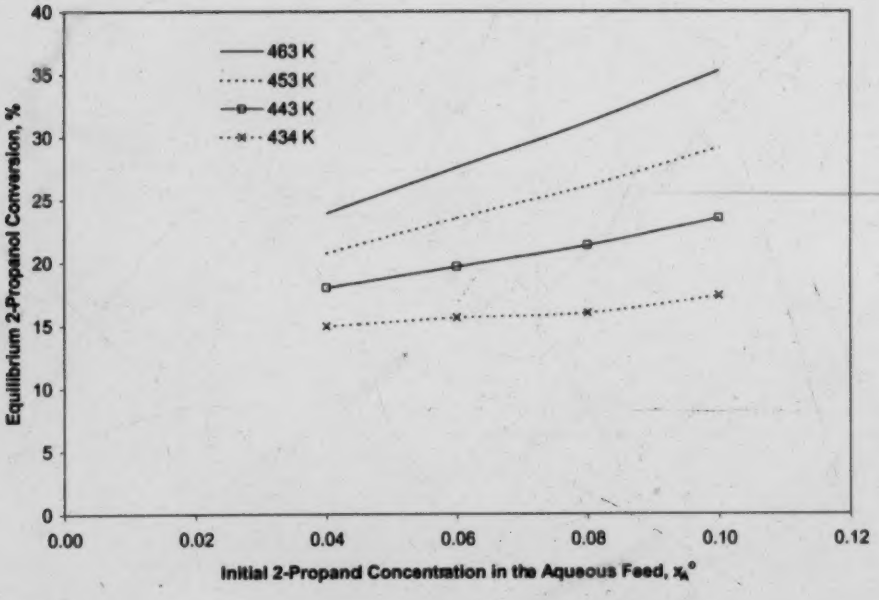

Figure 4.9 – Influence of Reactor Temperature and Initial 2-Propanol Concentration on the Equilibrium Conversion of 2-Propanol to Propylene in a Batch Slurry Reactor

that the assumption of an irreversible reaction in the development of the kinetic model in Chapter 3 (section 3.2) appears to be reasonable.

4.3 – Mass Transfer Limitations

Heterogeneous catalytic reactions can be said to occur through the following steps

Step 1 – Transport of reactant material to the catalyst surface

Step 2 – Diffusion of the reactant through the porous structure to the active catalyst surface

Step 3 – Chemisorption of the reactant on to the active site(s)

Step 4 – Catalytic surface reaction to form reaction product(s)

Step 5 – Desorption of reactants from the active site(s)

Step 6 – Diffusion of reaction products through the porous structure to the bulk phase

Step 7 – Transport of the reactant material through boundary layer to the bulk media

The external mass transfer is described in steps 1 and 7. Internal mass transfer through the porous catalyst via molecular and pore diffusion is described in steps 2 and 6. The surface reaction, which consists of the adsorption/desorption of the reactants/products and the surface reaction are detailed in steps 3-5. The observed rate of reaction depends on all of the above steps. True surface reaction rates can only be directly determined from rate data if the experiments are performed under conditions where the observed rate is not limited by diffusional processes, otherwise the mass transfer processes must be modeled.

The region where the external mass transfer is no longer rate limiting was determined by varying the stirrer speed. Tests with silicalite S-115 Al_2O_3 ExT. at 463 K with a catalyst loading of 1.57 weight %, an initial 2-propanol concentration of 10 mol % and a catalyst particle size of 90 - 150 μm indicates that external mass transfer is no longer rate limiting at stirrer speeds greater than 1080 rpm (Figure 4.10). It can be expected that when an initial concentration less than 10 mol % is used, the kinetic experiments will still be performed in a region where the external mass transfer is not rate limiting.

The transport of reactant molecules from the surface of the catalyst to the bulk fluid through the boundary layer can be expressed as [Levenspiel, 1972]

$$\frac{1}{-S_{ex}} = \frac{dN_A}{dt} = k_L' (C_{Ab} - C_{As}) \qquad (4.3.1)$$

where C_{Ab} and C_{As} are the liquid phase concentrations of 2-propanol in the bulk and at the surface respectively. The liquid phase mass transfer coefficient k_L' can be expressed using the following correlation for highly turbulent mixers [Geankoplis, 1993]

$$k_L' N_{sc}^{2/3} = 0.13 \left(\frac{[P/V]\mu_C^2}{\rho_C^2} \right)^{1/4} \qquad (4.3.2)$$

where the Schmidt number, N_{sc}, is defined as

$$N_{sc} = \frac{\mu_C}{\rho_C D_{AW}} \qquad (4.3.3)$$

The above correlation is valid when the agitation power is increased beyond that needed for the suspension of solid particles and the turbulent forces become larger than the gravitational forces. The ratio [P/V] is the power input per unit volume. Power consumption is related to the fluid viscosity of the continuous phase μ_C, the fluid density

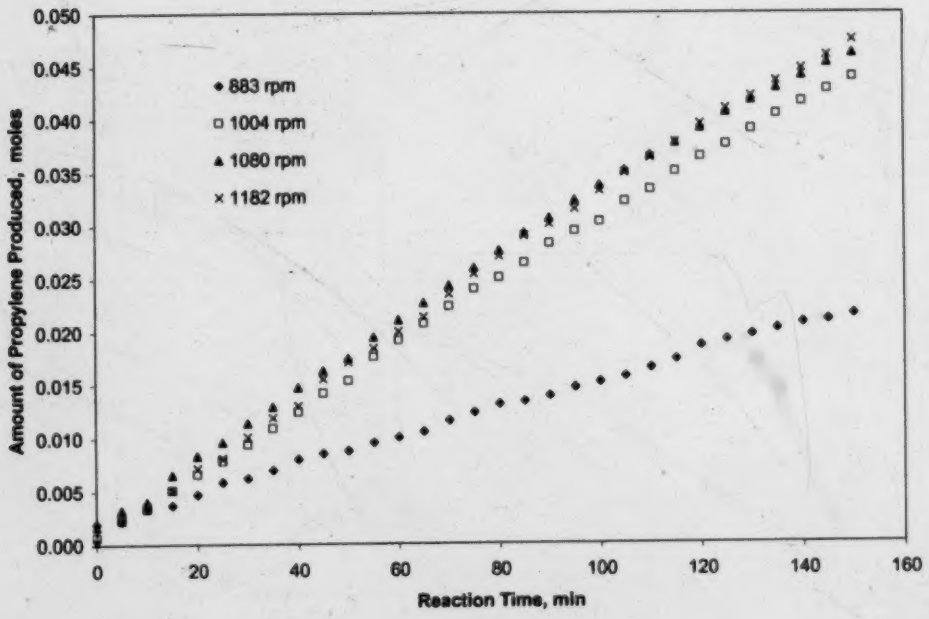

Figure 4.10 – Effect of Stirrer Speed on the Observed Rate of Propylene Formation over Silicalite S-115 Al_2O_3 : 10 mol % 2-propanol/water feed, 90 - 150 μm particle size, 463 K Reaction Temperature

of the continuous phase ρ_C, the impeller rotation speed N, and the impeller diameter D_a. The power consumption, P, can be related to the above physical conditions through experimental curves for various impeller types [Geankoplis, 1993] using the following dimensionless parameters

$$N_{Re} = \frac{D_a^2 N \rho_C}{\mu_C} \tag{4.3.4}$$

and

$$N_P = \frac{P}{\rho_C N^3 D_a^5} \tag{4.3.5}$$

From equations 4.3.3 - 4.3.5, it can be seen that the Schmidt number and the power consumption will remain nearly constant for initial 2-propanol concentrations less than 10 mol % because of the weak concentration dependency of the bulk fluid properties. It can then be concluded that the external mass transfer coefficient k_L' will remain nearly constant at a constant impeller stirrer speed. For this reason, the stirrer speed which minimizes the influence of external mass transfer on the observed rate of propylene formation for a 10 mol % 2-propanol feed will also minimize the influence of external mass transfer on initial 2-propanol concentrations slightly lower than 10 mol %.

The region where the internal mass transfer is no longer rate limiting was determined by varying the catalyst particle size and observing its influence on the observed rate of propylene formation. Tests at 463 K at a catalyst loading of 1.57 weight %, an initial 2-propanol concentration of 10 mol % and a stirrer speed of 1080 rpm indicate that internal mass transfer is not rate limiting at particle size ranges of 595 - 850 μm, 400 - 595 μm and 90 - 150 μm (Figure 4.11).

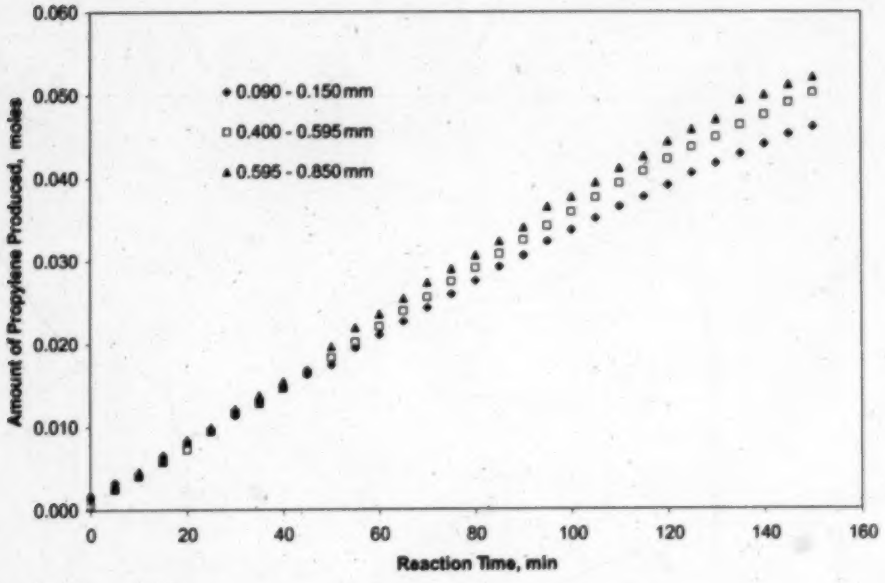

Figure 4.11 - Effect of Particle Size on the Observed Rate of Propylene Formation over Silicalite S-115 Al_2O_3 : 10 mol % 2-propanol/water feed, 1080 rpm Stirrer Speed, 463 K Reaction Temperature

4.4 – Kinetic Study

All kinetic experiments were conducted at a stirrer speed of 1080 rpm with 400 - 595 μm particle sizes. A 10 mol % 2-propanol/water mixture was fed to the reactor along with 1.57 weight % silicalite S-115 Al_2O_3 ExT. catalyst. Reaction rates were determined at 434, 444, 453, and 463 K. The experimental data were fitted with several Langmuir-Hinshelwood-Hougen-Watson (LHHW) type rate equations derived in Chapter 3 (equations 3.2.7, 3.2.11, 3.2.15, and 3.2.16). Model parameters, such as activation energies and the heats of adsorption, calculated from the above fitted models are given in Table 4.3.

A good kinetic model should not only be able to fit the experimental data, but it should be able to predict the reaction rates under different conditions. To this end, additional kinetic runs were carried out at 463 K for 2-propanol feed concentrations of 4, 6, and 8 mol %. This concentration range was chosen because it is in a dilute region, which would correspond to typical wastewater concentrations. A concentration of 2 mol % 2-propanol was not performed because the van Laar equation did not fit this dilute region well (Figure 4.4). The kinetic parameters established using the 10 mol % initial 2-propanol concentration kinetic runs were in turn used to predict the rate of propylene formation at other initial 2-propanol concentrations.

It can be seen in Table 4.3 that the SSM-2 model, which has single-site adsorption of both 2-propanol and water in the rate model is best able to predict the rate of propylene formation for 2-propanol concentrations ranging from 4 – 10 mol %. This is consistent with the E_1 type mechanism, involving only acid sites, which was proposed for 2-propanol dehydration to propylene over zeolite catalysts (Chapter 1). Both models that

include the water adsorption/desorption parameter were better able to predict the rate of propylene formation than the models that did not include this term in the equation. This indicates that water does in fact inhibit the rate of propylene formation, despite the relative high hydrophobicity of silicalite. This partly explains the poor dehydration activity of some of the hydrophilic catalysts such as zeolite 13X and SAPO-5 found during the catalyst screening (Figure 4.7).

Figure 4.12 illustrates the amount of propylene produced with varying time at several reaction temperatures with the fitted SSM-2 model. The model gives a good fit of the experimental data for temperatures between 434 and 463 K. The temperature dependency of the rate constant, as seen in Chapter 3 (equation 3.2.17) is shown in Figure 4.13. As can be seen from Figures 4.12 and 4.13, the rate of propylene formation is strongly dependent on temperature. This high activation energy indicates that the kinetic data were obtained in a region where the diffusional effects are not rate limiting. The temperature variation of the adsorption constants for the SSM-2 rate model is shown in Figure 4.14. The adsorption plots have positive slopes, which indicates that the heat of adsorption is exothermic. It should be noted that these calculated heats of adsorptions are model parameters only and do not necessarily reflect any real physical phenomena. It has been found in the literature that calculated heats of adsorption are strongly dependent on the type of model used, i.e. single versus dual-site [Yue and Oloafe, 1984]. The calculated heats of adsorption for the SSM-2 model are much lower than one would expect to find for chemisorption.

The ability of the SSM-2 model to predict the rates of propylene formation at lower 2-propanol concentrations is demonstrated in Figure 4.15. It can be seen that the

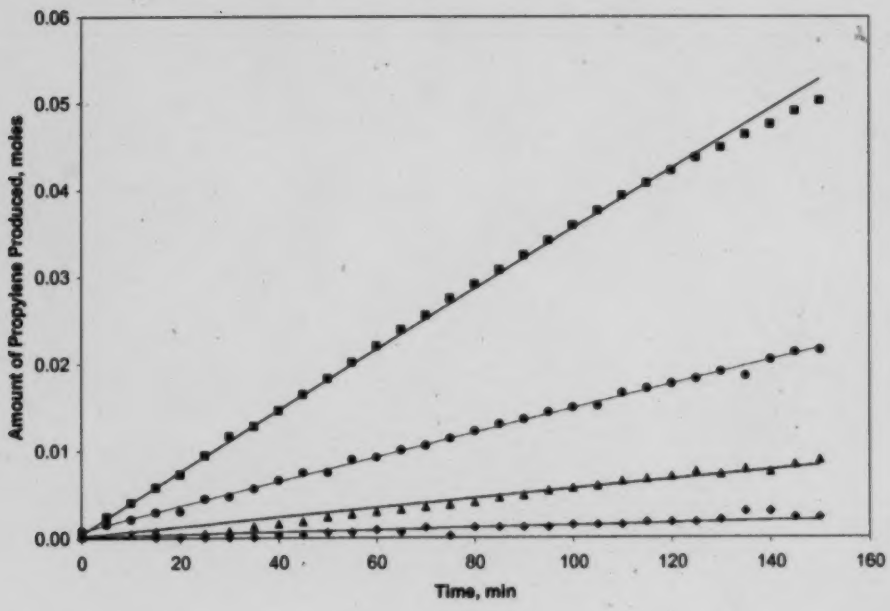

Figure 4.12 - Comparison of Experimental Rate Data with the Fitted SSM-2 Model at a Temperature Range of 434 – 463 K: (◆) 434 K, (▲) 444 K, (●) 453 K, (■) 463 K, (—) SSM-2 Model Fit

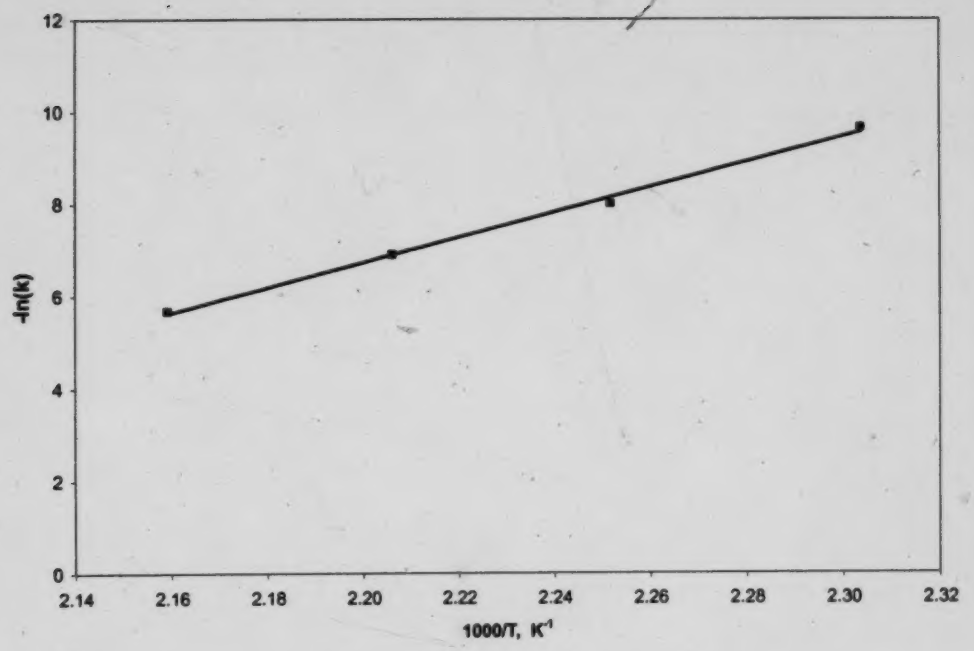

Figure 4.13 - Temperature Dependence of the Kinetic Parameters k, Determined from the Fitted SSM-2 LHHW Model

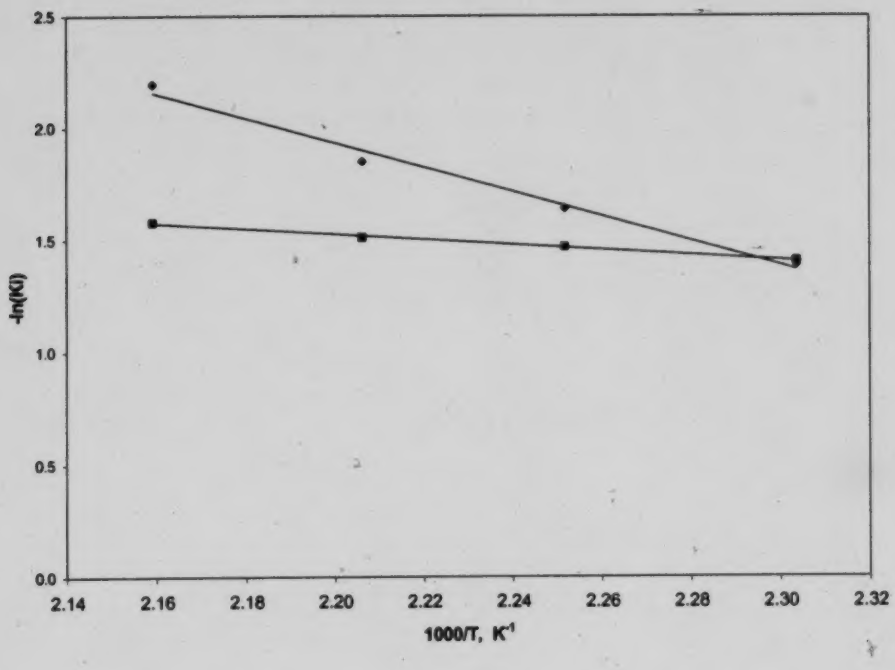

Figure 4.14 - Temperature Dependence of the Adsorption/Desorption Equilibrium Constants Determined from the Fitted SSM-2 LHHW Model: (◆) 2-Propanol, (■) Water

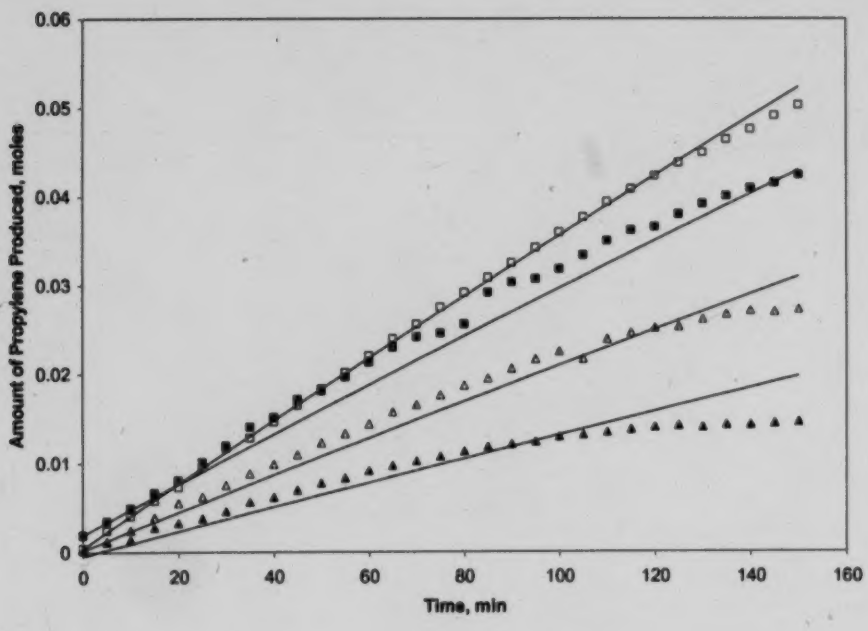

Figure 4.15 - Comparison of SSM-2 Model Prediction with the Rate of Propylene Produced under Different Initial 2-Propanol Mole Fraction: (▲) 4 mol % 2-Propanol Feed, (Δ) 6 mol % 2-Propanol Feed, (■) 8 mol % 2-Propanol Feed, (□) 10 mol % 2-Propanol Feed, (—) SSM-2 Model

SSM-2 model is able to adequately predict the rates of propylene formation, but the fit is not perfect. Upon inspection of Figure 4.15, one would assume that a reverse reaction is occurring during the reaction. However, as was illustrated in section 4.2.2 of this Chapter, a reversible reaction was not significant during the kinetic runs. Another possible explanation for the apparent drop in propylene formation would be due to catalyst deactivation. Fresh and used samples of silicalite S-115 Al_2O_3 ExT. were examined using x-ray diffraction and BET. The used sample indicates a catalyst that was used for a typical kinetic run at a reaction temperature of 463 K for a duration of 2 hours. An observable change in the catalyst structure before and after the kinetic run would indicate that deactivation does occur during the run. The x-ray diffraction pattern for the fresh and 'used' catalyst is illustrated in Figure 4.16. From the x-ray diffraction pattern, there does not appear to be any noticeable difference in the catalyst structure before and after the dehydration run. The BET surface area for the fresh and used catalyst was determined to be 320.9 and 342.0 $m^2 g^{-1}$ respectively; this difference in surface area is not significant. Based on the above measurements, the structure of the silicalite catalyst does not appear to undergo any significant structural change during the course of the kinetic run. Kinetic experiments on silicalite were performed using a fresh catalyst and a used catalyst that was reacted at 463 K with an initial 2-propanol concentration of 10 mol % for 2.5 hours. As can be seen in Figure 4.17, there does not appear to be any significant deactivation of the catalyst after the kinetic run. The apparent drop in propylene formation illustrated in Figure 4.15 cannot be attributed to the reversible reaction or catalytic deactivation. This indicates that a simple LHHW type rate equation is not sufficient to completely describe the observed phenomena, especially at high water

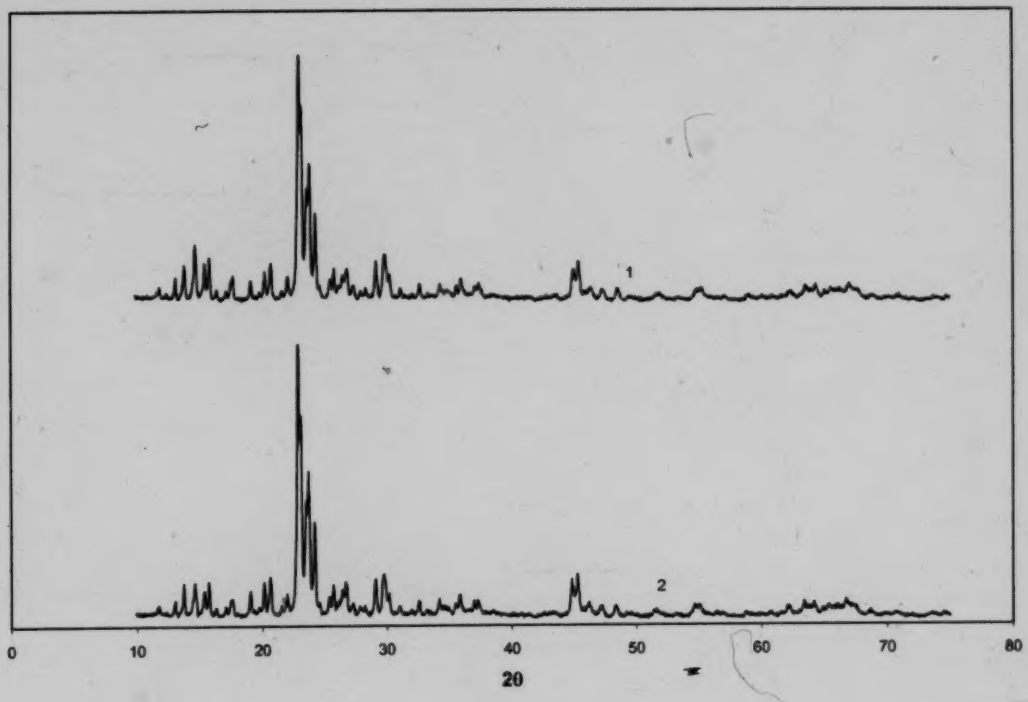

Figure 4.16 – Comparison of X-Ray Diffraction Pattern of Fresh Silicalite (S-115 Al_2O_3 ExT.) with Reacted Silicalite: 1 = Fresh, 2 = Reacted

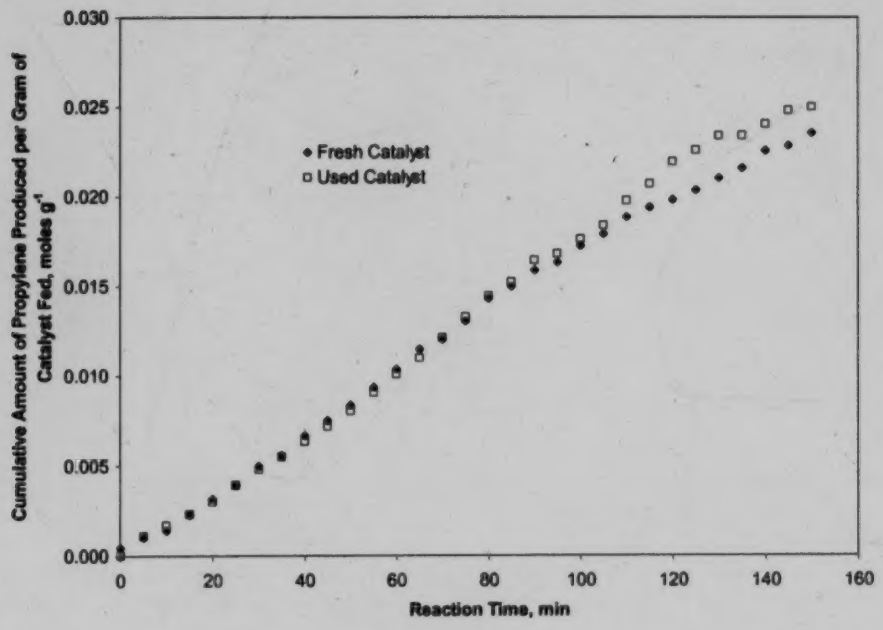

Figure 4.17 – Silicalite S-115 Al_2O_3 ExT. Catalyst Reusability: Initial 2-propanol Concentration of 10 mol %, 30-40 Mesh Particle Size, 1080 rpm Stirrer Speed, Reaction Temperature of 463 K: Used Catalyst Reacted for 2.5 Hours

concentrations. It is possible that a change in the reaction mechanism at very high water concentration may occur. Despite the deviations, the SSM-2 model does provide a very reasonable prediction of propylene formation. This kinetic model can be used in a suitable simulation package to design an appropriate wastewater purification process at an accuracy of ± 8.8 %.

4.5 – Catalyst Loading

The effect of the catalyst loading on the rate of propylene formation was determined by performing kinetic runs at catalyst loadings of 0.762 wt %, 1.106 wt % and 1.556 wt %. The experiments were performed at 463 K at an initial 2-propanol concentration of 10 mol %. The results of these experiments and the fitted SSM-2 model are given in Figure 4.18. The calculated kinetic parameters should not be affected by the catalyst loading, otherwise the assumption of a uniformly mixed vessel is invalid. As can be seen in Figure 4.19, the calculated kinetic parameters appear to be independent of the catalyst loading.

The established LHHW rate equation is:

$$r = \frac{1}{m_C}\frac{d\alpha}{dt} = \frac{k_S K_A C_A}{1 + K_A C_A + K_W C_W} \tag{4.4.1}$$

$$k_S = 1.406 \cdot 10^{23} \exp\left(-\frac{25148}{T}\right) \tag{4.4.2}$$

$$K_A = 8.32 \cdot 10^{-7} \exp\left(\frac{5472}{T}\right) \tag{4.4.3}$$

$$K_W = 1.66 \cdot 10^{-2} \exp\left(\frac{1154}{T}\right) \tag{4.4.4}$$

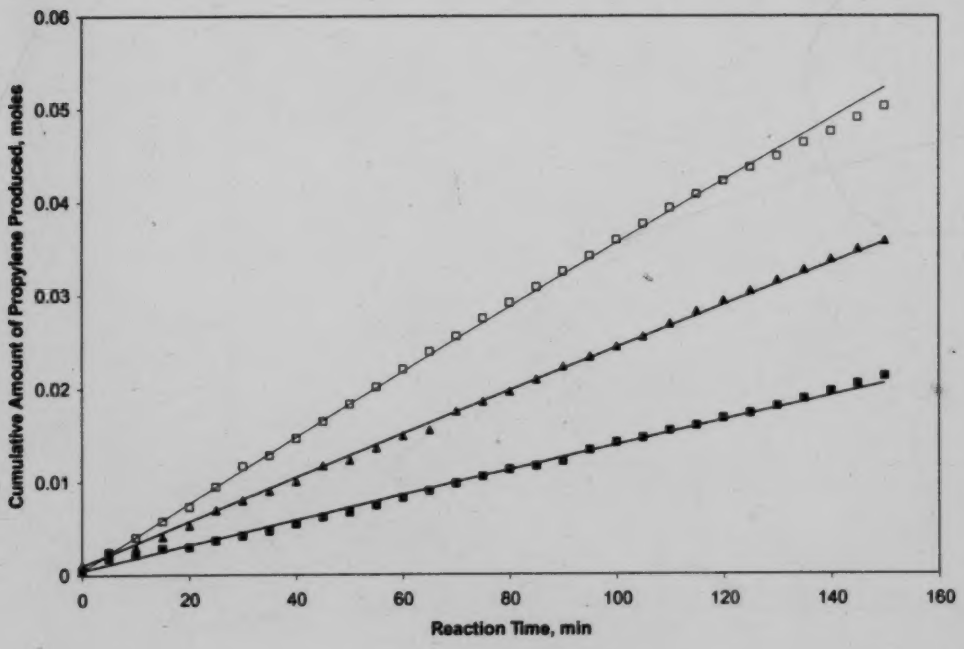

Figure 4.18 – Effect of Silicalite S-115 Al_2O_3 ExT. Loading on the Rate of Propylene Formation: 10 mol % 2-Propanol Feed at a Reaction Temperature of 463 K: (□) 1.556 wt %, (▲) 1.106 wt %, (■) 0.762 wt %, (—) SSM-2 Model Fit

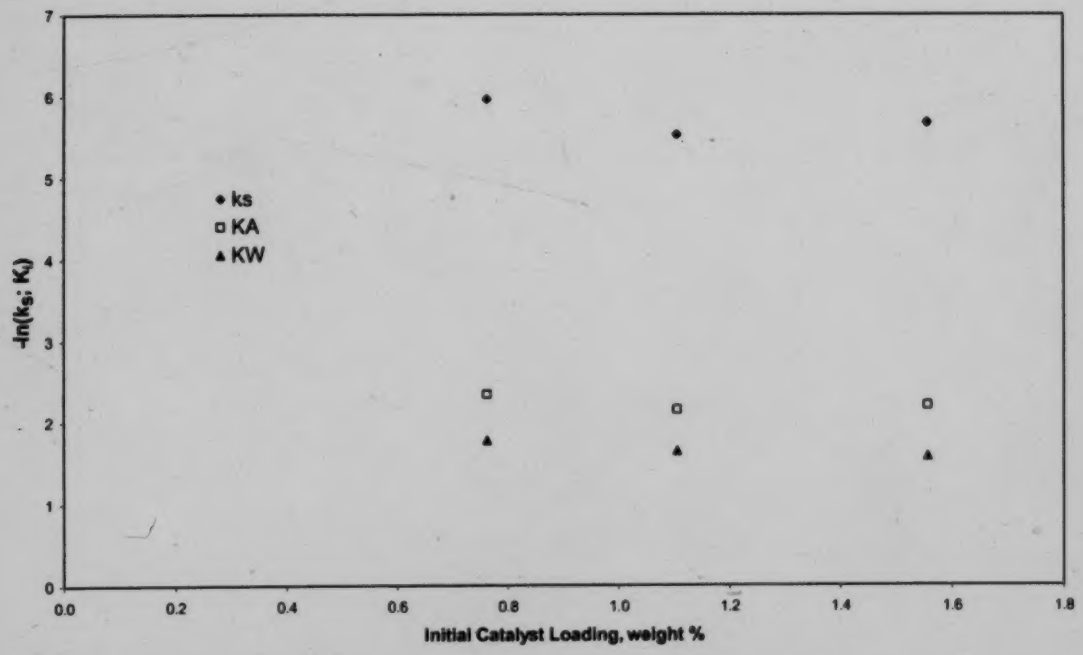

Figure 4.19 – Effect of Silicalite S-115 Al_2O_3 ExT. Loading on the Kinetic Parameters: 10 mol % 2-Propanol Feed at a Reaction Temperature of 463 K

4.6 – First Order Model

The previous chapters outlined a method which can be used to fit experimental rate data for the liquid-phase dehydration of 2-propanol. LHHW rate models were derived and fitted with experimental data because of their wide acceptance in vapor phase alcohol dehydration reactions. With this in mind, it should be noted that the experimental data was fitted over a fairly narrow range of 2-propanol concentrations and that a six-parameter model is perhaps too complex for such a small range. A simple firstconcentrations. Figure 4.20 illustrates the first order model fit at 463 K over a 2-propanol concentration range of 4 – 10 mol %. The temperature dependence of the rate of propylene formation at reaction temperatures ranging from 434 to 463 K is illustrated in Figure 4.21. The Arrhenius temperature dependence of the rate constant (equation 3.2.17) is illustrated in Figure 4.22. As was previously concluded, the high activation energy (195.8 kJ $mole^{-1}$) indicates that the kinetic experiments were performed in a region where the influence of internal and external mass transfer is not significant. The first order rate model is expressed mathematically as:

$$r = \frac{1}{m_C}\frac{d\alpha}{dt} = k_S C_A \tag{4.6.1}$$

$$k_S = 6.488 \cdot 10^{17} \exp\left(-\frac{23548}{T}\right) \tag{4.6.2}$$

It is recommended that for the purposes of simulating a wastewater purification process, where 2-propanol will be present in dilute concentrations, that the first order model be used due to it's mathematical simplicity and accuracy. This model should not be used to extrapolate rates of propylene formation beyond the experimental concentration range. If

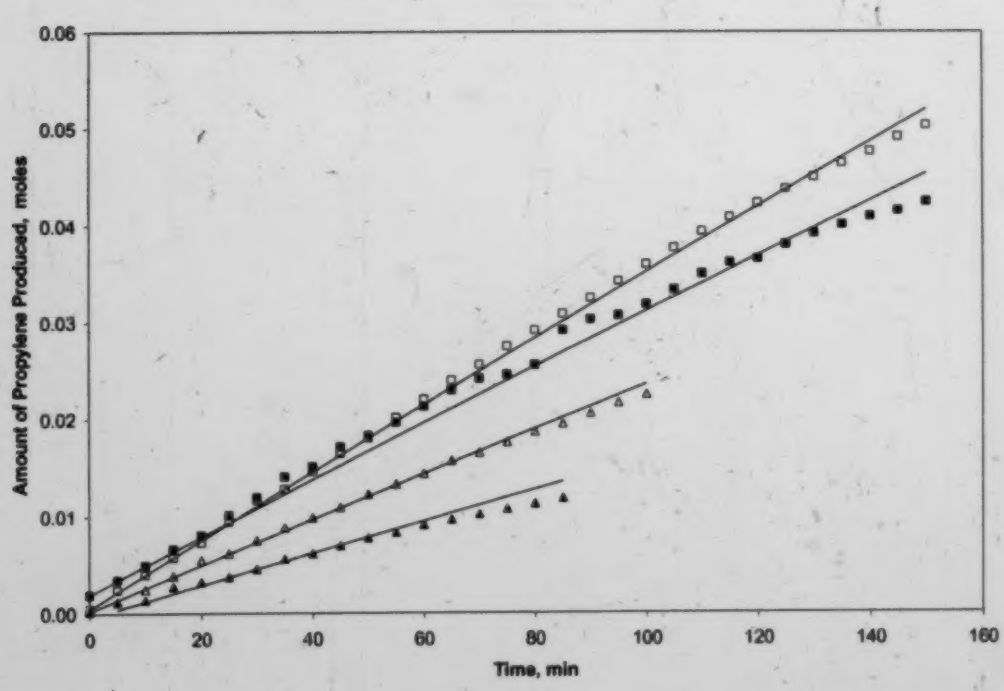

Figure 4.20 – Concentration Dependence of 2-Propanol on the Rate of Propylene Formation at 463 K:(▲) 4 mol % 2-Propanol Feed, (Δ) 6 mol % 2-Propanol Feed, (■) 8 mol % 2-Propanol Feed, (□) 10 mol % 2-Propanol Feed, (—) 1st Order Model Fit

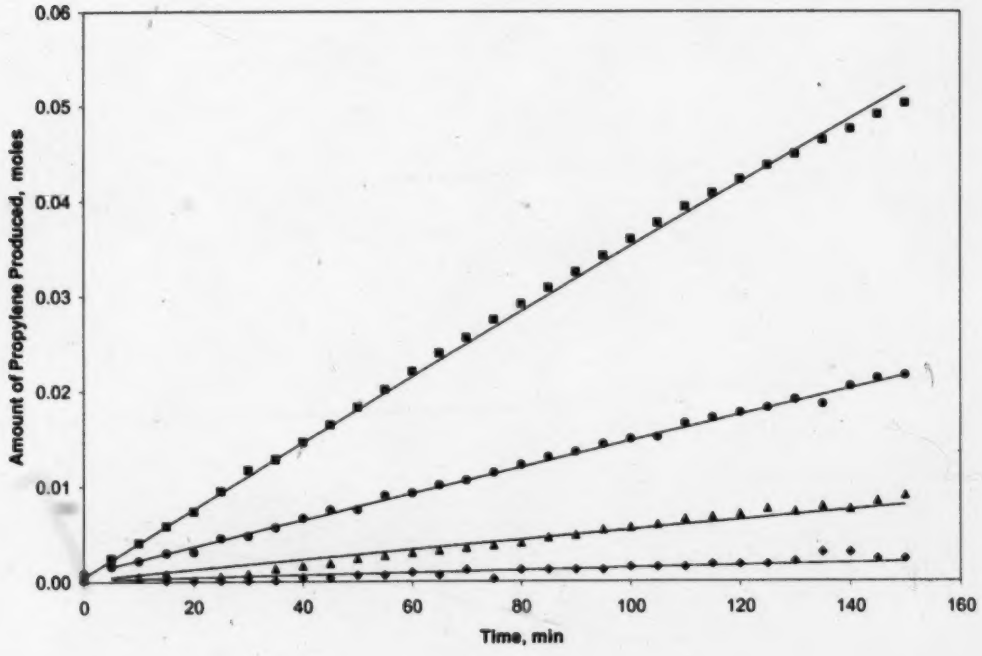

Figure 4.21 - Comparison of Experimental Rate Data with the Fitted 1st Order Model at a Temperature Range of 434 – 463 K: (◆) 434 K, (▲) 444 K, (●) 453 K, (■) 463 K, (—) 1st Order Model Fit

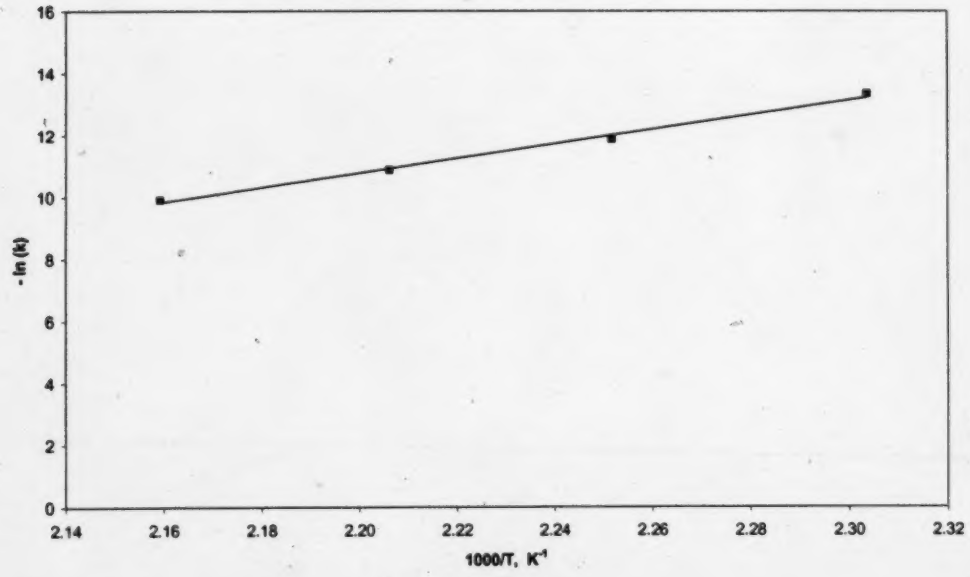

Figure 4.22 - Temperature Dependence of the Kinetic Parameters k, Determined from the Fitted 1st Order Model

rate data is acquired over a large range of 2-propanol concentrations, it is recommended that the LHHW models previously derived be used to fit the experimental data because of their wide acceptance in vapor-phase dehydration kinetics.

4.7 – Nomenclature

a = activity

C = binary constant for the van Laar equation

= liquid phase concentration of component, mole L^{-1}

C_P^0 = constant pressure heat capacity, J $mole^{-1}$ K^{-1}

D = diameter, m

= diffusivity, m^2 /s

E_A = acitvation energy, kJ $mole^{-1}$

f = fugacity, kPa

ΔH_A = heat of adsorption, kJ $mole^{-1}$

ΔH^0 = standard enthalpy change for the reaction, kJ $mole^{-1}$

K = adsorption/desorption equilibrium constant, L $mole^{-1}$

= chemical equilibrium constant

k = rate constant for 2-propanol dehydration, mole g^{-1} min^{-1}

k_L' = liquid mass transfer coefficient, m/s

L = moles of liquid, mole

m = mass, g

M = moles of component prior to reaction, mole

Mw = molecular weight of component, g / mole

N = moles of compound, mole

= impeller rotation speed, rev/s

N_P = number of data points

= power consumption number

N_{sc} = Schmidt number

P = pressure, kPa

= agitator power consumption, kJ

R = gas constant, 8.31451 J $mole^{-1}$ K^{-1}

r = rate of formation, mole g^{-1} min^{-1}

S_{ex} = external catalyst surface area, m^2

T = temperature, K

t = time, min; sec

V = moles of vapor, mole

= volume, m^3

x = liquid mole fraction

y = vapor mole fraction

Z = compressibility factor

Greek Letters

α = cumulative amount of propylene produced at time t, mole

ϕ = fugacity coefficient

γ = activity coefficient

μ = liquid-phase viscosity, kg/m s

ρ = saturated liquid density, g/cc; kg/m^3

Σ = summation

υ = stoichiometric coefficient

Subscripts

0 = standard state, 298 K, 1 atm

a = impeller/agitator

A = 2-propanol

b = bulk phase

C = catalyst

= continuous phase

f = formation

H = helium

i = component

P = propylene

S = surface

T = total

W = water

Superscripts

0 = pure phase

G = gas phase

L = liquid phase

SAT = saturated

V = vapor phase

Table 4.1 – BET Surface Area for the Screened Catalysts

Catalyst	BET Surface Area (m^2/g)
S-115 Al_2O_3 ExT.	320.89
S-115 SiO_2 ExT.	348.33
SAPO-5	327.05
Zeolite 13X	239.52
Alumina	323.21

Table 4.2 – Enthalpy and Gibbs Free Energy of Formation and the Temperature Dependence of the Heat Capacity for Reactant and Products

Compound	$\Delta H°f$ (J/mol)	$\Delta G°f$ (J/mol K)	a (J/mol K)	b (J/mol K^2)	c (J/mol K^3)	d (J/mol K^4)
2-Propanol	-318200	-180500	331.2	-2.7507	0.010227	-1E-05
Water	-286000	-237400	65.656	0.12677	-0.00051	6.66E-07
Propylene	20400	62760	3.14754	0.237884	-0.00012	2.46E-08
Σvi	52600	5860	-262.396	3.115354	-0.01086	1.06E-05

Table 4.3 – Parameters and Predictions of the Developed LHHW Kinetic Models

Model	E_A (kJ mol^{-1})	r^2	$\Delta H_{A,A}$ (kJ mol^{-1})	r^2	$\Delta H_{A,W}$ (kJ mol^{-1})	r^2	model fit * (%)
SSM-1	209.1	0.994	-26.9	0.991	-	-	18.2
DSM-1	199.7	0.996	-36.4	0.842	-	-	26.7
SSM-2	226.8	0.996	-45.5	0.987	-9.6	0.994	8.8
DSM-2	166.6	0.981	-30.3	0.870	-30.5	0.835	11.8

$$* \ \% \text{ Model Fit} = \frac{100}{N_P}\sum_{i=1}^{N}\left|\frac{\alpha_{EXP} - \alpha_{PRED}}{\alpha_{EXP}}\right|$$

4.8 – Literature Cited

Flanigen, E. M., J. M. Bennett, R. W. Grose, J. P. Cohen, R. L. Patton, R. M. Kirchner, and J. V. Smith, "Silicalite, a New Hydrophobic Crystalline Silica Molecular Sieve", *Nature* **271**, 512-516 (1978)

Geankoplis, C. J., "Transport Processes and Unit Operations", 3rd. Ed., Prentice-Hall, Englewood Cliffs (1993)

Hedge, S. G., P. Ratnasamy, L. M. Kustov, and V. B. Kazansky, "Acidity and Catalytic Activity of SAPO-5 and AlPO-5 Molecular Sieves", *Zeolites* **8**, 137-141 (1988)

Kyle, B. G., "Chemical and Process Thermodynamics", 2nd. Ed. Prentice Hall, Englewood Cliffs (1992)

Le van Mao, R., T. M. Nguyen and J. Yao, "Conversion of Ethanol in Aqueous Solution over ZSM-5 Zeolites. Influence of Reaction Parameters and Catalyst Acidic Properties as Studied by Ammonia TPD Technique", *Appl. Catal.* **61**, 161-173 (1990)

Levenspiel, O., "Chemical Reaction Engineering", 2nd. Ed., John Wiley and Sons, New York (1972)

Olson, D. H., W. O. Haag and R. M. Lago, "Chemical and Physical Properties of the ZSM-5 Substitutional Series", *J. Catal.* **61**, 390-396 (1980)

Oudejans, J. C., P. F. van den Oosterkamp and H. van Bekkum, "Conversion of Ethanol over Zeolite H-ZSM-5 in the Presence of Water", *Appl. Catal.* **3**, 109-115 (1982)

Phillips, C. B., and R. Datta, "Production of Ethylene from Hydrous Ethanol on H-ZSM-5 Under Mild Conditions", *Ind. Eng. Chem. Res.* **36**, 4466-4475 (1997)

Rees, L. V. C., "When is a Zeolite not a Zeolite?", *Nature* **296**, 491-492 (1982)

Schulz, J., and F. Bandermann, "Conversion of Ethanol over Zeolite H-ZSM-5", *Chem. Eng. Tech.* **17**, 179-186 (1994)

Yue, P. L. and O. Olaofe, "Kinetic Analysis of the Catalytic Dehydration of Alcohols over Zeolties", *Chem. Eng. Res. Des.* **62**, 81-91 (1984)

Chapter 5

Conclusions and Recommendations

5.1 – Conclusions

2-Propanol dehydrates over solid acid catalyst in an aqueous medium to form propylene and trace amounts of diisopropyl ether and acetone. Alumina, zeolite 13X, silicoaluminophosphate, silicalite with a silica binder (S-115 SiO_2 ExT.) and silicalite with an alumina binder (S-115 Al_2O_3 ExT.) were active for the catalytic dehydration of 2-propanol at 463 K. Of these catalysts, silicalite with an alumina binder (S-115 Al_2O_3 ExT.) was the most active in the dehydration of 2-propanol in the aqueous medium. The use of alumina as a binder greatly influences the 2-propanol dehydration activity of silicalite.

The kinetics of the catalytic dehydration in an aqueous medium was determined for 2-propanol concentrations between 4 - 10 mol % and temperatures ranging between 434 and 463 K in a batch slurry reactor system. The influence of stirrer speed, catalyst particle size, catalyst loading, reaction temperature, and 2-propanol concentration on the rate of propylene formation was investigated. The influence of external mass transfer on the rate of propylene formation was insignificant at stirrer speeds greater than 1000 rpm. The influence of internal mass transfer on the rate of propylene formation was insignificant at particle diameters ranging from 90 - 850 μm.

Several Langmuir-Hinshelwood-Hougen-Watson (LHHW) mechanisms were proposed and screened. The equilibrium conversion of 2-propanol to propylene is much higher than what was attained during the kinetic runs, hence all LHHW models assumed a negligible reversible reaction. The models which include the adsorption/desorption of

water on the active sites were better able to predict the rate of propylene formation than models in which fast desorption of water was assumed. A single site LHHW type mechanism was found to describe the kinetic data well. This model is consistent with the E_1 type mechanism involving only acid sites proposed in the literature for the 2-propanol dehydration to propylene over zeolite catalysts.

The developed rate equation is:

$$r = k K_A C_A / (1 + K_A C_A + K_W C_W)$$

The influence of reactor temperature on the rate of propylene formation is significant. The activation energy was determined to be 226.8 kJ/mol while the heat of adsorption for 2-propanol and water was -45.5 and -9.6 kJ/mol, respectively. These heats of adsorptions are model parameters only and do not necessarily reflect any real physical phenomena. The high activation energy indicates that the kinetic data were obtained in a region where the diffusional effects were not rate limiting.

A simplified first order model was also found to fit the experimental data well. The activation energy was determined to be 195.8 kJ/mol. For the purpose of designing an appropriate separation process for wastewater purification it is recommended that the simple first order model be used, due to its simplicity and accuracy at low 2-propanol concentrations. Due to the small range of 2-propanol concentrations studied in this thesis, a six-parameter model may be too complex. Rate data over a wider range of 2-propanol concentrations need to be determined in order to make the LHHW models more feasible.

5.2 – Recommendations for Future Work

5.2.1 – Simulation of Wastewater Purification Process

In order to determine whether a separation process, such as catalytic distillation, is more economically feasible than a conventional separation process, such as distillation, a computation simulation must be performed using the developed kinetic model. A commercial software package such as Aspen plus could be used for the simulation. The influence of operating parameters on the number of stages would be performed for both the catalytic distillation and the conventional distillation process. The catalytic distillation process may be more economical than conventional distillation.

5.2.2 – Hydration of Propylene over Solid Acid Catalysts

Recent work on the hydration of propylene over H-ZSM-5 catalysts have been found in the literature [Sonnermans, 1993ab]. Catalytic hydration of alkenes to give alcohols and ethers is an established commercial technology of significant commercial interest [Waddams, 1978]. However, like the dehydration of 2-propanol, propylene hydration has only been studied in the vapor-phase. In studying the kinetics of the liquid-phase catalytic hydration of propylene the reverse reaction (dehydration of 2-propanol) must be known. The techniques developed in this thesis for the dehydration of 2-propanol can be used for this end.

The reaction temperatures used to determine the dehydration kinetics in this thesis ranged from 434-463 K. At these temperatures, the forward reaction is dominant. The liquid-phase hydration of propylene is more thermodynamically favorable at a lower reaction temperature, hence it would occur at more moderate reaction temperatures

ranging between 363 – 393 K. The dehydration of 2-propanol over silicalite requires reaction temperatures higher than 434 K for any significant conversion. It is unlikely that any significant conversion would occur at the low reaction temperatures required for propylene hydration. It was recently determined that Amberlyst 38, a commercial ion-exchange resin, is active at reaction temperatures as low at 373 K. The 2-propanol dehydration kinetics should be determined for Amberlyst 38 at reaction temperature ranging from 363 K to 423 K. The 2-propanol dehydration kinetics would be used with the propylene hydration kinetics (determined separately) for the complete reaction model.

5.2.3 – Effect of Silica/Alumina Ratio on the Rate of Propylene Formation

As was recently concluded by Olson and co-workers (1980), the acidity and hydrophilicity of H-ZSM-5 catalysts are directly proportional to the alumina content. As was seen in section 4.2.2, the type of binder used in silicalite had a great effect on the rate of propylene formation in the aqueous phase. The alumina present in the binder appeared to influence the rate of propylene formation greatly.

The influence of the silica/alumina ratio of H-ZSM-5 type zeolites on the rate of propylene formation should be determined. It is hypothesized that an ideal Si/Al ratio could be determined because a high alumina content would contain a high amount of acid sites necessary for 2-propanol dehydration, but would also be more hydrophilic which is detrimental to propylene formation.

5.2.4 – Effect of Metal Ion Concentration in Wastewater on the Rate of Propylene Formation

The experiments used to determine the reaction kinetics of silicalite were performed using deionized water. It can be assumed that wastewater containing 2-

propanol may contain metal ions in a significant concentration which may be detrimental to the life of the catalyst and the rate of propylene formation. It has been determined that cation exchanged alumina is less active in 2-propanol dehydration than alumina which has not been exchanged [Saad et al., 1993; Gervasini et al., 1995; 1997].

Kinetic experiments performed using tap water instead of deionized water indicate that cations present in tap water has a detrimental effect on the rate of propylene formation. Figure 5.1 illustrates that the resulting catalyst, which was reacted with a mixture of 2-propanol and tap water at 463 K, is less active in propylene formation. It is concluded that silicalite can undergo an ion exchange with the cations present in water and that the resulting catalyst is more basic in nature.

A more scientific and systematic method in studying this phenomena should be performed in future experiments. The influence of the loading of various ions present in industrial wastewater on the rate of propylene formation and on the catalyst deactivation should be studied.

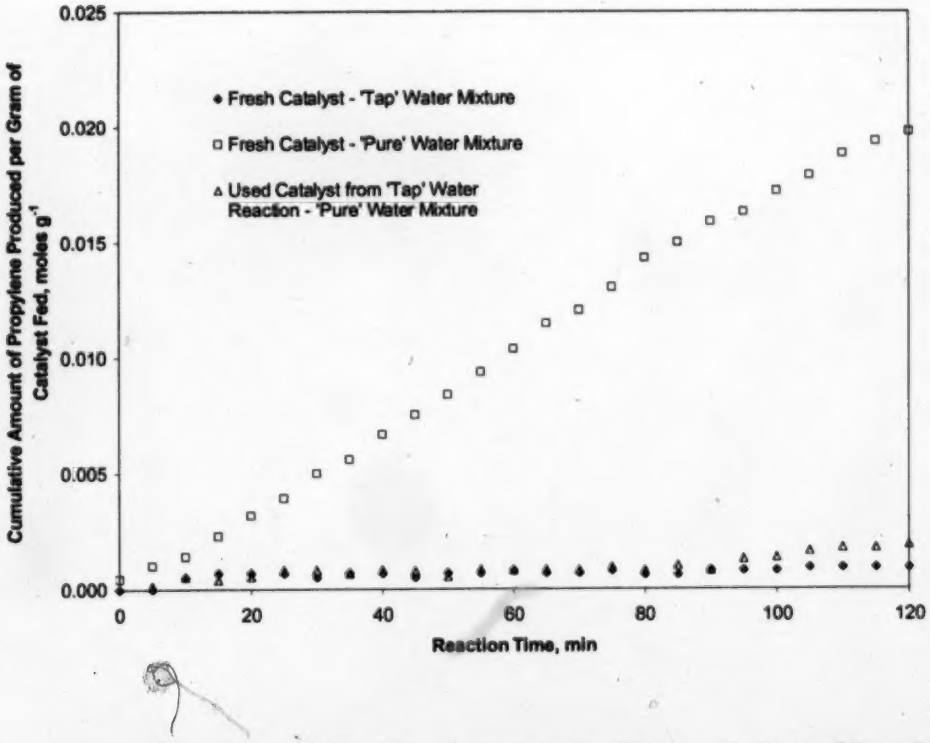

Figure 5.1 – Effect of Metal Ions Present in Tap Water on the Rate of Propylene Formation and Catalyst Deactivation: 10 mol % 2-Propanol Feed, Reaction Temperature of 463 K (Used Catalyst from Tap Water Reaction used in Kinetic Run with Deionized Water in the Feed)

5.3 – Literature Cited

Gervasini, A., G. Bellussi, J. Fenyvesi, and A. Auroux, "Microcalorimetric and Catalytic Studies of the Acidic Character of Modified Metal Oxide Surfaces. 1. Doping Ions on Alumina, Magnesia, and Silica", *J. Phys. Chem.* **99**, 5117-5125 (1995)

Gervasini, A., J. Fenyvesi and A. Auroux, "Study of the Acidic Character of Modified Metal Oxide Surfaces Using the Test of Isopropanol Dehydration", *Cat. Letters*. **43**, 219-228 (1997)

Olson, D. H., W. O. Haag and R. M. Lago, "Chemical and Physical Properties of the ZSM-5 Substitutional Series", *J. Catal.* **61**, 390-396 (1980)

Saad, A. B. M., V. A. Ivanov, J. C. Lavalley, P. Nortier, and F. Luck, "Comparitive Study on the Effects of Sodium Impurity and Amorphisation on the Lewis Acidity of γ-Alumina", *Appl. Catal. A*. **94**, 71-83 (1993)

Sonnemans, M. H. W., "Hydration and Etherification of Propene over H-ZSM-5. 2. Deposition of Carbonaceous Compounds on the Catalysts", *Ind. Eng. Chem. Res*. **32**, 2512-2515 (1993a)

Sonnemans, M. W. H., "Hydration of Propene over Acidic Zeolites", *Appl. Catal. A*. **94**, 215-229 (1993b)

Waddams, A. L., "Chemicals from Petroleum : An Introductory Survey", 4th Ed., Murray, London (1978)

Appendix A1

Maple V Worksheet for the Determination of the Amount of Propylene Produced

Note : 'Pgauge' is the gauge pressure measured by the pressure transducer in psig
'T' is the reaction temperature in degrees Celsius
'massA' and 'massW' are the grams of isopropanol and water added to the reactor, respectively
'Tnaught' is the reactor temperature prior to heating in degrees Celsius
'Pnaught' is the gauge pressure prior to heating (after helium purge) in psig
Units of the calculated parameters are found at the end of Chapter 3

Determination of the Amount of Propylene Produced at T and P Physical Conditions - Initial and Final T and P, Initial Moles of Inert and Reactant

```
> Pgauge:=451:
> P:=(Pgauge+14.7+4)*101.325/14.7:
> T:=190:
> massA:=38.109:
> massW:=100.173:
> Tnaught:=24:
> Pnaught:=-1.5:
> Ma:=massA/60.096:
> Mw:=massW/18.015:
> Mh:=(Pnaught+14.7+4)*101325*(319-massA/0.75-massW)*1e-6/(8.31451*(Tnaught+273.15)*14.7);

                    Mh := .008062382275
> Mt:=Ma+Mw+Mh;

                    Mt := 6.202730655
> R:=8.31451:
```

Determination of the Liquid Phase Fugacity of Pure Components 2-Propanol (1) and Water (2)

Modified Peng-Robinson Equation of State (PRSV)

```
> Tc1:=508.40:Pc1:=4764.25:omega1:=0.66372:kappa11:=0.23264:
> Tc2:=647.286:Pc2:=22089.75:omega2:=0.34380:kappa12:=-0.06635:
> Tr1:=(T+273.15)/Tc1:Tr2:=(T+273.15)/Tc2:
> kappa1:=(0.378893+1.4897153*omega1-0.17131848*(omega1)^2+0.0196554*(omega1)^3)+kappa11*(1+sqrt(Tr1))*(0.7-Tr1):
> kappa2:=(0.378893+1.4897153*omega2-0.17131848*(omega2)^2+0.0196554*(omega2)^3)+kappa12*(1+sqrt(Tr2))*(0.7-Tr2):
> a11:=(0.457235*R^2*Tc1^2/Pc1)*(1+kappa1*(1-sqrt(Tr1)))^2:
> a22:=(0.457235*R^2*Tc2^2/Pc2)*(1+kappa2*(1-sqrt(Tr2)))^2:
> b1:=0.077796*R*Tc1/Pc1:
> b2:=0.077796*R*Tc2/Pc2:
> A1L:=a11*P/(R*(T+273.15))^2:
> A2L:=a22*P/(R*(T+273.15))^2:
```

```
> B1L:=b1*P/(R*(T+273.15)):
> B2L:=b2*P/(R*(T+273.15)):
> q:=Z1L^3+(B1L-1)*(Z1L)^2+(A1L-3*(B1L)^2-2*B1L)*Z1L+((B1L)^3+(B1L)^2-
A1L*B1L)=0:
> w:=solve(q,Z1L):
> e:=w[1]:
> r:=Z2L^3+(B2L-1)*(Z2L)^2+(A2L-3*(B2L)^2-2*B2L)*Z2L+((B2L)^3+(B2L)^2-
A2L*B2L)=0:
> t:=solve(r,Z2L):
> y:=t[1]:
> phi1L:=exp(e-1-ln(e-B1L)-A1L/(2*sqrt(2)*B1L)*ln((e+(1+sqrt(2))*B1L)/(e+(1-
sqrt(2))*B1L))):
> phiAL:=simplify(phi1L):
> phi2L:=exp(y-1-ln(y-B2L)-A2L/(2*sqrt(2)*B2L)*ln((y+(1+sqrt(2))*B2L)/(y+(1-
sqrt(2))*B2L))):
> phiWL:=simplify(phi2L):
> fugAL:=phiAL*P;

                    fugAL := 1691.188114
> fugWL:=phiWL*P;

                    fugWL := 1195.745861
```

Determination of the Saturated Liquid Molar Volume of Pure Components 2-Propanol(1) and Water (2)

COSTALD (1979) Correlation

```
> Vo1:=0.2313:omega1SRK:=0.6637:
> Vo2:=0.0435669:omega2SRK:=-0.65445:
> ax:=-1.52816:bx:=1.43907:cx:=-0.81446:dx:=0.190454:ex:=-0.296123:fx:=0.386914:
> gx:=-0.0427258:hx:=-0.0480645:
> Vro1:=1+ax*(1-Tr1)^(1/3)+bx*(1-Tr1)^(2/3)+cx*(1-Tr1)+dx*(1-Tr1)^(4/3):
> Vro2:=1+ax*(1-Tr2)^(1/3)+bx*(1-Tr2)^(2/3)+cx*(1-Tr2)+dx*(1-Tr2)^(4/3):
> Vrd1:=(ex+fx*(Tr1)+gx*(Tr1)^2+hx*(Tr1)^3)/(Tr1-1.00001):
> Vrd2:=(ex+fx*(Tr2)+gx*(Tr2)^2+hx*(Tr2)^3)/(Tr2-1.00001):
> Vsat1:=Vo1*Vro1*(1-omega1SRK*Vrd1):
> Vsat2:=Vo2*Vro2*(1-omega2SRK*Vrd2):
> rhoA:=1/(Vsat1*1000/60.096);

                    rhoA := .5441071276
> rhoW:=1/(Vsat2*1000/18.015);

                    rhoW := .8644972067
```

Temperature Dependent Binary Constants for the van Laar Excess Gibbs Free Energy Equation

```
> C21:=-2228.6/(T+273.15)+5.953:
> C12:=2299.1/(T+273.15)-3.624:
```

```
        Critical/Reduced Variables and Other Constants for 'Volatile' Components
Propylene (3) and Helium (4)
        Used to Determine Compressibility of a Gas Mixture with PRSV
> Tc3:=365.57:Pc3:=4664.55:omega3:=0.14080:
> Tc4:=5.3:Pc4:=2.26*101.325:omega4:=-0.365:
> kappa3:=0.378893+1.4897153*omega3-
0.17131848*(omega3)^2+0.0196554*(omega3)^3:
> kappa4:=0.378893+1.4897153*omega4-
0.17131848*(omega4)^2+0.0196554*(omega4)^3:
> Tr3:=(T+273.15)/Tc3:
> Tr4:=(T+273.15)/Tc4:
> a33:=(0.457235*R^2*Tc3^2/Pc3)*(1+kappa3*(1-sqrt(Tr3)))^2:
> a44:=(0.457235*R^2*Tc4^2/Pc4)*(1+kappa4*(1-sqrt(Tr4)))^2:
> b3:=0.077796*R*Tc3/Pc3:
> b4:=0.077796*R*Tc4/Pc4:
> a12:=sqrt(a11*a22):
> a21:=a12:
> a13:=sqrt(a11*a33):
> a31:=a13:
> a14:=sqrt(a11*a44):
> a41:=a14:
> a23:=sqrt(a22*a33):
> a32:=a23:
> a24:=sqrt(a22*a44):
> a42:=a24:
> a34:=sqrt(a33*a44):
> a43:=a34:
      Define Mole Fractions
> xw:=1-xa:
> V:=Mt+alpha-L:
> yh:=Mh/V:
> yp:=alpha/V:
    Activity Coefficients - van Laar Gibbs Free Energy Equation
> gammaa:=exp(C12/(1+C12*xa/(C21*xw))^2):
> gammaw:=exp(C21/(1+C21*xw/(C12*xa))^2):
       Modified Peng-Robinson Equation of State Parameters - Determination of the
       Compressibility Factor for a Gas Mixture, Z and Vapor Phase Fugacity
Coefficients
>
a:=(ya)^2*a11+2*ya*yw*a12+2*ya*yp*a13+2*ya*yh*a14+(yw)^2*a22+2*yw*yp*a23
+2*yw*yh*a24+(yp)^2*a33+2*yp*yh*a34+(yh)^2*a44:
> b:=ya*b1+yw*b2+yp*b3+yh*b4:
> A:=a*P/(R*(T+273.15))^2:
> B:=b*P/(R*(T+273.15)):
```

```
> phiAV:=exp(b1/b*(Z-1)-ln(Z-B)-
A/(2*sqrt(2)*B)*(2*(ya*a11+yw*a12+yp*a13+yh*a14)/a-
b1/b)*ln((Z+(1+sqrt(2))*B)/(Z+(1-sqrt(2))*B))):
> phiWV:=exp(b2/b*(Z-1)-ln(Z-B)-
A/(2*sqrt(2)*B)*(2*(ya*a21+yw*a22+yp*a23+yh*a24)/a-
b2/b)*ln((Z+(1+sqrt(2))*B)/(Z+(1-sqrt(2))*B))):
      Set of Equations to be Solved to Determine xa, ya, yw, L, alpha and Z
      Z : Modified Peng-Robinson Equation of State for a Gas Mixture
> qq:=Z^3+(B-1)*Z^2+(A-3*B^2-2*B)*Z+(B^3+B^2-A*B)=0: xa: Water Component
Balance - Reaction Stoichiometry
> ww:=L*xw+V*yw=Mw+alpha:
      ya: Liquid 2-Propanol Fugacity = Vapor 2-Propanol Fugacity, VLE
> ee:=ya*P*phiAV=xa*gammaa*fugAL:
      yw: Liquid Water Fugacity = Vapor Water Fugacity, VLE
> rr:=yw*P*phiWV=xw*gammaw*fugWL:
      L : Summation of Vapor Phase Mole Fractions = 1
> tt:=ya+yw+yp+yh=1:
      alpha: 'Force Balance', i.e. PV=nZRT - assume negligible change of volume on
mixing
> yy:=P*1000*(319e-6-
L*(xa*60.096/(rhoA*1e6)+xw*18.015/(rhoW*1e6)))=V*R*Z*(T+273.15):
>
fsolve({qq,ww,ee,rr,tt,yy},{Z,xa,ya,yw,L,alpha},{Z=0.5..1,xa=0..1,ya=0..1,yw=0..1,L=0.
.9,alpha=-1..1});

 {alpha = .05032457627, Z = .8267580817, L = 6.108746232,

    ya = .1950923325, xa = .09096092816, yw = .4003108739}
> clear;

                    clear
> reset;

                    reset
```

Appendix A2
Raw Data for the Kinetic Runs

Table A2.1 – Catalyst Screening Raw Data : Alumina

T avg	190°C	Ma,°	38.274g	cat	2.185g
	463.15K	Mw,°	100.078g	Mh,°	0.0063moles

time (min)	T (°C)	P (psig)	x_A	x_W	α (moles)	Conv (%)
0	190	259	0.10033	0.89967	0.00002	0.003
5	191	266	0.10022	0.89978	0.00050	0.078
10	190	260	0.10028	0.89972	0.00026	0.041
15	188	253	0.10020	0.89980	0.00097	0.153
20	188.5	256	0.10017	0.89983	0.00111	0.174
25	190	263	0.10015	0.89985	0.00100	0.157
30	191	269	0.10009	0.89991	0.00123	0.193
35	190	264	0.10011	0.89989	0.00124	0.195
40	190	265	0.10007	0.89993	0.00149	0.233
45	189	260	0.10009	0.89991	0.00149	0.233
50	191	268	0.10014	0.89986	0.00099	0.155
55	189.5	262	0.10010	0.89990	0.00137	0.214
60	190	263	0.10015	0.89985	0.00100	0.157
65	191.5	272	0.10006	0.89994	0.00134	0.210
70	190.5	265	0.10012	0.89988	0.00087	0.137
75	190	264	0.10011	0.89989	0.00124	0.195
80	190	264	0.10011	0.89989	0.00124	0.195
85	190	264	0.10011	0.89989	0.00124	0.195
90	190	265	0.10007	0.89993	0.00149	0.233

Table A2.2 – Catalyst Screening Raw Data: Zeolite 13X

T avg	190.03°C	Ma,°	38.497g	cat	2.168g
	463.18K	Mw,°	99.710g	Mh,°	0.006303moles

time (min)	T (°C)	P (psig)	x_A	x_W	α (moles)	Conv (%)
0	190	263	0.10103	0.89897	0.00088	0.138
5	190	261	0.10111	0.89889	0.00040	0.062
10	189.5	261	0.10102	0.89898	0.00101	0.157
15	190.5	266	0.10100	0.89900	0.00100	0.156
20	190.5	266	0.10100	0.89900	0.00100	0.156
25	190	265	0.10094	0.89906	0.00137	0.214
30	190	264	0.10099	0.89901	0.00113	0.176
35	190	266	0.10090	0.89910	0.00162	0.253
40	189.5	264	0.10089	0.89911	0.00175	0.272
45	190.5	267	0.10096	0.89904	0.00125	0.194
50	190	264	0.10099	0.89901	0.00113	0.176
55	190	264	0.10099	0.89901	0.00113	0.176
60	190	265	0.10094	0.89906	0.00137	0.214
65	190	265	0.10094	0.89906	0.00137	0.214
70	190	264	0.10099	0.89901	0.00113	0.176
75	190	264	0.10099	0.89901	0.00113	0.176
80	190	264	0.10099	0.89901	0.00113	0.176
85	190	265	0.10094	0.89906	0.00137	0.214
90	190	264	0.10099	0.89901	0.00113	0.176

Table A2.3 – Catalyst Screening Raw Data: Silicalite S-115 SiO_2 ExT.

T avg	190.16°C	Ma,°	38.064g	cat	2.184g
	463.31K	Mw,°	99.577g	Mh,o	0.006823moles

time (min)	T (°C)	P (psig)	x_A	x_W	α (moles)	Conv (%)
0	190	261	0.10025	0.89975	0.00003	0.005
5	189.5	260	0.10019	0.89981	0.00040	0.063
10	190	265	0.10007	0.89993	0.00101	0.160
15	191	277	0.09975	0.90025	0.00273	0.430
20	190	272	0.09977	0.90023	0.00275	0.434
25	190	274	0.09968	0.90032	0.00325	0.513
30	189.5	272	0.09967	0.90033	0.00338	0.533
35	189	270	0.09965	0.90035	0.00351	0.554
40	191	280	0.09962	0.90038	0.00347	0.548
45	189	271	0.09961	0.90039	0.00376	0.593
50	190.5	278	0.09960	0.90040	0.00361	0.570
55	190	276	0.09959	0.90041	0.00375	0.591
60	192	288	0.09947	0.90053	0.00417	0.658
65	190	282	0.09932	0.90068	0.00525	0.829
70	190	284	0.09923	0.90077	0.00575	0.908
75	191	285	0.09940	0.90060	0.00471	0.744
80	190.5	287	0.09920	0.90080	0.00586	0.925
85	190	287	0.09910	0.90090	0.00651	1.028
90	190	287	0.09910	0.90090	0.00651	1.028

Table A2.4 – Catalyst Screening Raw Data: SAPO-5

T avg	190.18°C	Ma,°	38.482g	cat	2.184g
	463.33K	Mw,°	99.803g	Mh,°	0.006792moles

time (min)	T (°C)	P (psig)	x_A	x_W	α (moles)	Conv (%)
0	190	263	0.10100	0.89900	0.00039	0.061
5	190	262	0.10104	0.89896	0.00015	0.023
10	190.5	265	0.10101	0.89899	0.00026	0.041
15	191	270	0.10089	0.89911	0.00086	0.135
20	190	270	0.10070	0.89930	0.00211	0.329
25	190	269	0.10074	0.89926	0.00186	0.290
30	190	269	0.10074	0.89926	0.00186	0.290
35	190	269	0.10074	0.89926	0.00186	0.290
40	190	270	0.10070	0.89930	0.00211	0.329
45	190	270	0.10070	0.89930	0.00211	0.329
50	190	270	0.10070	0.89930	0.00211	0.329
55	190	270	0.10070	0.89930	0.00211	0.329
60	190	270	0.10070	0.89930	0.00211	0.329
65	190	271	0.10065	0.89935	0.00235	0.367
70	190	271	0.10065	0.89935	0.00235	0.367
75	190	271	0.10065	0.89935	0.00235	0.367
80	190	271	0.10065	0.89935	0.00235	0.367
85	190	270	0.10070	0.89930	0.00211	0.329
90	192	280	0.10066	0.89934	0.00205	0.319

Table A2.5 – External Mass Transfer Raw Data: Stirrer Speed = 883 rpm

stirrer speed	883rpm	Mw^{o}	100.235g
cat. loading	1.57wt %	Ma^{o}	38.06g
T avg	463.13K	cat	2.171g

time (min)	T (°C)	P (psig)	x_W	x_A	α (moles)
0	189	269	0.90066	0.09934	0.00198
5	190	275	0.90072	0.09928	0.00222
10	191	285	0.90095	0.09905	0.00343
15	190	281	0.90098	0.09902	0.00371
20	190	285	0.90116	0.09884	0.00470
25	189.5	287	0.90135	0.09865	0.00585
30	190	291	0.90142	0.09858	0.00621
35	190	294	0.90156	0.09844	0.00696
40	190	298	0.90173	0.09827	0.00797
45	190	300	0.90182	0.09818	0.00848
50	190	301	0.90187	0.09813	0.00873
55	190	304	0.90200	0.09800	0.00950
60	190	306	0.90209	0.09791	0.01000
65	190	308	0.90218	0.09782	0.01052
70	190	312	0.90236	0.09764	0.01154
75	190	315	0.90250	0.09750	0.01232
80	190	318	0.90264	0.09736	0.01309
85	190	319	0.90268	0.09732	0.01335
90	190	321	0.90277	0.09723	0.01387
95	190	324	0.90291	0.09709	0.01465
100	190	326	0.90300	0.09700	0.01517
105	190	328	0.90310	0.09690	0.01569
110	190	331	0.90323	0.09677	0.01648
115	190	334	0.90337	0.09663	0.01727
120	190	339	0.90361	0.09639	0.01859
125	190	341	0.90370	0.09630	0.01912
130	190	343	0.90379	0.09621	0.01965
135	190	345	0.90389	0.09611	0.02019
140	190	347	0.90398	0.09602	0.02072
145	190	348	0.90403	0.09597	0.02099
150	190	350	0.90413	0.09587	0.02153

Table A2.6 – External Mass Transfer Raw Data: Stirrer Speed = 1004 rpm

stirrer speed	1004rpm	Mw°	100.67g
cat. loading	1.54wt %	Ma°	38.32g
T avg	463.17K	cat	2.146g

time (min)	T (°C)	P (psig)	x_W	x_A	α (moles)
0	190	269	0.90019	0.09981	0.00068
5	190	276	0.90050	0.09951	0.00239
10	190	280	0.90067	0.09933	0.00338
15	190	287	0.90097	0.09903	0.00511
20	190	293	0.90123	0.09877	0.00660
25	190	298	0.90145	0.09855	0.00785
30	190	304	0.90172	0.09828	0.00937
35	190	310	0.90199	0.09801	0.01089
40	190	316	0.90226	0.09774	0.01242
45	190	323	0.90257	0.09743	0.01422
50	190.5	330	0.90278	0.09722	0.01534
55	190	336	0.90317	0.09683	0.01760
60	190	342	0.90344	0.09656	0.01918
65	190	348	0.90372	0.09628	0.02077
70	190	354	0.90400	0.09600	0.02237
75	190	360	0.90429	0.09571	0.02398
80	190	364	0.90448	0.09552	0.02506
85	190	369	0.90472	0.09528	0.02641
90	189.5	373	0.90503	0.09497	0.02827
95	190	380	0.90525	0.09475	0.02943
100	190.5	386	0.90542	0.09459	0.03031
105	190	390	0.90574	0.09427	0.03220
110	190	394	0.90593	0.09407	0.03332
115	190	400	0.90623	0.09377	0.03501
120	190	405	0.90648	0.09352	0.03642
125	190	409	0.90668	0.09332	0.03756
130	190	414	0.90693	0.09307	0.03899
135	190	419	0.90718	0.09282	0.04043
140	190	423	0.90739	0.09261	0.04159
145	190	427	0.90759	0.09241	0.04276
150	190	431	0.90780	0.09220	0.04393

Table A2.7 – External Mass Transfer Raw Data: Stirrer Speed = 1182 rpm

stirrer speed	1182rpm	Mw^o	100.284g
cat. loading	1.57wt %	Ma^o	37.92g
T avg	463.15K	cat	2.175g

time (min)	T (°C)	P (psig)	x_W	x_A	α (moles)
0	189	262	0.90074	0.09926	0.00031
5	190	275	0.90111	0.09889	0.00228
10	190.5	283	0.90136	0.09864	0.00363
15	190.5	289	0.90162	0.09838	0.00513
20	189.5	292	0.90196	0.09804	0.00718
25	190	298	0.90212	0.09788	0.00804
30	190	306	0.90248	0.09752	0.01008
35	190	313	0.90280	0.09720	0.01188
40	190.5	320	0.90301	0.09699	0.01300
45	190	327	0.90344	0.09656	0.01552
50	190	333	0.90372	0.09628	0.01709
55	190	338	0.90395	0.09605	0.01842
60	190	344	0.90424	0.09576	0.02001
65	190	349	0.90447	0.09553	0.02135
70	190	357	0.90485	0.09515	0.02351
75	190	364	0.90519	0.09481	0.02541
80	190	370	0.90548	0.09452	0.02706
85	190	377	0.90582	0.09418	0.02899
90	190	381	0.90602	0.09398	0.03011
95	190	386	0.90626	0.09374	0.03150
100	190	392	0.90656	0.09344	0.03319
105	190	398	0.90686	0.09314	0.03489
110	190	403	0.90712	0.09289	0.03632
115	190	408	0.90737	0.09263	0.03775
120	190	414	0.90767	0.09233	0.03949
125	190	419	0.90793	0.09207	0.04094
130	190	423	0.90814	0.09186	0.04211
135	190	428	0.90840	0.09160	0.04358
140	190	432	0.90861	0.09139	0.04476
145	190	436	0.90882	0.09118	0.04595
150	190	441	0.90908	0.09092	0.04745

Table A2.8 – Internal Mass Transfer Raw Data: 90 - 150 μm Particle Diameters

particle size	100-170 mesh		
stirrer speed	1080rpm	Mw°	100.537g
cat. loading	1.58wt %	Ma°	37.918g
T avg	463.21K	cat	2.186g

time (min)	T (°C)	P (psig)	x_W	x_A	α (moles)
0	189.5	270	0.90121	0.09879	0.00169
5	191	284	0.90152	0.09848	0.00326
10	191	287	0.90166	0.09834	0.00400
15	190	292	0.90208	0.09792	0.00653
20	190	299	0.90239	0.09761	0.00830
25	190	304	0.90261	0.09739	0.00957
30	190	311	0.90292	0.09708	0.01136
35	190	317	0.90320	0.09680	0.01291
40	190	324	0.90352	0.09648	0.01472
45	190	330	0.90379	0.09621	0.01629
50	190.5	337	0.90400	0.09600	0.01742
55	190	342	0.90435	0.09565	0.01946
60	190	348	0.90464	0.09536	0.02106
65	190	354	0.90492	0.09508	0.02267
70	190	360	0.90520	0.09480	0.02429
75	190	366	0.90549	0.09451	0.02593
80	190	372	0.90578	0.09422	0.02757
85	190	378	0.90607	0.09393	0.02923
90	190	383	0.90632	0.09368	0.03062
95	190	389	0.90661	0.09339	0.03230
100	190	394	0.90686	0.09314	0.03371
105	190	399	0.90711	0.09289	0.03512
110	190	404	0.90736	0.09264	0.03655
115	190	408	0.90756	0.09244	0.03769
120	190	413	0.90782	0.09218	0.03913
125	190	418	0.90807	0.09193	0.04058
130	190	422	0.90828	0.09172	0.04175
135	190	426	0.90848	0.09152	0.04292
140	190	430	0.90869	0.09131	0.04410
145	190	434	0.90890	0.09110	0.04528
150	190	437	0.90906	0.09094	0.04617

Table A2.9 – Internal Mass Transfer Raw Data: 595 - 850 μm Particle Diameters

particle size	20-30mesh		
stirrer speed	1080rpm	Mw°	100.459g
cat. loading	1.56wt %	Ma°	38.257g
T avg	463.17K	cat	2.158g

time (min)	T (°C)	P (psig)	x_W	x_A	α (moles)
0	189	268	0.90032	0.09968	0.00168
5	190	277	0.90051	0.09949	0.00265
10	190	285	0.90086	0.09914	0.00463
15	190.5	293	0.90111	0.09889	0.00598
20	190	300	0.90152	0.09848	0.00839
25	190	306	0.90188	0.09812	0.00990
30	189.5	312	0.90216	0.09784	0.01211
35	190	321	0.90246	0.09754	0.01375
40	190.5	330	0.90277	0.09723	0.01539
45	191	338	0.90302	0.09698	0.01676
50	190.5	346	0.90350	0.09650	0.01958
55	190	352	0.90390	0.09610	0.02190
60	190	358	0.90418	0.09582	0.02351
65	190	365	0.90452	0.09548	0.02540
70	190	372	0.90486	0.09514	0.02731
75	190	378	0.90515	0.09485	0.02896
80	190	384	0.90544	0.09456	0.03062
85	190	390	0.90573	0.09427	0.03230
90	190	396	0.90603	0.09397	0.03398
95	189.5	402	0.90646	0.09354	0.03649
100	190	409	0.90668	0.09332	0.03767
105	190	415	0.90699	0.09301	0.03940
110	190	421	0.90729	0.09271	0.04113
115	190	426	0.90755	0.09245	0.04259
120	190	432	0.90786	0.09214	0.04435
125	190	437	0.90812	0.09188	0.04583
130	190	441	0.90833	0.09167	0.04701
135	190	446	0.90874	0.09127	0.04939
140	190	451	0.90886	0.09114	0.05001
145	190	455	0.90907	0.09093	0.05122
150	190	458	0.90923	0.09077	0.05213

Table A2.10 – Temperature Dependence Raw Data: 463 K

T avg	189.98°C	Ma,°	38.109g
	463.13K	Mw,°	100.173g
		cat	2.151g
		Mh,°	0.00806moles

time (min)	T (°C)	P (psig)	x_A	x_W	α (moles)	L (moles)	V (moles)	C_A (moles/L)	C_W (moles/L)
0	189	263	0.09978	0.90022	0.00048	6.125	0.078	3.358	30.300
5	190	276	0.09941	0.90059	0.00245	6.124	0.081	3.342	30.275
10	190.5	285	0.09912	0.90088	0.00404	6.123	0.084	3.331	30.276
15	190.5	292	0.09881	0.90119	0.00579	6.122	0.086	3.324	30.314
20	190	298	0.09855	0.90145	0.00729	6.122	0.088	3.321	30.383
25	190	304	0.09817	0.90183	0.00947	6.122	0.091	3.313	30.430
30	189.5	310	0.09779	0.90221	0.01168	6.122	0.093	3.307	30.513
35	190	317	0.09758	0.90242	0.01281	6.121	0.095	3.299	30.504
40	190	324	0.09726	0.90274	0.01462	6.120	0.097	3.291	30.545
45	190	331	0.09694	0.90306	0.01645	6.119	0.100	3.283	30.586
50	190	338	0.09661	0.90339	0.01830	6.119	0.102	3.275	30.627
55	190	345	0.09629	0.90371	0.02016	6.118	0.105	3.268	30.669
60	190	352	0.09595	0.90405	0.02203	6.118	0.107	3.260	30.711
65	190	359	0.09562	0.90438	0.02392	6.117	0.110	3.252	30.754
70	190	365	0.09533	0.90467	0.02556	6.117	0.112	3.245	30.791
75	190	372	0.09499	0.90501	0.02748	6.116	0.114	3.236	30.834
80	190	378	0.09470	0.90530	0.02913	6.115	0.116	3.229	30.872
85	190	384	0.09440	0.90560	0.03080	6.115	0.119	3.222	30.910
90	190	390	0.09411	0.90589	0.03248	6.114	0.121	3.215	30.948
95	190	396	0.09381	0.90619	0.03418	6.114	0.123	3.208	30.986
100	190	402	0.09351	0.90649	0.03588	6.113	0.125	3.200	31.025
105	190	408	0.09320	0.90680	0.03760	6.113	0.128	3.193	31.065
110	190	414	0.09290	0.90710	0.03933	6.112	0.130	3.185	31.104
115	190	419	0.09264	0.90736	0.04078	6.112	0.132	3.179	31.138
120	190	424	0.09238	0.90762	0.04224	6.111	0.134	3.173	31.171
125	190	429	0.09212	0.90788	0.04371	6.111	0.136	3.166	31.205
130	190	433	0.09191	0.90809	0.04489	6.110	0.137	3.161	31.233
135	190	438	0.09165	0.90835	0.04638	6.110	0.139	3.155	31.267
140	190	442	0.09144	0.90856	0.04757	6.110	0.141	3.150	31.295
145	190	447	0.09117	0.90883	0.04907	6.109	0.143	3.143	31.329
150	190	451	0.09096	0.90904	0.05028	6.109	0.144	3.138	31.358

Table A2.11 – Temperature Dependence Raw Data: 453 K

T avg	180.13°C	Ma,°	38.19g
	453.28K	Mw,°	99.944g
		cat	2.175g
		Mh,°	0.00954moles

time (min)	T (°C)	P (psig)	x_A	x_W	α (moles)	L (moles)	V (moles)	C_A (moles/L)	C_W (moles/L)
0	180	222	0.10034	0.89966	0.00085	6.124	0.070	3.439	30.836
5	180.5	227	0.10020	0.89980	0.00156	6.123	0.071	3.432	30.821
10	180	227	0.10011	0.89989	0.00214	6.123	0.072	3.434	30.865
15	180	230	0.09997	0.90003	0.00292	6.123	0.073	3.430	30.882
20	181	235	0.09992	0.90008	0.00305	6.122	0.074	3.422	30.823
25	180	236	0.09970	0.90030	0.00448	6.123	0.075	3.424	30.916
30	180	237	0.09965	0.90035	0.00475	6.123	0.075	3.422	30.922
35	181	245	0.09946	0.90054	0.00561	6.121	0.077	3.411	30.880
40	180	244	0.09933	0.90067	0.00659	6.122	0.077	3.415	30.962
45	179.5	245	0.09919	0.90081	0.00745	6.123	0.078	3.415	31.012
50	181	252	0.09914	0.90086	0.00749	6.121	0.079	3.403	30.921
55	180	253	0.09891	0.90109	0.00898	6.122	0.080	3.404	31.015
60	180	254	0.09886	0.90114	0.00924	6.122	0.081	3.403	31.021
65	180	257	0.09872	0.90128	0.01005	6.121	0.082	3.400	31.038
70	180	259	0.09863	0.90137	0.01058	6.121	0.082	3.398	31.050
75	180	262	0.09849	0.90151	0.01139	6.121	0.083	3.394	31.068
80	180	265	0.09835	0.90165	0.01220	6.121	0.084	3.391	31.086
85	180	268	0.09820	0.90180	0.01301	6.121	0.085	3.387	31.104
90	180	270	0.09811	0.90189	0.01356	6.120	0.086	3.385	31.116
95	180	273	0.09796	0.90204	0.01437	6.120	0.087	3.381	31.134
100	180	275	0.09787	0.90213	0.01492	6.120	0.088	3.379	31.146
105	180.5	278	0.09782	0.90218	0.01510	6.119	0.088	3.374	31.120
110	180	281	0.09758	0.90242	0.01656	6.120	0.090	3.372	31.183
115	180	283	0.09748	0.90252	0.01712	6.120	0.090	3.369	31.195
120	180	285	0.09739	0.90261	0.01767	6.119	0.091	3.367	31.207
125	180	287	0.09729	0.90271	0.01822	6.119	0.092	3.365	31.220
130	180	290	0.09714	0.90286	0.01906	6.119	0.093	3.361	31.238
135	180.5	293	0.09720	0.90280	0.01856	6.118	0.093	3.359	31.199
140	180	295	0.09690	0.90310	0.02045	6.119	0.095	3.355	31.269
145	180	298	0.09675	0.90325	0.02129	6.118	0.096	3.351	31.288
150	180	299	0.09670	0.90330	0.02157	6.118	0.096	3.350	31.294

Table A2.12 – Temperature Dependence Raw Data: 444 K

T avg	170.95°C	Ma,°	37.904g
	444.10K	Mw,°	100.708g
		cat	2.15g
		Mh,°	0.00779moles

time (min)	T (°C)	P (psig)	x_A	x_W	α (moles)	L (moles)	V (moles)	C_A (moles/L)	C_W (moles/L)
0	170	177	0.09939	0.90061	0.00022	6.172	0.057	3.485	31.578
5	171	179	0.09944	0.90056	-0.00028	6.171	0.057	3.480	31.511
10	170	178	0.09934	0.90066	0.00049	6.172	0.057	3.484	31.583
15	170	179	0.09930	0.90070	0.00075	6.172	0.058	3.483	31.589
20	171	180	0.09940	0.90060	-0.00002	6.171	0.058	3.478	31.516
25	171	182	0.09931	0.90069	0.00052	6.171	0.058	3.476	31.528
30	171	183	0.09926	0.90074	0.00078	6.171	0.059	3.475	31.534
35	171	185	0.09917	0.90083	0.00132	6.171	0.059	3.473	31.545
40	171	186	0.09912	0.90088	0.00159	6.171	0.060	3.471	31.551
45	171	187	0.09908	0.90092	0.00186	6.171	0.060	3.470	31.557
50	171	189	0.09898	0.90102	0.00240	6.171	0.061	3.468	31.569
55	171	190	0.09894	0.90106	0.00266	6.171	0.061	3.467	31.574
60	171	191	0.09889	0.90111	0.00293	6.170	0.061	3.466	31.580
65	171	192	0.09884	0.90116	0.00320	6.170	0.062	3.465	31.586
70	171	193	0.09880	0.90120	0.00347	6.170	0.062	3.463	31.592
75	171	194	0.09875	0.90125	0.00375	6.170	0.062	3.462	31.598
80	171	195	0.09870	0.90130	0.00402	6.170	0.063	3.461	31.604
85	171	197	0.09861	0.90139	0.00456	6.170	0.063	3.459	31.616
90	171	198	0.09856	0.90144	0.00483	6.170	0.064	3.457	31.622
95	171	200	0.09847	0.90153	0.00538	6.170	0.064	3.455	31.634
100	171	201	0.09842	0.90158	0.00565	6.170	0.065	3.454	31.640
105	171	202	0.09837	0.90163	0.00592	6.170	0.065	3.453	31.646
110	171	204	0.09828	0.90172	0.00647	6.170	0.066	3.450	31.658
115	171	205	0.09823	0.90177	0.00674	6.170	0.066	3.449	31.663
120	171	206	0.09818	0.90182	0.00702	6.170	0.066	3.448	31.669
125	171	208	0.09809	0.90191	0.00757	6.169	0.067	3.446	31.682
130	171.5	209	0.09812	0.90188	0.00728	6.169	0.067	3.443	31.647
135	171	210	0.09804	0.90196	0.00784	6.169	0.067	3.444	31.688
140	172	212	0.09806	0.90194	0.00755	6.168	0.068	3.438	31.624
145	171	211	0.09795	0.90205	0.00839	6.169	0.068	3.442	31.700
150	171	213	0.09785	0.90215	0.00895	6.169	0.069	3.440	31.712

Table A2.13 – Temperature Dependence Raw Data: 434 K

T avg	160.94°C	Ma,°	37.802g
	434.09K	Mw,°	99.963g
		cat	2.168g
		Mh,°	0.00757moles

time (min)	T (°C)	P (psig)	x_A	x_W	α (moles)	L (moles)	V (moles)	C_A (moles/L)	C_W (moles/L)
0	160	140	0.10013	0.89987	0.00018	6.138	0.048	3.568	32.066
5	161	142	0.10016	0.89984	-0.00020	6.137	0.048	3.563	32.006
10	161	142	0.10016	0.89984	-0.00020	6.137	0.048	3.563	32.006
15	161	143	0.10011	0.89989	0.00008	6.137	0.049	3.561	32.012
20	161	143	0.10011	0.89989	0.00008	6.137	0.049	3.561	32.012
25	161	143	0.10011	0.89989	0.00008	6.137	0.049	3.561	32.012
30	161	143	0.10011	0.89989	0.00008	6.137	0.049	3.561	32.012
35	161	143	0.10011	0.89989	0.00008	6.137	0.049	3.561	32.012
40	161	144	0.10007	0.89993	0.00036	6.137	0.049	3.560	32.018
45	161	144	0.10007	0.89993	0.00036	6.137	0.049	3.560	32.018
50	161	145	0.10002	0.89998	0.00064	6.137	0.049	3.559	32.024
55	161	145	0.10002	0.89998	0.00064	6.137	0.049	3.559	32.024
60	161	146	0.09997	0.90003	0.00092	6.137	0.050	3.558	32.030
65	161	145	0.10002	0.89998	0.00064	6.137	0.049	3.559	32.024
70	161	147	0.09992	0.90008	0.00120	6.137	0.050	3.556	32.036
75	162	147	0.10005	0.89995	0.00024	6.136	0.050	3.553	31.963
80	161	147	0.09992	0.90008	0.00120	6.137	0.050	3.556	32.036
85	161	147	0.09992	0.90008	0.00120	6.137	0.050	3.556	32.036
90	161	147	0.09992	0.90008	0.00120	6.137	0.050	3.556	32.036
95	161	147	0.09992	0.90008	0.00120	6.137	0.050	3.556	32.036
100	161	148	0.09987	0.90013	0.00148	6.137	0.050	3.555	32.042
105	161	148	0.09987	0.90013	0.00148	6.137	0.050	3.555	32.042
110	161	148	0.09987	0.90013	0.00148	6.137	0.050	3.555	32.042
115	161	149	0.09982	0.90018	0.00176	6.137	0.051	3.554	32.048
120	161	149	0.09982	0.90018	0.00176	6.137	0.051	3.554	32.048
125	161	149	0.09982	0.90018	0.00176	6.137	0.051	3.554	32.048
130	161	150	0.09978	0.90022	0.00205	6.137	0.051	3.553	32.054
135	160	150	0.09964	0.90036	0.00301	6.137	0.051	3.556	32.128
140	160	150	0.09964	0.90036	0.00301	6.137	0.051	3.556	32.128
145	161	151	0.09973	0.90027	0.00233	6.137	0.051	3.551	32.061
150	161	151	0.09973	0.90027	0.00233	6.137	0.051	3.551	32.061

Table A2.14 – Concentration Dependence Raw Data: 8 mol % Initial 2-Propanol/Water Concentration in the Feed at 463 K

T avg	190.06°C	xa^0	0.0811	Mh,°	0.00722moles
	463.21K	Ma,°	31.786g	cat	2.156g
		Mw,°	107.93g		

time (min)	T (°C)	P (psig)	x_A	x_W	α (moles)	L (moles)	V (moles)	C_A (moles/L)	C_W (moles/L)
0	190	258	0.07874	0.92126	0.00193	6.452	0.077	2.823	33.026
5	191	269	0.07847	0.92153	0.00348	6.451	0.080	2.809	32.992
10	190	270	0.07824	0.92176	0.00497	6.452	0.081	2.809	33.097
15	190.5	279	0.07796	0.92204	0.00664	6.451	0.083	2.799	33.102
20	191	287	0.07772	0.92228	0.00806	6.450	0.086	2.789	33.100
25	190	290	0.07740	0.92260	0.01012	6.450	0.087	2.787	33.218
30	190	297	0.07710	0.92290	0.01195	6.450	0.090	2.779	33.261
35	189	300	0.07677	0.92323	0.01406	6.450	0.091	2.776	33.380
40	190	309	0.07658	0.92342	0.01512	6.449	0.094	2.764	33.336
45	189.5	314	0.07625	0.92375	0.01713	6.449	0.096	2.759	33.418
50	190	320	0.07609	0.92391	0.01806	6.448	0.097	2.751	33.405
55	191	331	0.07582	0.92418	0.01963	6.446	0.100	2.738	33.373
60	190	332	0.07556	0.92444	0.02131	6.447	0.101	2.737	33.482
65	190	338	0.07529	0.92471	0.02295	6.447	0.104	2.729	33.521
70	189.5	340	0.07509	0.92491	0.02412	6.447	0.104	2.727	33.586
75	191	349	0.07502	0.92498	0.02453	6.445	0.107	2.716	33.490
80	192	358	0.07483	0.92517	0.02554	6.444	0.109	2.705	33.443
85	189	355	0.07429	0.92571	0.02913	6.446	0.110	2.708	33.738
90	189	359	0.07411	0.92589	0.03026	6.446	0.112	2.703	33.765
95	189.5	363	0.07404	0.92596	0.03065	6.445	0.113	2.698	33.740
100	191	375	0.07382	0.92618	0.03179	6.443	0.116	2.683	33.663
105	190	375	0.07359	0.92641	0.03332	6.444	0.117	2.683	33.770
110	189.5	378	0.07333	0.92667	0.03495	6.444	0.118	2.678	33.843
115	189.5	382	0.07314	0.92686	0.03611	6.444	0.120	2.673	33.871
120	190	386	0.07307	0.92693	0.03649	6.443	0.121	2.668	33.846
125	190	391	0.07283	0.92717	0.03794	6.443	0.123	2.661	33.881
130	190	395	0.07264	0.92736	0.03911	6.442	0.124	2.656	33.910
135	190	398	0.07250	0.92750	0.03999	6.442	0.125	2.652	33.931
140	190	401	0.07235	0.92765	0.04087	6.442	0.126	2.648	33.952
145	190	403	0.07225	0.92775	0.04146	6.442	0.127	2.645	33.967
150	190	406	0.07211	0.92789	0.04235	6.441	0.128	2.641	33.988

Table A2.15 – Concentration Dependence Raw Data: 6 mol % Initial 2-Propanol/Water Concentration in the Feed at 463 K

T avg	189.97°C	xa^0	0.06	Mh,°	0.00707 moles
	463.12K	Ma,°	25.06g	cat	2.169g
		Mw,°	117.7g		

time (min)	T (°C)	P (psig)	x_A	x_W	α (moles)	L (moles)	V (moles)	C_A (moles/L)	C_W (moles/L)
0	189	233	0.05844	0.94156	0.00023	6.888	0.069	2.245	36.180
5	189	237	0.05828	0.94172	0.00124	6.888	0.071	2.241	36.205
10	191	251	0.05808	0.94192	0.00247	6.886	0.074	2.226	36.096
15	190	252	0.05787	0.94213	0.00390	6.886	0.075	2.224	36.201
20	189.5	256	0.05763	0.94237	0.00552	6.887	0.076	2.219	36.276
25	190	261	0.05753	0.94247	0.00621	6.886	0.078	2.213	36.258
30	190	266	0.05733	0.94267	0.00751	6.886	0.079	2.207	36.290
35	190	271	0.05714	0.94286	0.00881	6.885	0.081	2.201	36.322
40	190	275	0.05698	0.94302	0.00985	6.885	0.082	2.196	36.348
45	190	279	0.05682	0.94318	0.01090	6.885	0.083	2.191	36.374
50	190	284	0.05662	0.94338	0.01222	6.884	0.085	2.185	36.406
55	190	288	0.05646	0.94354	0.01328	6.884	0.086	2.180	36.433
60	190	292	0.05630	0.94370	0.01435	6.884	0.088	2.175	36.459
65	190	297	0.05610	0.94390	0.01568	6.884	0.089	2.169	36.492
70	190	300	0.05598	0.94402	0.01649	6.883	0.090	2.165	36.512
75	190	304	0.05582	0.94418	0.01757	6.883	0.092	2.160	36.539
80	190	308	0.05565	0.94435	0.01865	6.883	0.093	2.155	36.566
85	190	311	0.05553	0.94447	0.01947	6.883	0.094	2.151	36.586
90	190	315	0.05537	0.94463	0.02056	6.882	0.095	2.146	36.613
95	190	319	0.05520	0.94480	0.02163	6.882	0.097	2.141	36.641
100	190	322	0.05508	0.94492	0.02248	6.882	0.098	2.137	36.661
105	192	329	0.05518	0.94482	0.02166	6.880	0.099	2.132	36.501
110	190	327	0.05487	0.94513	0.02386	6.882	0.100	2.130	36.696
115	189.5	327	0.05477	0.94523	0.02455	6.882	0.100	2.129	36.748
120	189.5	329	0.05469	0.94531	0.02510	6.882	0.100	2.127	36.762
125	190	332	0.05466	0.94534	0.02525	6.881	0.101	2.124	36.731
130	190	335	0.05454	0.94546	0.02608	6.881	0.102	2.120	36.752
135	190	337	0.05445	0.94555	0.02664	6.881	0.103	2.117	36.766
140	189.5	336	0.05439	0.94561	0.02706	6.881	0.103	2.117	36.811
145	190	338	0.05441	0.94559	0.02692	6.881	0.103	2.116	36.773
150	190	339	0.05437	0.94563	0.02720	6.881	0.104	2.115	36.780

Table A2.16 – Concentration Dependence Raw Data: 4 mol % Initial 2-Propanol/Water Concentration in the Feed at 463 K

T avg	189.98°C	xa^0	0.039	Mh,°	0.00431moles
	463.13K	Ma,°	17.113g	cat	2.178g
		Mw,°	126.38g		

time (min)	T (°C)	P (psig)	x_A	x_W	α (moles)	L (moles)	V (moles)	C_A (moles/L)	C_W (moles/L)
0	190	209	0.03803	0.96197	-0.00041	7.240	0.064	1.568	39.675
5	190	215	0.03781	0.96219	0.00115	7.240	0.065	1.561	39.716
10	190	216	0.03777	0.96223	0.00141	7.240	0.066	1.559	39.723
15	189.5	219	0.03759	0.96241	0.00276	7.240	0.067	1.554	39.792
20	190	223	0.03752	0.96248	0.00324	7.240	0.068	1.550	39.771
25	190	225	0.03744	0.96256	0.00377	7.239	0.069	1.548	39.785
30	190	228	0.03733	0.96267	0.00456	7.239	0.070	1.544	39.806
35	190	232	0.03718	0.96282	0.00562	7.239	0.071	1.538	39.834
40	190	234	0.03711	0.96289	0.00616	7.239	0.071	1.536	39.848
45	190	237	0.03700	0.96300	0.00696	7.239	0.072	1.532	39.869
50	190	240	0.03689	0.96311	0.00776	7.239	0.073	1.528	39.890
55	190	242	0.03681	0.96319	0.00829	7.239	0.074	1.525	39.905
60	190	245	0.03670	0.96330	0.00910	7.238	0.075	1.521	39.926
65	190	247	0.03662	0.96338	0.00964	7.238	0.076	1.518	39.940
70	190	249	0.03655	0.96345	0.01018	7.238	0.076	1.516	39.955
75	190	251	0.03647	0.96353	0.01072	7.238	0.077	1.513	39.969
80	190	253	0.03640	0.96360	0.01126	7.238	0.078	1.510	39.983
85	190	255	0.03632	0.96368	0.01181	7.238	0.078	1.507	39.998
90	190	256	0.03628	0.96372	0.01208	7.238	0.079	1.506	40.005
95	190	257	0.03624	0.96376	0.01235	7.238	0.079	1.505	40.012
100	190	259	0.03617	0.96383	0.01290	7.238	0.080	1.502	40.027
105	190	260	0.03613	0.96387	0.01317	7.238	0.080	1.501	40.034
110	190	261	0.03609	0.96391	0.01344	7.237	0.080	1.499	40.041
115	190	262	0.03605	0.96395	0.01372	7.237	0.081	1.498	40.049
120	190	263	0.03601	0.96399	0.01399	7.237	0.081	1.496	40.056
125	190	263.5	0.03600	0.96400	0.01413	7.237	0.081	1.496	40.060
130	190	263	0.03601	0.96399	0.01399	7.237	0.081	1.496	40.056
135	190	264	0.03598	0.96402	0.01427	7.237	0.081	1.495	40.063
140	190	264	0.03598	0.96402	0.01427	7.237	0.081	1.495	40.063
145	190	264.5	0.03596	0.96404	0.01440	7.237	0.081	1.494	40.067
150	190	265	0.03594	0.96406	0.01454	7.237	0.082	1.494	40.071

Table A2.17 – Catalyst Reusability Raw Data: Used Catalyst at 463 K

T	190°C	xa^0	0.1026	Mh,°	0.009moles
	463.2K	Ma,°	38.149g	cat	1.825g
		Mw,°	100.07g		

time (min)	T (°C)	P (psig)	x_A	x_W	α (moles)	L (moles)	V (moles)	C_A (moles/L)	C_W (moles/L)
0	190	274	0.10002	0.89998	0.00005	6.120	0.079	3.356	30.199
5	190	282	0.09967	0.90033	0.00202	6.119	0.082	3.348	30.242
10	190.5	289	0.09947	0.90053	0.00311	6.118	0.084	3.339	30.232
15	190	291	0.09928	0.90072	0.00425	6.118	0.085	3.339	30.291
20	190	296	0.09906	0.90094	0.00550	6.118	0.086	3.334	30.319
25	189.5	300	0.09878	0.90122	0.00716	6.118	0.088	3.331	30.390
30	190	309	0.09848	0.90152	0.00878	6.117	0.091	3.320	30.392
35	190	314	0.09825	0.90175	0.01006	6.116	0.092	3.315	30.420
40	190	320	0.09798	0.90202	0.01159	6.116	0.094	3.308	30.454
45	190	326	0.09771	0.90229	0.01314	6.116	0.096	3.302	30.489
50	190	332	0.09743	0.90257	0.01470	6.115	0.098	3.295	30.523
55	190	339	0.09711	0.90289	0.01654	6.114	0.101	3.287	30.564
60	190	346	0.09678	0.90322	0.01838	6.114	0.103	3.279	30.606
65	190.5	355	0.09648	0.90352	0.02005	6.113	0.106	3.268	30.609
70	190	360	0.09612	0.90388	0.02212	6.113	0.108	3.264	30.690
75	189.5	365	0.09576	0.90424	0.02422	6.113	0.110	3.259	30.771
80	189	370	0.09540	0.90460	0.02634	6.113	0.112	3.254	30.852
85	189.5	378	0.09513	0.90487	0.02779	6.112	0.115	3.244	30.852
90	189	383	0.09476	0.90524	0.02995	6.112	0.117	3.238	30.934
95	190	391	0.09462	0.90538	0.03062	6.110	0.119	3.227	30.882
100	191	402	0.09433	0.90567	0.03211	6.108	0.123	3.213	30.848
105	191	407	0.09408	0.90592	0.03351	6.108	0.125	3.207	30.880
110	190.5	413	0.09365	0.90635	0.03603	6.108	0.127	3.200	30.971
115	190.5	419	0.09334	0.90666	0.03774	6.107	0.129	3.193	31.011
120	190	424	0.09295	0.90705	0.04002	6.107	0.132	3.187	31.097
125	190	428	0.09275	0.90725	0.04119	6.107	0.133	3.182	31.124
130	190	433	0.09249	0.90751	0.04265	6.106	0.135	3.175	31.157
135	190.5	436	0.09247	0.90753	0.04268	6.106	0.136	3.171	31.124
140	190	437	0.09228	0.90772	0.04383	6.106	0.137	3.170	31.185
145	189	436	0.09206	0.90794	0.04526	6.107	0.137	3.172	31.285
150	190	443	0.09197	0.90803	0.04561	6.105	0.139	3.163	31.226

Table A2.18 – Catalyst Loading Raw Data: 0.762 wt %

T	189.95°C	Ma,°	38.128g	cat	1.053g
	463.10K	Mw,°	100.09g	Mh,°	0.00807moles

time (min)	T (°C)	P (psig)	x_A	x_W	α (moles)	L (moles)	V (moles)	C_A (moles/L)	C_W (moles/L)
0	189	263	0.09990	0.90010	0.00051	6.121	0.078	3.361	30.285
5	189	268	0.09968	0.90032	0.00174	6.121	0.079	3.356	30.312
10	190	275	0.09958	0.90042	0.00223	6.120	0.081	3.346	30.254
15	189.5	275	0.09948	0.90052	0.00285	6.120	0.081	3.339	30.231
20	190	278	0.09944	0.90056	0.00297	6.119	0.082	3.339	30.235
25	190	281	0.09931	0.90069	0.00371	6.119	0.083	3.340	30.287
30	190	283	0.09923	0.90077	0.00421	6.119	0.084	3.338	30.298
35	190	285	0.09914	0.90086	0.00471	6.119	0.084	3.335	30.309
40	190	288	0.09900	0.90100	0.00546	6.119	0.085	3.332	30.326
45	190	291	0.09887	0.90113	0.00621	6.118	0.086	3.329	30.342
50	190	293	0.09878	0.90122	0.00672	6.118	0.087	3.327	30.354
55	190	296	0.09865	0.90135	0.00747	6.118	0.088	3.324	30.370
60	190	299	0.09852	0.90148	0.00823	6.118	0.089	3.321	30.387
65	190	302	0.09838	0.90162	0.00899	6.117	0.090	3.318	30.404
70	190	305	0.09825	0.90175	0.00976	6.117	0.091	3.314	30.421
75	190	308	0.09811	0.90189	0.01052	6.117	0.092	3.311	30.438
80	190	311	0.09797	0.90203	0.01129	6.117	0.093	3.308	30.455
85	190.5	315	0.09790	0.90210	0.01164	6.116	0.094	3.302	30.429
90	190.5	317	0.09781	0.90219	0.01216	6.116	0.095	3.300	30.440
95	190	319	0.09761	0.90239	0.01336	6.116	0.096	3.299	30.501
100	190	322	0.09747	0.90253	0.01414	6.116	0.097	3.296	30.518
105	190	324	0.09738	0.90262	0.01466	6.116	0.097	3.294	30.530
110	190	327	0.09724	0.90276	0.01544	6.115	0.098	3.290	30.548
115	190	329	0.09715	0.90285	0.01596	6.115	0.099	3.288	30.559
120	190	332	0.09701	0.90299	0.01675	6.115	0.100	3.285	30.577
125	190	334	0.09692	0.90308	0.01728	6.115	0.101	3.283	30.589
130	190	337	0.09678	0.90322	0.01807	6.115	0.102	3.279	30.606
135	190	340	0.09664	0.90336	0.01887	6.114	0.103	3.276	30.624
140	190	343	0.09650	0.90350	0.01966	6.114	0.104	3.273	30.642
145	190	346	0.09635	0.90365	0.02046	6.114	0.105	3.269	30.660
150	190	349	0.09621	0.90379	0.02127	6.114	0.106	3.266	30.678

Table A2.19 - Catalyst Loading Raw Data: 1.106 wt %

T	190.06°C	Ma,°	38.153g	cat	1.106g
	463.21K	Mw,°	100.58g	Mh,°	0.00804moles

time (min)	T (°C)	P (psig)	x_A	x_W	α (moles)	L (moles)	V (moles)	C_A (moles/L)	C_W (moles/L)
0	189	265	0.09945	0.90055	0.00103	6.149	0.078	3.351	30.341
5	191	281	0.09915	0.90085	0.00247	6.146	0.082	3.328	30.236
10	191	283	0.09907	0.90093	0.00296	6.146	0.083	3.326	30.247
15	190.5	285	0.09888	0.90112	0.00408	6.147	0.084	3.325	30.306
20	190.5	290	0.09866	0.90134	0.00532	6.146	0.085	3.320	30.333
25	190	294	0.09838	0.90162	0.00697	6.146	0.087	3.318	30.404
30	190	298	0.09821	0.90179	0.00798	6.146	0.088	3.313	30.426
35	190	302	0.09803	0.90197	0.00899	6.146	0.090	3.309	30.448
40	190	306	0.09785	0.90215	0.01000	6.145	0.091	3.305	30.471
45	189.5	310	0.09756	0.90244	0.01169	6.145	0.092	3.294	30.471
50	190	315	0.09745	0.90255	0.01230	6.145	0.094	3.295	30.522
55	190	320	0.09722	0.90278	0.01359	6.144	0.096	3.290	30.550
60	190	325	0.09699	0.90301	0.01488	6.144	0.097	3.284	30.579
65	190.5	330	0.09687	0.90313	0.01549	6.143	0.099	3.278	30.559
70	190	335	0.09653	0.90347	0.01749	6.143	0.101	3.273	30.638
75	190	339	0.09635	0.90365	0.01855	6.143	0.102	3.269	30.661
80	190	343	0.09616	0.90384	0.01961	6.142	0.103	3.265	30.685
85	190	348	0.09593	0.90407	0.02093	6.142	0.105	3.259	30.715
90	190	353	0.09569	0.90431	0.02227	6.141	0.107	3.253	30.745
95	190	357	0.09550	0.90450	0.02335	6.141	0.108	3.249	30.769
100	190	361	0.09531	0.90469	0.02444	6.141	0.110	3.244	30.793
105	190	365	0.09512	0.90488	0.02551	6.140	0.111	3.240	30.817
110	190	370	0.09488	0.90512	0.02687	6.140	0.113	3.234	30.848
115	190	375	0.09464	0.90536	0.02824	6.140	0.115	3.228	30.879
120	190	379	0.09445	0.90555	0.02935	6.139	0.116	3.223	30.904
125	190	383	0.09425	0.90575	0.03045	6.139	0.118	3.218	30.929
130	190	387	0.09405	0.90595	0.03157	6.139	0.119	3.214	30.955
135	190	391	0.09386	0.90614	0.03269	6.138	0.121	3.209	30.980
140	190	395	0.09366	0.90634	0.03381	6.138	0.122	3.204	31.006
145	190	399	0.09346	0.90654	0.03494	6.137	0.124	3.199	31.031
150	190	402	0.09331	0.90669	0.03579	6.137	0.125	3.196	31.051